THE UNIVERSITY OF CHICAGO

MORPHOLOGY AND EVOLUTION OF THE AVIAN FLIGHT APPARATUS IN RELATION TO ECOLOGY AND FUNCTION

A DISSERTATION SUBMITTED TO

THE FACULTY OF THE DIVISION OF THE BIOLOGICAL SCIENCES

AND THE PRITZKER SCHOOL OF MEDICINE

IN CANDIDACY FOR THE DEGREE OF

DOCTOR OF PHILOSOPHY

GRADUATE PROGRAM IN INTEGRATIVE BIOLOGY

BY

STEPHANIE LYNN BAUMGART

CHICAGO, ILLINOIS

AUGUST 2021

In memory of my loving grandmother, Beverly May.

TABLE OF CONTENTS

LIST OF FIGURES

LIST OF TABLES

Supplemental materials: Any **s**upplementary material for Chapter 2 not found in the appendices can be found in the supplemental data for Baumgart et al. (2021), DOI: 10.1093/iob/obab011.

There are also three interactive plots on FigShare that accompany Chapter 3, DOIs: 10.6084/m9.figshare.15054381, 10.6084/m9.figshare.15054423, and 10.6084/m9.figshare.15054477.

ACKNOWLEDGEMENTS

First, I would like to thank my adviser, Paul Sereno. Coming into undergrad, I knew I wanted to major in biology and had always been interested in paleontology, but it was not clear to me how to do so. Taking his Vertebrate Structure and Function class during my second year of undergrad introduced me to the wonderful world of comparative anatomy and made me realize that this is what I wanted to do. I asked him what else I could do to become a paleontologist and he welcomed me into his lab – I learned how to prepare fossils, watch the construction of an exhibit and help where needed, got to go on multiple dinosaur digs, got to TA his classes, and learned how to segment CT scans of fossils. Paul taught me how to improve my writing, how to design courses, how outreach is also a very critical part of science. He has always been very supportive of my ideas – research, teaching, or outreach – and encouraged me and believed in me when I start doubting myself. I honestly am not sure how my career path would have turned out without Paul's welcome and mentorship, and I cannot thank him enough.

Second, I would like to thank my committee. I met Mark Westneat my fourth year of undergrad in his anatomy class. I had a blast learning about even more awesome animals (sling-jaw wrasse!) and dissecting many specimens in labs, all with healthy dose of puns. Mark has always been very supportive and pushed me to learn new techniques and keep thinking about how to take my research in new directions. He has taught me a lot about biomechanics, has provided valuable guidance with regards to shaping my research, and invited me to his lab's SICB talk practice sessions. When I was working on my undergrad thesis, Zhe-Xi Luo let me use one of his student computers to use Mimics for segmenting CT scans. But every time I was in there, he would stop by and check up on me and was very excited about what I was doing.

During my gap year, I ran into him carrying a platypus skeleton to his classroom, and he invited me to sit in on his mammal evolution course. He and Ken Angielczyk then proceeded to blow my mind with the coolness of synapsids, which I then was able to share with the next round of students as a TA. I will always appreciate Luo encouraging me to get trained to use the microCT scanner, little did I know just how much I would use it for my research and other projects. Luo has always provided me with great insight and feedback on my work and has really welcomed me into his lab. I would like to thank Michael Coates for agreeing to sit down with a confused undergrad me to discuss grad school. I had been told that you do not apply to graduate programs at the same school you went to undergrad, but he encouraged me to apply here and the rest is history. Since then, he has pushed me with his "So what?" question to really think about the bigger picture of my research and working with him as a TA has really improved my teaching abilities. I met John Bates through the openVertebrate "oVert" TCN CT scanning project, and though our time together has been shorter, it has been no less influential. Coming into my thesis on extant birds from the perspective of a paleontologist, my background in ornithology was based mostly on anatomy and skeletons. Talking with him brought the birds to life and included many fascinating conversations on bird behavior, migration patterns, and bizarre facts that were constantly reshaping the way I was thinking about birds.

I would also like to thank my collaborator Leon Claessens for feedback and discussions regarding sternum morphology (Chapter 3) as well as access to the sternum models on Aves3D.org using specimens from the Yale Peabody Museum and the Harvard Museum of Comparative Zoology. I thank the numerous undergraduate students who have worked hard with him to create these sternum models, and I could not have done this work without them. I also thank Rossy Natale for providing the *Actiphilornis* sternum model from the Field Museum of

Natural History. I would like to thank Michael Habib for access to the *Bennettazhia* scan and discussion about the specimen and aerodynamics.

This work was funded by the U.S. Department of Education Graduate Assistance in Areas of National Need (GAANN) in Integrative Neuromechanics (P200A150077), a generous donation from SC Johnson to Paul Sereno, the University of Chicago Hinds Fund, and the oVert TCN (NSF DBI 1701714).

I need to give special thanks to Michael Guerra and Garnett Kirk, our department's IT staff, for all of their hard work during the pandemic, trying to keep computers working and giving me remote access to five different computers throughout the department so I could continue to work on my thesis throughout the lockdown and remote work. And thank you to Zeray Alemseged and Zhe-Xi Luo for giving me remote access to your student computers, I could not have finished my thesis when I did without that access. I would also like to thank Audrey Aronowsky for her amazing admin skills and her patience and excellent advice as I was trying to figure out what was supposed to be happening at different stages of grad school.

I would also like to give a general thank you to those who make their data accessible online – my thesis has been composed of wing images from the University of Puget Sound's Slater Museum of Natural History online Wing and Tail Image Collection (Chapter 2) maintained by Peter Wimberger and Gary Shugart, three-dimensional sternum models from Aves3D.org provided by Leon Claessens and Scott Edwards and created with the work of many undergrads (Chapter 3), and humerus CT data from a number of museum collections around the world downloaded from Morphosource.org (Chapter 4). I could not have completed my thesis without those resources, and, if anything, the pandemic lockdown has underlined the great

importance of accessibility to datasets for the continuation of research and learning about our world.

I definitely could not have made it through this whole process without the support of amazing labmates, past and present: Erin Fitzgerald, Lauren Conroy, Tyler Keillor, Jessica Schwartz, Caleb Wang, Maria Viteri, Alexander Okamoto, Hadley Eichengreen, Grace Broderick, Kate Hodge, Amaury Michel, Spiro Sullivan, Spencer Pevsner, Aneila Hogan, and many more. You all inspire me every day with your amazing skills and ideas and thank you for listening to the mad ravings of a stressed grad student, feeding said stressed grad student, and making the past six years – nine and counting in the Sereno lab – truly enjoyable. It is going to be incredibly hard to leave the lab when it's time, because you have become a second family to me.

I would also like to thank April Neander and Daryl Coldren. April has taught me all I know about CT scanning, has patiently helped me troubleshoot tricky specimens or odd CT scanner behaviors, and is always ready with cute cat pictures when I am stressed. Daryl has taught me so much about birds while we CT scanned them in the Culver basement for oVert. I came to studying birds and working on the oVert project from a paleontological background with an interest in bones, so working with whole birds with skin and feathers was a new experience. Daryl patiently answered my many questions and corrected my pronunciations, and we have had so many fascinating conversations about birds. I have also greatly enjoyed the hilarious (to me) stories involving his farm animals. I am so excited we get to continue working together for another year, because it has been truly wonderful working with you two.

And to the lifelong friends I have made through the department: Gayani Senevirathne, Noor Singh, Melvin Bonilla, Kelsey Stilson, Sam Gartner, Megan Kennedy, Rossy Natale,

Stephanie Sang, Aileen Tartanian, Vish Venkat, Dakota Lane, Ben Sulser, Courtney Orsbon, Dave Grossnickle, Aaron Olsen, Jackie Lungmus (and countless others that are no less loved!), I thank you for the adventures, the serious discussions, the not-so-serious discussions, troubleshooting, research feedback, HMart trips, Bachelor nights, craft nights, and happy hours at 710. You all kept me sane and laughing, and I have learned so much from all of you. And thank you to my dear college friends, Noelle Turtur and Prathima Radhakrishnan, for constant love and support, mutual ranting sessions, and wonderful adventures in the States and abroad. I miss you so much and love you both.

Last but definitely not least, I would like to thank my family. My parents, John and Linda, fostered my lifelong obsession with dinosaurs and encouraging me to apply to the University of Chicago for my undergrad, pointing to Paul's Dinosaur Science course as a fun reason to go. Little did any of us know that I would still be here, eleven years later, putting the last touches on my PhD dissertation. My younger sister, Alexandra, has had to tolerate playing with dinosaurs and learning about them for various games, but she seemed to have fun. She has grown into an amazing scientist and has helped me with more nuanced biomechanical concepts, explaining a picture of a vulture I saw on Twitter that was able to fly with no secondary feathers, for example. I would finally like to thank my grandparents, Bill and Kathy, and my late grandmother, Bev, for sitting through The Land Before Time (and sequels!) a bajillion times, for buying me tons of paleontology books and toys, and for encouraging me in my fascination with paleontology throughout the years. A supportive family is so important, and I truly could not have gotten through this without you.

ABSTRACT

Powered flight evolved three times independently among tetrapods (Pterosauria, Aves, Chiroptera), each transition involving a distinctive retooling of forelimbs into wings in response to similar aerodynamic functional constraints. In this dissertation I examine three aspects of the avian flight apparatus —wing shape, sternum shape, and humeral pneumaticity (internal air space)— using a range of comparative techniques that may be extended in future research to the other two clades of powered fliers. Although avian wing shape has long been correlated with general aerodynamic demands (flight function, speed, lift, etc.), that correlation more recently has been shown to be less significant when considering the range of distinctive avian flight styles and migratory habits. Instead, phylogenetic proximity has left an imprint with closely related birds showing similar wing shapes. To rigorously test the association of wing shape with ecology and flight behavior, and to test the strength of association of wing morphology with other behavioral and ecological variables, I chose a functionally and ecologically diverse assemblage of birds known as waterbirds. In this group I found that wing shape is highly convergent and correlated strongly with foraging behavior, but not with habitat, flight style or migration pattern. The sternum, anchor to the major flight muscles, varies markedly in shape like the wing but has not been as intensively studied. I found that sternum shape, like wing shape, is highly convergent and retains phylogenetic signal but also is significantly correlated with flight style. The sternum may thus be more strongly linked than the wing to some biomechanical flight variables. Humeral pneumaticity has been shown to be correlated with body mass, particular flight styles, and some behaviors and ecological habitats, such as diving. Previous studies, however, were based only on the presence/absence of pneumatic foramina rather than the actual volume of internal air space. Using CT scans of a sample of avian humeri, I calculated pneumatic volume and showed that

body mass is only weakly correlated with pneumaticity. Although pneumaticity is clearly an evolutionary solution for reduced mass in response to the challenge of aerial flight, pneumaticity may be correlated with other functions and behaviors as well. Considering wing shape, sternum shape, and pneumaticity more broadly in an evolutionary framework yields a wider range of insights about flight. Extending the comparative approach to pterosaurs and bats broadens the scope to outlining the general patterns of form and function in the wing, sternum and bone structure among vertebrate powered fliers.

CHAPTER 1

> Whether it be the sweeping eagle in his flight, or the open apple-blossom, the toiling workhorse, the blithe swan, the branching oak, the winding stream at its base, the drifting clouds, over all the coursing sun, *form ever follows function*, and this is the law. Where function does not change form does not change. The granite rocks, the ever-brooding hills, remain for ages; the lightning lives, comes into shape, and dies in a twinkling.
>
> It is the pervading law of all things organic and inorganic, of all things physical and metaphysical, of all things human and all things superhuman, of all true manifestations of the head, of the heart, of the soul, that the life is recognizable in its expression, that form ever follows function. *This is the law.*
>
> Louis Sullivan, *The Tall Office Building Artistically Considered*

Introduction

The advent of *powered flight*—a profound locomotor transitions for any terrestrial organism—opens an entirely new ecological landscape to evolutionary exploration. Powered fliers, unlike the many kinds of engineered aircraft (Jenkinson et al. 1999), are built from an ancient aquatic vertebrate Bauplan that has been retooled over millions of years across many habitats. Nonetheless, both powered fliers and manufactured aircraft need to follow aerodynamic first principles to achieve flight and stay aloft. As Louis Sullivan wrote in 1896, "form ever follows function," a central principle in the discipline of functional morphology, although Sullivan was referring to architecture. With more sophisticated techniques in recent years, our ability to record, measure and then explore the relationship between form and function has brought to the fore how this dynamic plays out in real world habitats and environments. In this dissertation, I focus on avian powered fliers to learn more about the relationship between the *form* of the avian

flight apparatus and its ecological and biomechanical *functions*. My long-term aims are to expand that focus comparatively to incorporate all vertebrate powered fliers.

Vertebrate powered flight has evolved three times independently. Pterosaurs took to the air first (~220 Mya) using wing and tail membranes, the former held taut led by a hypertrophied fourth finger; birds were next (~160 Mya) using fore and hind wings covered with and extended by feathers, a novel integumentary invention; late on the scene were bats (~52 Mya) using multiple membranes including a wing membrane stretched across elongate fingers, hind limb and tail (Alexander 2015; Dalla Vecchia 2019). These three radiations differ in body size range and the structure of bony supports, which led to varying ecological strategies. Using modern techniques to capture and analyze new forms of data (CT-based visualization, morphometric capture and analysis, calibrated phylogenetic relationships, and comparative statistical analysis), their similarities as well as their differences may lead to significant comparative insights.

Birds and pterosaurs are archosaurs and therefore likely share a highly efficient, unidirectional respiratory system with the potential for pneumatized bones and body cavities (Schachner et al. 2013), whereas bats utilize the less efficient mammalian respiratory system with tidal airflow and an apneumatic postcranial anatomy (West et al. 2007). Birds have flight muscle structure powering wingbeat on the ventral side of the body (Ghetie et al. 1976), whereas pterosaurs and bats power the upstroke using muscles attaching to the lateral and dorsal aspect of their ribcage (Bennett 2003; Hermanson and Altenbach 1983). The wingspan of the largest bat is approximately 1.5 m and the largest bird approximately 6.4 m (extinct *Pelagornis*), whereas wingspans exceeding an estimated 10 m characterize the largest pterosaurs (Alexander 2015; Ksepka 2014).

I chose the avian flight apparatus as the central focus of work in this dissertation for reasons of data and diversity. Aves includes approximately 10,000 extant species of global distribution that occupy a wide range of ecological space, including the cold and deep water habitats of the Antarctic penguins, some of which can dive up to 500m (*Aptenodytes forsteri*, Myers et al. 2020). Unlike the other two volant clades, fossil avians record the transition between non-volant and volant species, and extant species have repeatedly reduced and lost the ability to fly. Birds have long attracted the attention of functional morphologists, the dynamic between avian bill shape and its functional role in diet most famously captivating Darwin (1845). Here birds provide a rich resource for studying the interplay between structure, function and evolutionary history.

1.1 HYPOTHESES

The central aim of this PhD dissertation is to address central questions in the ecomorphology of bird flight using the techniques of morphometrics, phylogenetics and comparative methods approaches to the analysis of structural and functional traits. This work specifically aims to test hypotheses of the association of general shape factors and particular functional traits with bird ecology and flight behavior, as well as explore patterns of convergence among bird clades. I aim to quantify relationships between form and function in three key areas of the flight apparatus: the wing as the principal flight structure (Chapter 2), the sternum as the principal anchor for flight muscles (Chapter 3), and the humerus as the principal attachment to the wing with a variably air-filled interior (Chapter 4).

1.1.1 Wing shape in waterbirds: morphometrics and evolution

The central goal of Chapter 2 is to explore wing shape in waterbirds, a non-monophyletic group of birds united by aquatic habitats that are incredibly diverse in morphology and behavior.

Wing shape has been extensively studied in vertebrate powered fliers (ex: Wang and Clarke 2015; Dyke et al. 2006; Norberg and Rayner 1987; Findley et al. 1972; Taylor et al. 2012; Palmer and Dyke 2012; Hone et al. 2015; Lockwood et al. 1998; Hansen 2003; Martin-Silverstone et al. 2020; Bahlman et al. 2013; David Lentink and Biewener 2010) by those studying the natural world and manmade aircraft. Aspect ratio and wing loading have been linked to aerial performance (ex: fast takeoff or metabolically efficient) or migratory ability (migrant or non-migrant) (Gómez-Bahamon et al. 2020; Lockwood et al. 1998), although many of these studies were not undertaken in the light of phylogenetic context. A recent study has tested wing shape against various factors and found that phylogenic relationships provided the best explanation for the diversity in avian wing shapes (Wang and Clarke 2015). The ecological variable tested was flight style (Viscor and Fuster 1987), capturing only one aspect of flight — wingbeat pattern in steady horizontal flight. I hypothesize that testing ecological variables that are more reflective of a bird's lifestyle (foraging behavior, habitat, migration with geographical context) may yield a clearer link between wing shape and behavior. This hypothesis is tested with linear and geometric morphometric analyses and phylogenetic comparative methods.

1.1.2 Sternum shape

One of the central questions in bird flight mechanisms that remains relatively unexplored is the anatomical variability and functional relevance of the sternum. The sternum serves as the anchor for major flight muscles as well as a bone whose movement is tied to respiration and whose internal surface supports viscera. Most birds have a keel on the ventral surface of the sternum providing additional attachment area for the major flight muscles, the pectoralis and supracoracoideus. The keel can be shallow or deep and inclined or not. The sternal plate, the main body of the sternum, can be long and narrow or short and wide. With this diversity in shape

and close relationship to avian flight musculature, it is surprising that the ecomorphology of this bone has not been detailed. Three linear sternal measures were compared to various ecological characteristics (Düzler et al. 2006; Zhang et al. 2011), but there has yet to be a landmark-based morphometric analysis. I hypothesize that sternum shape is related to flight style (short bursts of flight or long periods of soaring) but is modular in how it evolves, given the other roles the sternum plays in the avian body. This hypothesis is tested with a large sample of avian sterna using three-dimensional morphometrics, phylogenetic comparative methods, and modularity and integration tests.

1.1.3 Humeral pneumaticity

Postcranial skeletal pneumaticity, or air-filled outpocketings of the respiratory tract, lightens the body cavities and skeletal elements in both birds and pterosaurs (Butler et al. 2012; P. M. O'Connor 2009; Smith 2012). Some soaring birds have pneumatic sacs that invade every bone. Diving birds, in contrast, have little or no skeletal pneumaticity to reduce buoyancy. O'Connor (2009) and Smith (2012) tabulated bones that had pneumatic foramina (pores for entry of pneumatic sacs), using a pneumaticity index (the ratio of bones with and without pneumatic foramina) that they found correlated with body mass and ecology. A few studies have focused in on vertebral pneumaticity (Fajardo et al. 2007; Gutzwiller et al. 2013; Moore 2020), using CT scans to quantify the volume of bone to air. This technique has not been extended to other skeletal bones. I hypothesize that "pneumaticity index" is a coarse measure that may mask differences in pneumaticity important to correlations with body mass or behavior. I test this hypothesis using CT scans of the humerus from a wide sampling of birds differing in body mass, behavior and taxonomic group. The humerus is almost always pneumatized in birds and reduces the chance of confusion with marrow-filled spaces.

Collectively, these studies are the beginnings of a deeper investigation into the structure of the avian flight apparatus and its relation to function and ecology and set up future comparisons with other vertebrate powered fliers.

CHAPTER 2

Wing shape in waterbirds: morphometric patterns associated with behavior, habitat, migration, and phylogenetic convergence

Published as: Baumgart, Stephanie L., Sereno, Paul C., Westneat, Mark W. "Wing shape in waterbirds: morphometric patterns associated with behavior, habitat, migration, and phylogenetic convergence." *Integrative Organismal Biology* Vol. 3. (2021). DOI: 10.1093/iob/obab011.

S.L.B. and M.W.W. devised the project and created WingMorph, S.L.B. wrote the R code and performed the data analyses, S.L.B. made the figures, S.L.B. interpreted the results with input from M.W.W. and P.C.S., S.L.B. wrote the manuscript with critical feedback from M.W.W. and P.C.S.

2.1 ABSTRACT

Wing shape plays a critical role in flight function in birds and other powered fliers and has been shown to be correlated with flight performance, migratory distance, and the biomechanics of generating lift during flight. Avian wing shape and flight mechanics have also been shown to be associated with general foraging behavior and habitat choice. We aim to determine if wing shape in waterbirds, a functionally and ecologically diverse assemblage united by their coastal and aquatic habitats, is correlated with various functional and ecological traits. We applied geometric morphometric approaches to the spread wings of a selection of waterbirds to search for evolutionary patterns between wing shape and foraging behavior, habitat and migratory patterns.

We found strong evidence of convergent evolution of high and low aspect ratio wing shapes in multiple clades. Foraging behavior also consistently exhibits strong evolutionary correlations with wing shape. Habitat, migration and flight style, in contrast, do not exhibit significant correlation with wing shape in waterbirds. Although wing shape is critical to aerial flight function, its relationship to habitat and periodic locomotor demands such as migration is complex.

2.2 INTRODUCTION

Wing shape has long been known to exhibit a strong correlation with a generalized description of aerodynamic performance: long, narrow wings (high aspect ratio) characterize large-bodied gliding and soaring organisms, whereas short, broad wings (low aspect ratio) characterize smaller-bodied organisms with more maneuverable flight (Norberg 1990; Tobalske 2007; Alexander 2015). This general correlation between wing shape and aerodynamic function has also been found in every group of aerial or aquatic powered fliers, including cephalopods, insects, fishes, pterosaurs and bats, and has often been applied to airfoil design in mechanized flight (Da Vinci 1505; Norberg 1990; 1995; Hansen 2003; David Lentink and Biewener 2010; Martin-Silverstone et al. 2020). Despite the extensive body of work on bird flight and wing shape, we are only beginning to understand the complexity of biological wings, the relationship between their form and their function, and their evolutionary history.

Previous work has shown a strong relationship between avian wing shape and various aspects of flight function. Aspect ratio has a significant relationship with maneuverability, rapid takeoff and efficient gliding (Hartman 1961; Greenewalt 1975; Norberg 1990). Wingtip shape has proven to be significant with regards to dispersal ability, takeoff and flight performance, and

relative migration distance within species or between closely related species (Mulvihill and Chandler 1990; Lockwood et al. 1998; Combes and Daniel 2001; Swaddle and Lockwood 2003; Brewer and Hertel 2007; Claramunt et al. 2012; Minias et al. 2015). Wang and Clarke (2014; 2015) discovered that wing bone shape and wing outlines have a strong phylogenetic signal when examined in an evolutionary context; wing shape was more closely associated with clade membership than flight style. In addition, recent work across birds has linked wing length and beak morphology to feeding behaviors and ecological habitats (Pigot et al. 2020). These large-scale analyses show convergence as a common evolutionary pattern across birds, underscoring the need to carefully assess avian morphological traits against the phylogenetic and ecologic background of birds selected for study.

Waterbirds comprise a diverse assemblage for exploring patterns of morphological and ecological diversity. They include water-adapted species from three clades: Aequiornithines (diving birds, wading birds, shorebirds), Gruiformes (containing rails and cranes) and Anseriformes (ducks and geese) (Prum et al. 2015). With sufficient ornithological interest for their own focus group (e.g., Waterbird Society), waterbirds have been subject to extensive research including recent exploration of the genetic basis underlying interdigital webbing in their feet (Tokita et al. 2020). Waterbirds, known conclusively now to be representatives of at least three phylogenetic assemblages, are nonetheless united ecologically by their proximity to, and dependence on, aquatic or nearshore habitats that has led to convergence in morphology, trophic strategy and locomotor behavior. Recent work shows that waterbird wing shapes are diverse, occupying roughly half of total avian wing shape space (Wang and Clarke 2014; 2015). These studies, among the first to analyze avian wing shape within phylogenetic context, demonstrated that some traditional functional and ecological variables showed little correlation with wing

shape. This result runs counter to the idea that form and function are correlated. Thus, exploration of wing shape among the diversity of waterbirds may yield unexpected insights in the relationship between structure and function.

We began with the hypothesis that using landmark-based geometric, rather than simple linear, morphometrics to capture waterbird wing shape would yield clearer relationships to important ecological traits. And given that no single variable fully captures the complexity of avian lifestyle, we tested several: flight style, foraging behavior, habitat, migratory status, and migratory status categorized by geographic location. Flight style has previously been used to describe the wingbeat pattern used in horizontal flight, i.e., frequent flapping vs. gliding (Viscor and Fuster 1987). Foraging behavior better captures the range of different behaviors that may require more or less agility, for example plunge diving vs. dabbling. Habitat categories often reflect differences in air currents or foliage density, which again would draw upon wing function. Finally, migration variables are used here to capture how much a bird requires long distance migratory flights, and determine whether long migratory distances over land rather than ocean results in any wing shape differences.

Our central aim is to explore the relation between wing metrics and a variety of ecological variables in waterbirds, which exhibit diverse behaviors in a range of habitats. We test the hypothesis that wing shape and foraging behavior are strongly correlated (Higham 2007; Webb 1984) and the strength of the correlation between wing shape indices and migratory patterns. Using geometric morphometric data in the context of a well-resolved phylogeny (Hackett et al. 2008; Jetz et al. 2012), we also examine biomechanical traits such as the distribution of wing area, wing loading and wing aspect ratio. Finally, we look anew at

phylogenetic convergence of wing shape in the light of an integrated phylomorphospace and comparative approach.

2.3 MATERIALS AND METHODS

2.3.1 Specimen selection, phylogeny and ecological data sources

We analyzed wing images for 136 species of waterbirds from eight clades to search for correlation with ecological or behavioral traits (**Suppl. Table 2.1**). A diversity of wing shapes is represented (**Figure 2.1**). Penguins are excluded, because their wing feather morphology is too divergent for many of the measurements in this study (e.g., no clear distinction between primary, secondary and covert feathers) and because previous work has shown their wing outlines differ markedly from that of other birds (Wang and Clarke 2015). All included species are documented by an adult wing (dorsal view) in the Wing and Tail Image Collection of the University of Puget Sound's Slater Museum of Natural History (2011). All included wing images are preserved in the standard "spread wing" position.

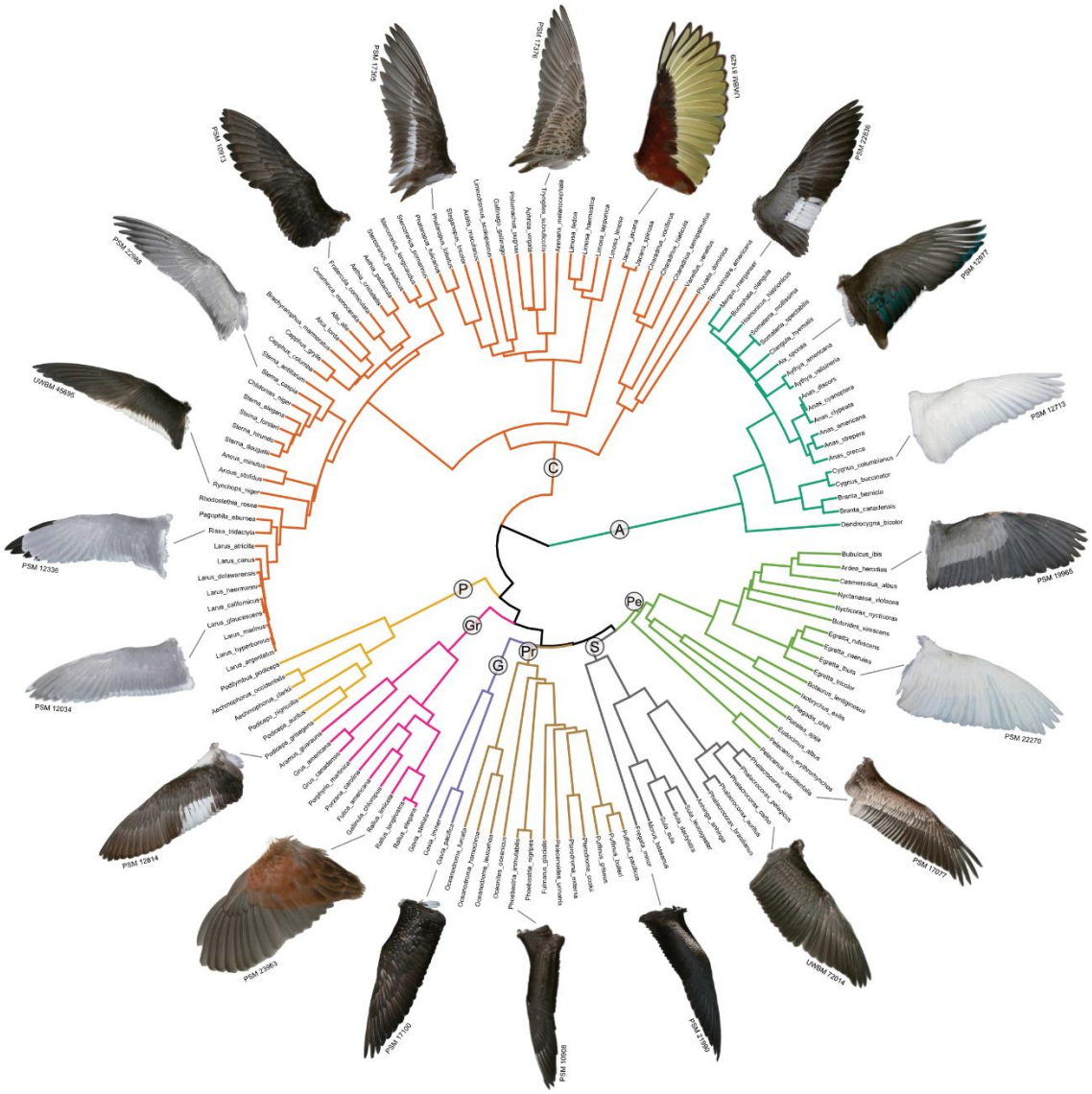

Figure 2.1 Waterbird wing shapes across the phylogeny with color-labeled clades: A, Anseriformes; C, Charadriiformes; P, Podicipediformes; Gr, Gruiformes; G, Gaviiformes; Pr, Procellariiformes; S, Suliformes; Pe, Pelecaniformes. Images reproduced with permission from the Puget Sound Wing and Tail Image Collection and the Burke Museum of Natural History and Culture.

Our phylogeny follows Pigot et al. (2020) in the use of the avian molecular tree of Jetz et al. (2012), the latter based on the earlier phylogenetic tree of Hackett et al. (2008). One thousand full molecular trees from the Hackett Sequenced Series were downloaded from BirdTree.org. A

maximum credibility tree was created from these 1000 trees with median node heights using TreeAnnotator from BEAST (Drummond and Rambaut 2007). The resulting tree contained a single negative branch length, which was converted to a branch length of 0.01. The tree was imported into R and pruned to our species with the *drop.tip()* function in the *ape* package (Paradis and Schliep 2019) for subsequent use in phylogenetic analyses.

We scored our sample of 136 waterbirds for body mass, phylogenetic relationships, and a suite of ecological traits including foraging behavior, habitat, and migration. For body mass we accessed data in Dunning Jr. (2007). We gathered ecological trait data from various traditional and recent compilations. “Flight style” came from Viscor and Fuster (1987) with species in our analysis coded according to their clade-level assignments. “Foraging behavior” was adapted from the “All About Birds” website (Cornell Lab of Ornithology 2015), *The Birder’s Handbook* (Ehrlich et al. 1988), and the Animal Diversity Web (Myers et al. 2020) (see “Terminology” in Suppl. text for list of terms). All terms were taken from the Cornell Lab of Ornithology, except "aerial hunter," which we use here to describe birds that hunt on the wing. Jaegers and frigatebirds, for example, prey on other birds in flight, and petrels often catch food on the wing rather than diving (Cornell Lab of Ornithology 2015). In both of these cases, significant time is spent in the air to catch prey. “Foraging niche” was defined and logged following Pigot et al. (2020). As we found no substantive differences between foraging niche and foraging behavior (**Suppl. Figure 2.2**), we used foraging behavior. “Habitat” data came from the Cornell Lab of Ornithology (2015), *The Birder’s Handbook* (Ehrlich et al. 1988), and the Animal Diversity Web (Myers et al. 2020).

“Migratory status” (full migrant, partial migrant, non-migrant) was obtained from the online *BirdLife International* database (2020). Most species in this compilation were logged as

full migrants or non-migrants. A single species, *Phalacrocorax carbo* (great cormorant), was registered as a third category, “partial migrant,” because only part of the population migrates. The majority of waterbirds have geographic ranges that were scored as either “continent-based” or “oceanic” using range maps from *BirdLife International* (2020). As a result, we scored our waterbirds for an additional variable that combines migratory status with geographic location. Only five species ranged across both continental and oceanic geography, and we scored these as “mixed range.” We combined these data with migratory status to generate our variable "Migration+Location" (i.e., continental migrant, continental non-migrant).

2.3.2 Digitization

To capture wing shape, wing images were digitized with a mixture of homologous and sliding semi-landmarks (**Figure 2.2**A for wing anatomy; **Figure 2.2**B for numbered landmarks). The trailing edge of the coverts was also included in wing shape, because overall covert shape was found to contribute significantly to wing shape disparity (Wang and Clarke 2015). The R package *StereoMorph* (Olsen and Westneat 2015; Olsen and Haber 2017) was used to digitize the images. Homologous landmarks (**Figure 2.2**B, larger red circles) include the anteroproximal point (approximate location of the humeral head), the anteriormost part of the wrist, the distal tips of the first five primary flight feathers, the division between primary and secondary flight feathers, the last secondary flight feather, the distalmost primary greater covert tip, the division between the primary and secondary greater coverts, and the last secondary greater covert. Six curves of sliding semi-landmarks (**Figure 2.2**B, smaller yellow circles) were created at the anterior edge of the wing (humeral head to wrist, wrist to distal tip of first primary flight feather), the posterior edge of the flight feathers (tip of fifth primary flight feather to tip of last primary

flight feather, tip of last primary flight feather to tip of last secondary flight feather), and the posterior edge of the greater coverts (distalmost tip of primary coverts to tip of last primary covert, tip of last primary covert to tip of last secondary covert). These points create the dataset for the whole-wing morphospace, subsets of which were used to calculate additional variables and morphospaces.

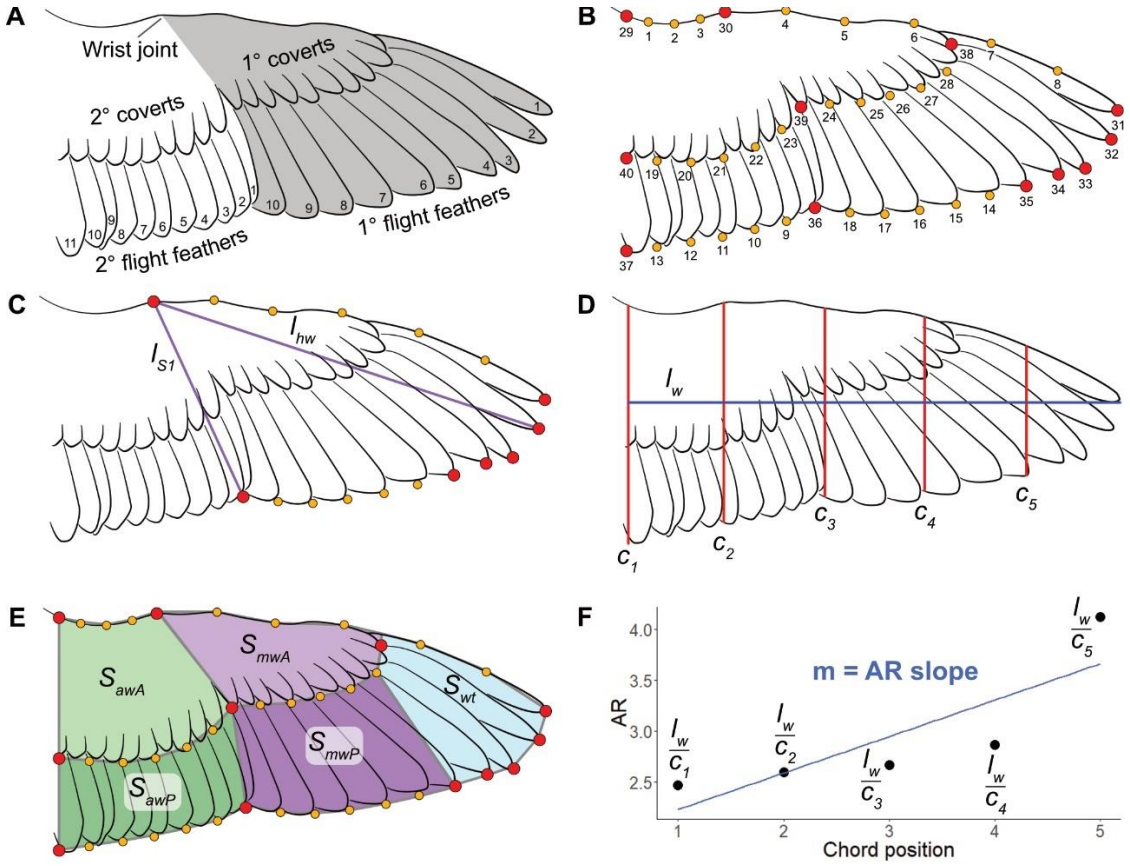

Figure 2.2 Landmark protocol for wings. A) Anatomy of a bird wing, handwing – grey portion, armwing – white portion; B) Numbered homologous landmarks (red) and sliding semi-landmarks (yellow); C) Subset of landmarks used for handwing morphospace, and measurements taken for hand-wing index calculations (purple, l_{S1} and l_{hw}); D) Wingspan (blue, l_w) chords (red,C_1-C_5) for AR distribution analysis; E) Wing area segments: anterior armwing (light green, S_{awA}), posterior armwing (dark green, S_{awP}), anterior midwing (light purple, S_{mwA}), posterior midwing (dark purple, S_{mwP}), wingtip (light blue, S_{wt}); F) Calculating slope for AR distribution of a wing.

2.3.3 Wing shape measurements and functional metrics

Wingspan, wing length, aspect ratio, wing area, wing loading, and pointedness of the wingtip (for symbols, see **Table 2.1**) comprise the most commonly used wing metrics for comparative functional analysis (Ellington 1984; Norberg 1990).

Table 2.1 Variables and abbreviations for wing and aerodynamic metrics (adapted from Norberg (1990).

AR = aspect ratio	l = length	Mg = body weight	S_w = area of one wing
wingspan, wingspread	l_{aw} = armwing length	m_w = mass of one wing	T_i = wingtip-shape index
wing chord	l_{hw} = handwing length	S = airfoil or wing area	T_l = wingtip-length ratio
mean wing chord	l_w = wing length	S_{aw} = armwing area	T_s = wingtip-area ratio
acceleration of gravity	M = body mass	S_{hw} = handwing area	WL = wing loading

We followed the terminology used in Norberg (1990): *wingspan, b,* is the distance between wingtips; *wing length, l_w,* is the distance from the shoulder joint to wingtip; *armwing length, l_{aw},* is the distance between the shoulder and wrist joints; and *handwing length, l_{hw},* is the distance between wrist joint and wingtip (**Figure 2.2**A). It is worth noting that ornithologists have often used 'wing length' as the measure from the wrist joint to the wingtip (equivalent to l_{hw}), because that has been the easiest measure to get from a museum specimen with a folded wing (Greenewalt 1962). Because we used spread wings, we can distinguish between the different regions of the wing.

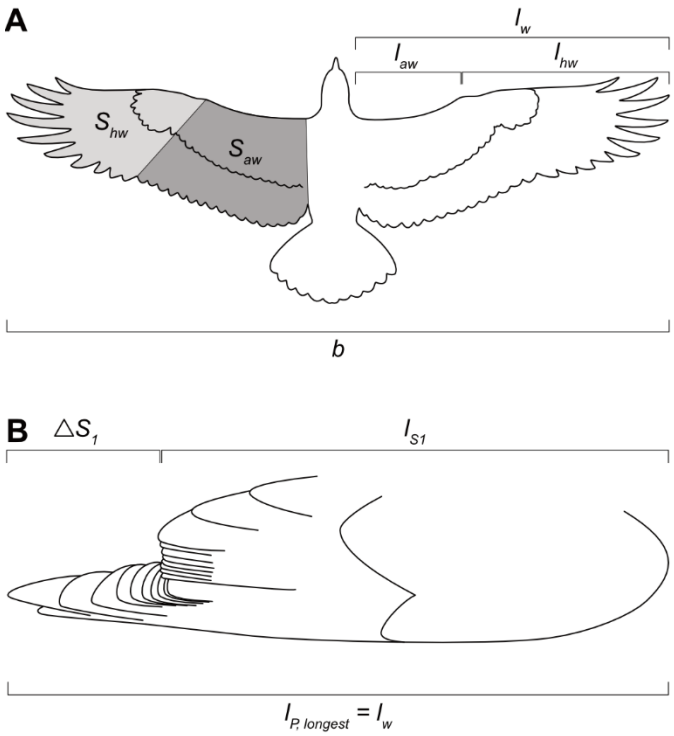

Figure 2.3 Wing measurements associated with flight performance. (A) Based on definitions in Norberg and Rayner (1987) and Norberg (1990). (B) Measurements on folded wings for Kipp's index (Lockwood et al. 1998), illustration adapted from Sibley (2018). Abbreviations: b, wingspan; l, length; S, area; $\boldsymbol{\Delta S_1}$, distance between longest primary and first secondary flight feathers.

Traditionally, aspect ratio is wingspan divided by mean chord, because the chord of a bird wing changes significantly over its length. However, most recent studies measure single-wing aspect ratio, as wing length squared divided by wing area (Norberg 1990). We followed that convention here as $AR = \frac{{l_w}^2}{S_w}$. We also developed an aspect ratio slope metric ("AR slope") using wing length and a series of five incrementally more distal chords to calculate an aspect ratio series along the wing. These points generated a linear regression (**Figure 2.2**F), from which was derived the AR slope. This metric measures the degree that aspect ratio changes along the length of the wing.

Airfoil area (S) refers to the lift-generating surface of an object (**Table 2.1**) (Norberg 1990). Single-wing area (S_w) refers solely to the area of one wing (Norberg 1990). Armwing area

(S_{aw}) is the area of the wing between the shoulder and wrist joints, which extends across the secondary feathers (**Figure 2.3**A), and *handwing area* (S_{hw}) is the area of the wing between the wrist joint and the wingtip, which extends across the primary feathers (**Figure 2.3**A) (Norberg 1990). Wing loading ($\frac{Mg}{S}$) is a measure of the force of body weight placed per unit of wing area (Norberg 1990). Pennycuick (2008) noted that wing loading needs to be calculated using total airfoil area (S), which includes the area of both wings and the body. This area represents the portion of the bird that is contributing to lift while gliding. Norberg and Rayner (1987) examined data from many birds and bats and found that the body area is approximately 20% of combined wing area. Because our dataset is composed of single wings, we approximated wing loading as $WL = \frac{Mg}{2S_w + (2S_w \times 0.2)}$ N·m^{-2}.

Handwing pointedness has been linked to flight performance and dispersal ability (Lockwood et al. 1998; Claramunt et al. 2012). "Kipp's distance" (ΔS_1) has been defined as the distance between the longest primary and secondary flight feathers, though has since changed to being the distance between the longest primary flight feather and first secondary flight feather: $l_w - l_{s1}$ (Kipp 1959; Lockwood et al. 1998; Claramunt et al. 2012; Sheard et al. 2020; Pigot et al. 2020), which is readily measured on the folded wings of museum specimens (**Figure 2.3**B). "Kipp's index" (I_K), or the "handwing index" (HWI), is a commonly used metric for wingtip shape. This index is often calculated as a proportion of Kipp's distance against the traditional wing length measurement: $I_K = \frac{l_w - l_{s1}}{l_w} \times 100$ (**Figure 2.3**B) (Lockwood et al. 1998; Baldwin et al. 2010).

WingMorph app for calculating functional metrics. We developed a Mac Xcode app called *WingMorph* (free for download; http://www.github.com/mwestneat/WingMorph) to calculate functional metrics for bird wings. The app imports the two-dimensional wing landmarks, from

which it computes functional metrics (wing spans, chords, aspect ratios, handwing index, regional wing areas, total wing area; **Figure 2.2**C-E) that are output as a trait matrix (.csv) file. The full set of wing metrics calculated for our waterbird dataset are available (Suppl. Table 2).

Morphometric analysis and phylogenetic comparative methods. The functional metric morphospace was calculated using aspect ratio, AR slope, wing area, wing loading, and handwing index. This data was size corrected by calculating the log shape ratios for wing area and wing loading, two variables strongly affected by body size. A single geometric mean was calculated between wing area and wing loading. Each of those variables was divided by that geometric mean, and those values were $\log_{10}$-transformed (Mosimann 1970; Price et al. 2019). Because each of the variables in morphospace use dramatically different ranges, each set of variables were z-scored for standardization before running the principal component analysis (PCA).

Geometric morphometric analysis was performed using the R packages *geomorph* (Adams et al. 2020) and *RRPP* (Collyer and Adams 2018; 2020), which included a General Procrustes analysis of coordinate data (used for standardizing landmark data in whole-wing and handwing data) and PCA to generate whole-wing and handwing morphospaces. The whole-wing morphospace was represented by the landmarks in **Figure 2.2**B, and the handwing morphospace was represented by a subset of those landmarks outlining the handwing, from the wrist, around the wingtip, to the last primary flight feathers (circles in **Figure 2.2**C). Wing area distribution data (calculated from polygons as presented in **Figure 2.2**E) were analyzed using PCA using the base *prcomp()* function (R Core Team 2020). *Phytools* (Revell 2012) was used for discerning phylogenetic signal (*phylosig()*, Pagel's lambda) and ancestral state estimation (discrete character: *reRootingMethod()*; continuous character: *contMap()*). The equal rates (ER) and

symmetric rates (SYM) models were recommended for *reRootingMethod()*(Revell 2012), and they had an equivalent log likelihood for this dataset, so the ER model was used in this analysis. *Ape* (Paradis and Schliep 2019) was used for setting up the phylogenetic tree, and *geiger* (Harmon et al. 2008) was used for phylogenetic analysis of covariance (*aov.phylo()*, 1000 simulations, Wilks test). Phylogenetic analysis of covariance was done with the first six PCs for whole-wing morphospace data (90.9% total variance) and with the first three PCs for handwing morphospace data (91.3% total variance). Data were plotted with *ggplot2* (Wickham 2016) and *plotly* (Sievert 2020), and phylomorphospaces were plotted using *ggphylomorpho* (Barr 2017). A few non-waterbird clades among our waterbird clades (Galliformes, Strisores, Columbaves, Inopinaves (=landbirds); following nomenclature of Prum et al. (2015)) are either arboreal or ground-dwelling. These birds were excluded so they would not introduce non-waterbird behaviors to the analyses.

Convergence in whole-wing shape among waterbirds was tested by using the R package *convevol* (Stayton 2015). We used the function *convratsig()* to test whether identified sets of tip species have converged more strongly on a region of morphospace than would be expected from that of a simulated null distribution. We used convergence measure C1, representing the proportion of the maximum distance between focal taxa that has been closed by evolution. For several larger groups of species, we also used the function *convnumsig()* to test whether the frequency of lineages independently evolving into a certain region of morphospace is significantly different from a simulated null distribution (convergence measure C5). Both tests were run with 1000 simulations. The *convnumsig()* function requires the number of species selected for comparison within a given group to be larger than the number of variables, in this case, PCs. As such, only the first five PCs were used for *convnumsig()* to enable tests for clusters

with six species or more. The *convratsig()* function does not have this restriction, allowing us to use ten PCs (~90% total variance) for clusters with 2-10 species and increase the robustness of the convergence analysis.

2.4 RESULTS

Our geometric morphometric analysis provided new information on wing shape and wing functional metrics in waterbirds. We found that whole-wing aspect ratio, wing area, wing loading, and body mass, are all significantly influenced by phylogenetic relationships (Suppl. Table 3). Our phylogenetic comparative analyses showed that wing shape in waterbirds is significantly associated with ecological traits, such as foraging behavior and habitat, but not with migratory behaviors. Phylomorphospace analysis revealed a strong phylogenetic pattern of repeated convergence in wing shape across waterbird clades.

2.4.1 Wing shape correlations with ecology and migration.

Results show a wide range of wing shapes in waterbirds, from short, broad low aspect ratio wings in the rail *Rallus limicola* (*AR* = 1.8) to long, slender, high aspect ratio wings in the albatross *Phoebastria immutabilis* (*AR* = 5.8) (**Figures 2.4-2.8**). Results show strong patterns of correlation between multiple wing metrics and ecological traits such as foraging behavior and habitat across the phylogeny of waterbirds. Some significant differences were found to be associated with taxonomic grouping as well, but there was no significant association of waterbird wing shape functional metrics with migratory status. Below is a summary of the functional metrics and discussion of key variables. We present the complete analysis of functional metrics and their ecological and migratory associations in the supplemental materials.

Both low and high aspect ratio wings appear to have evolved at least five times independently (**Figure 2.4**B). The waterbirds with higher aspect ratio wings tend to be plunge divers and aerial hunters (**Figure 2.4**, **Suppl. Figure 2.3**C), although albatrosses with very high aspect ratio wings dabble (surface skim or head submerged tipping downward) when they forage (**Figure 2.4**). Birds with lower aspect ratio wings tend to be probers and stalkers (**Figure 2.4**, **Suppl. Figure 2.3**C). Surface divers, ground foragers, and dabblers tend to have medium aspect ratio wings (**Figure 2.4**, **Suppl. Figure 2.3**C).

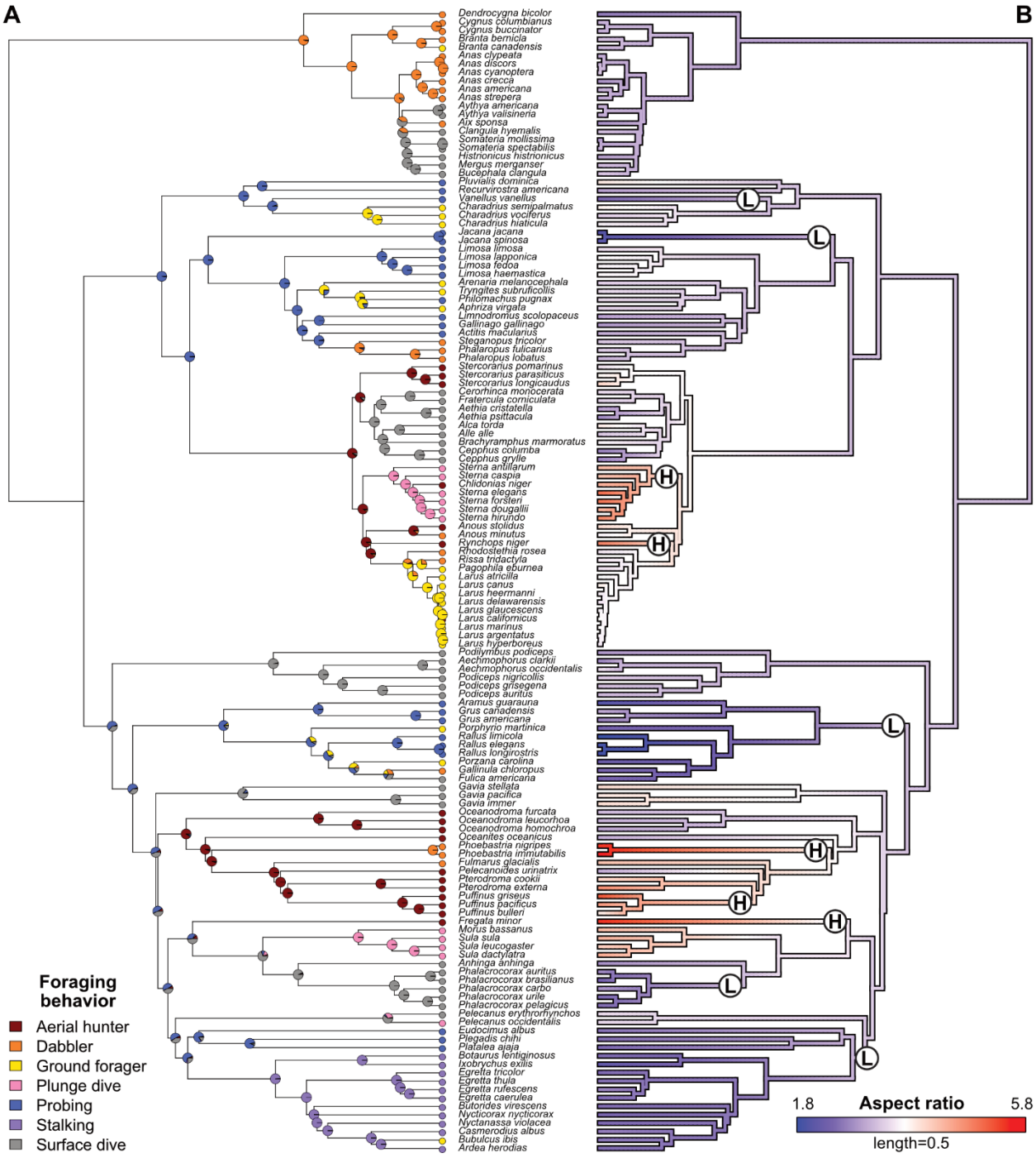

Figure 2.4 (A) Ancestral state estimation of waterbird foraging behavior. **(B)** Wing aspect ratio. Abbreviations: H, evolution of high aspect ratio wings, L, evolution of low aspect ratio wings.

Functional metrics plotted in morphospace suggest there exists significant overlap between major groups for foraging behavior and migration+location variables (**Figure 2.5**). The

loadings in **Figure 2.5**A and **Suppl. Table 2.4** shows that AR, AR slope, and HWI are positively correlated and provide most of the influence for PC1. Wing area and wing loading are also positively correlated and mostly influence PC2. The top left (low on PC1 and high on PC2) has birds with low aspect ratio wings and a low HWI. Moving towards the higher PC1 are birds with high aspect ratio wings and a high HWI. Birds with low PC2 values do not have a notably different AR than the birds with higher PCs, but it seems there is a complex interaction with wing area and/or wing loading to bring the species to the lower PC 2 values.

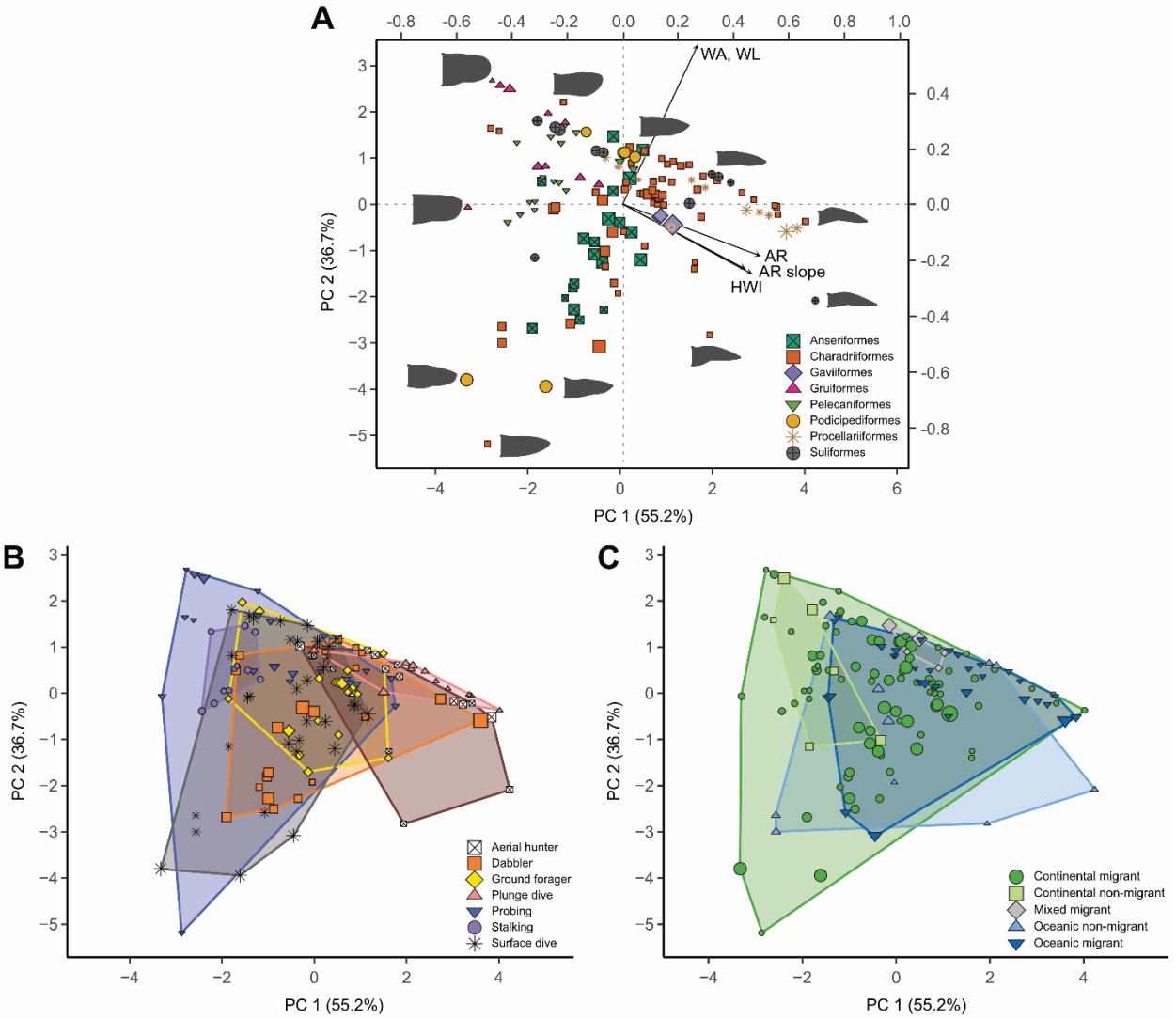

Figure 2.5 Morphospace of functional metrics: aspect ratio, AR slope, wing area (WA), wing loading (WL), and handwing index (HWI). **(A)** colored by taxonomy and includes loading plot,

(Figure 2.5 continued) **(B)** colored by foraging behavior, **(C)** colored by migration+location. Wing area and wing loading were corrected for size using Mosimann shape ratios, then all the variable distributions were standardized using z-scores before running the PCA. PCs 1-2 represent 91.9% of the total variance. Size of points indicates relative wing loading. Interactive plot in Suppl. Fig. 4.

2.4.2 Landmark-based morphospaces of waterbird wings

Whole-wing morphospace. Whole-wing morphospace shows some clustering by clade, whereas ecological specializations distinguish species from a central cluster that includes species with various behaviors in various habitats (**Figure 2.6**C-E). PC 1 and whole-wing aspect ratio are closely associated, boxplots following very similar trends for all phylogenetic and ecological categories (**Suppl. Figure 2.3**A-E, and **Suppl. Figure 2.4**A-E respectively; also **Suppl. Figure 2.6**A). This trend suggests that PC1 is driven largely by whole-wing aspect ratio, rather than body mass and wing loading traits (**Suppl. Figure 2.4**F-J). PC2 is an axis influenced strongly by the relative size of the armwing to the handwing, curvature of the leading edge of the wing (straight or curved), pointedness of the wingtip (rounded or pointed), and coverage of the primary coverts (more proximal or more distal) (**Suppl. Figure 2.6**B). The PC3 axis is influenced by coverage of the secondary coverts (anterior wing or extending to the trailing edge; **Suppl. Figure 2.6**C) and the curvature of the leading edge.

Considering whole-wing phylomorphospace by taxonomic group, Anseriformes, Gaviiformes, Pelecaniformes, Podicipediformes, and Suliformes score low and Charadriiformes high on PC 2 (**Figure 2.6**A-B). Gruiformes and Charadriiformes extend into lower PC 1 and PC 2 values, and Procellariiformes and Charadriiformes score high on PC 1 and PC 2 (**Figure 2.6**A-B). Different flight styles feature major overlap, with only gliding/soaring birds limited to high PC 1 values (**Figure 2.6**C). Foraging behavior is significantly correlated with whole-wing shape space (phylo-MANOVA: Wilks statistic = 0.178, p-value = 0.0170, **Suppl. Table 2.8**). Aerial

hunters and plunge divers are limited to higher PC 1 values, probing birds extend to lower PC 1 values, and the other foraging behaviors are more central (**Figure 2.6**D). The major habitat groups also feature a lot of overlap in the central region of wing morphospace (**Figure 2.6**E), with ocean, shoreline and a few marsh birds exhibiting higher PC 1 values. Marsh-dwelling birds also extend to lower PC 1 values. Migratory and continental birds occupy a huge range of wing morphospace (**Figure 2.6**F, G), whereas oceanic birds (migratory and non-migratory) are limited to higher PC 1 values (**Figure 2.6**G).

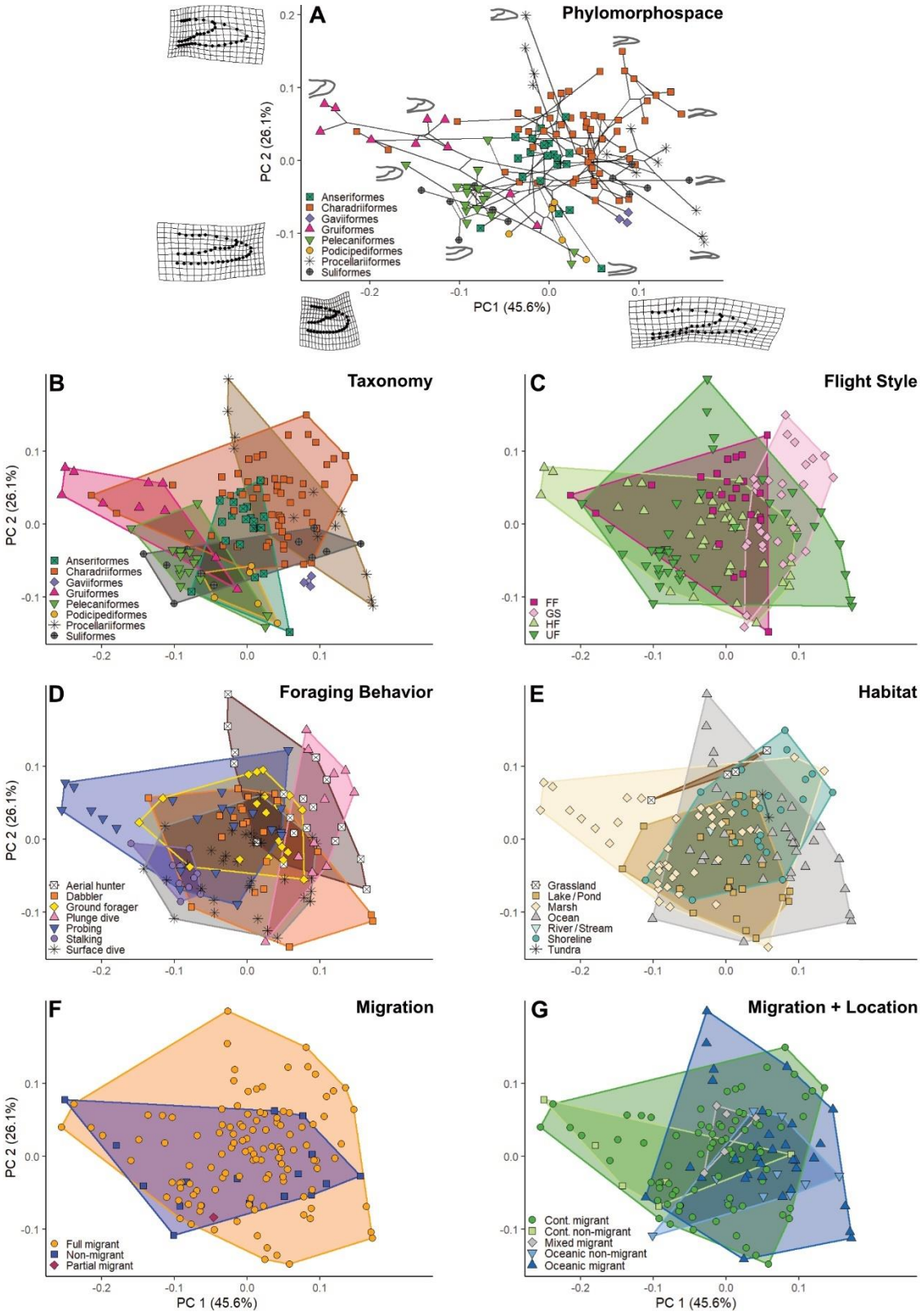

Figure 2.6 Whole-wing morphospace based on principal components (PC) 1 and 2, 71.7% of total variance. **(A)** Phylomorphospace with warp grids depicting wing shape at extremes of axes

(Figure 2.6 continued) and wing shapes of selected specimens. Subsequent morphospaces are colored for **(B)** major clades, **(C)** flight style, **(D)** foraging behavior, **(E)** habitat, **(F)** migration, and **(G)** migration + location. Abbreviations: FF, forward/bounding flight, GS, gliding/soaring flight, HF, high-frequency flapping flight, UF, undulating flapping flight. PC scores in Suppl. Table 2.7. Interactive plot in Suppl. Fig. 2.7.

Wing area morphospace. Like whole-wing morphospace, wing area morphospace shows a central cluster with some peripheral extensions. This analysis compares the distribution of the handwing to armwing areas, as well as the extent to which the dorsal greater coverts cover the wing surface. PC 1 (53.3%) represents the ratio between anterior and posterior armwing areas, with posterior armwing areas generating higher PC 1 values. PC 2 (34.4%) represents the change in relative wingtip area, with smaller wingtip areas generating higher PC 2 values.

Taxonomy provides the strongest separation between groups within wing area morphospace. Anseriformes, Gruiformes, Pelecaniformes and Podicipediformes compose the central cluster (**Figure 2.7**A, B). Charadriiformes are present in the central cluster but also extend into areas of higher (gulls and terns) and lower (a couple jacanas) PC 1 values. Suliformes are split between average and low PC 1 values. Procellariiformes and Gaviiformes tend to have high PC1 values. There is no major pattern in shape space with regard to flight style, although undulating flappers expand to fill the morphospace (**Figure 2.7**C). Considering foraging, aerial hunters have larger anterior than posterior wings with a range of wingtip sizes (**Figure 2.7**D). Some surface divers and a few probers have large posterior wing areas, a wing shape feature not observed in birds characterized by other foraging behaviors. Ocean-dwelling birds tend to have the widest range in morphospace (**Figure 2.7**E). The wing areas of other habitats largely overlap, although marsh-dwelling birds with small anterior and large posterior wing areas cluster together. Full migrants tend to have greater coverage of morphospace than non-migrants (**Figure 2.7**F). Oceanic migrants tend to have larger anterior than posterior wings

and exhibit a range of wingtip sizes (**Figure 2.7**G). Most categories (except mixed migrant) have representatives with larger posterior than anterior wing areas.

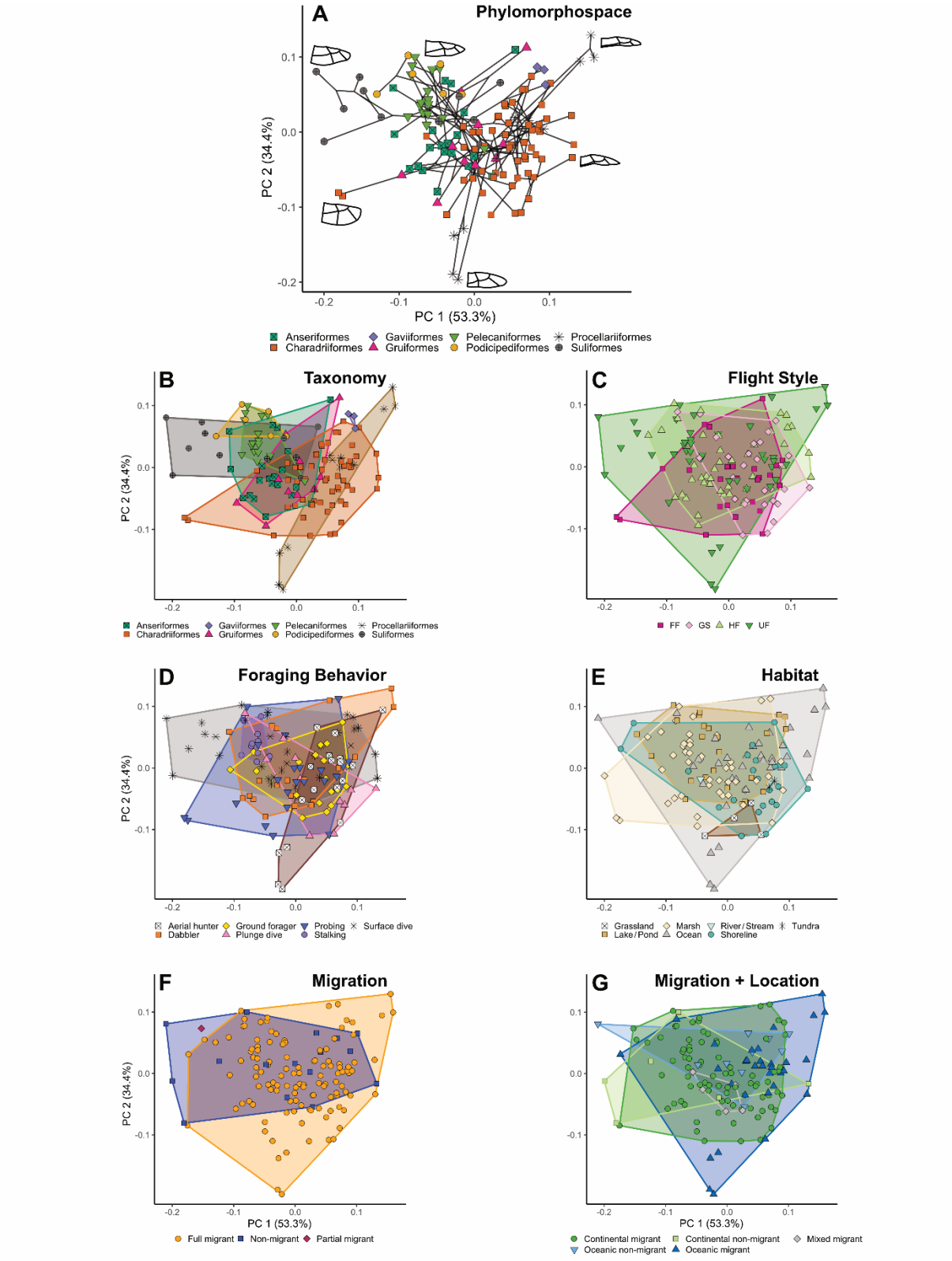

Figure 2.7 Wing-area morphospace based on principal components (PC) 1 and 2. **(A)** Phylomorphospace with icons depicting extremes of morphospace and wing area distributions of

(Figure 2.7 continued) selected specimens. Subsequent morphospaces are colored for **(B)** major clades, **(C)** flight style, **(D)** foraging behavior, **(E)** habitat, **(F)** migration, and **(G)** migration + location. Abbreviations: FF, forward/bounding flight, GS, gliding/soaring flight, HF, high-frequency flapping flight, UF, undulating flapping flight. PC scores available in Suppl. Table 2.9. Interactive plot in Suppl. Fig. 2.8.

Handwing morphospace. Handwing morphospace shows some clustering among the variables (**Figure 2.8**). PC 1 (69.0% of the variation) represents wing tip shape, and PC 2 (15.7% of the variation) records the location of the tip of the first secondary flight feather in relation to the wrist (inclined distally or proximally) and the curvature of the primary flight feathers (straight or curved trailing edge).

Phylogenetically, many of the same trends in the whole-wing morphospace are repeated in handwing morphospace (**Figure 2.8**A, B). Gruiformes and Pelecaniformes tend to have lower PC 1 values, Anseriformes average, and Procellariiformes high PC 1 values. Charadriifromes shows the greatest range in handwing morphospace, and two suliform clusters are on either side of the plot with both high and low PC 1 values. For flight style, forward/bounding flapping flight and gliding/soaring birds overlap very little, though they overlap with the high-frequency flapping and undulating flapping birds (**Figure 2.8**C). There is a lot of overlap within foraging behavior, aerial hunters and plunge divers tend towards the right and probing birds occupy the largest area of morphospace, and are the only ones expanding into the area with low PC 1 and PC 2 values (**Figure 2.8**D). Foraging behavior has a significant relationship with handwing morphospace (phylo-MANOVA: Wilks statistic = 0.369, corrected p-value = 0.032, **Suppl. Table 2.11**). Habitat morphospace does not differentiate clusters (**Figure 2.8**E). Unlike the other habitats, marsh-dwelling birds expand toward low PC 1 and PC 2 values. Habitat also shows a weakly significant relationship with handwing morphospace (phylo-MANOVA: Wilks statistic =

0.571, corrected p-value = 0.061, **Suppl. Table 2.11**). There is little difference in migratory versus non-migratory birds in wing morphospace (**Figure 2.8**F). Oceanic birds tend to have more pointed handwings than continental birds, which occupy a greater range in morphospace (**Figure 2.8**G).

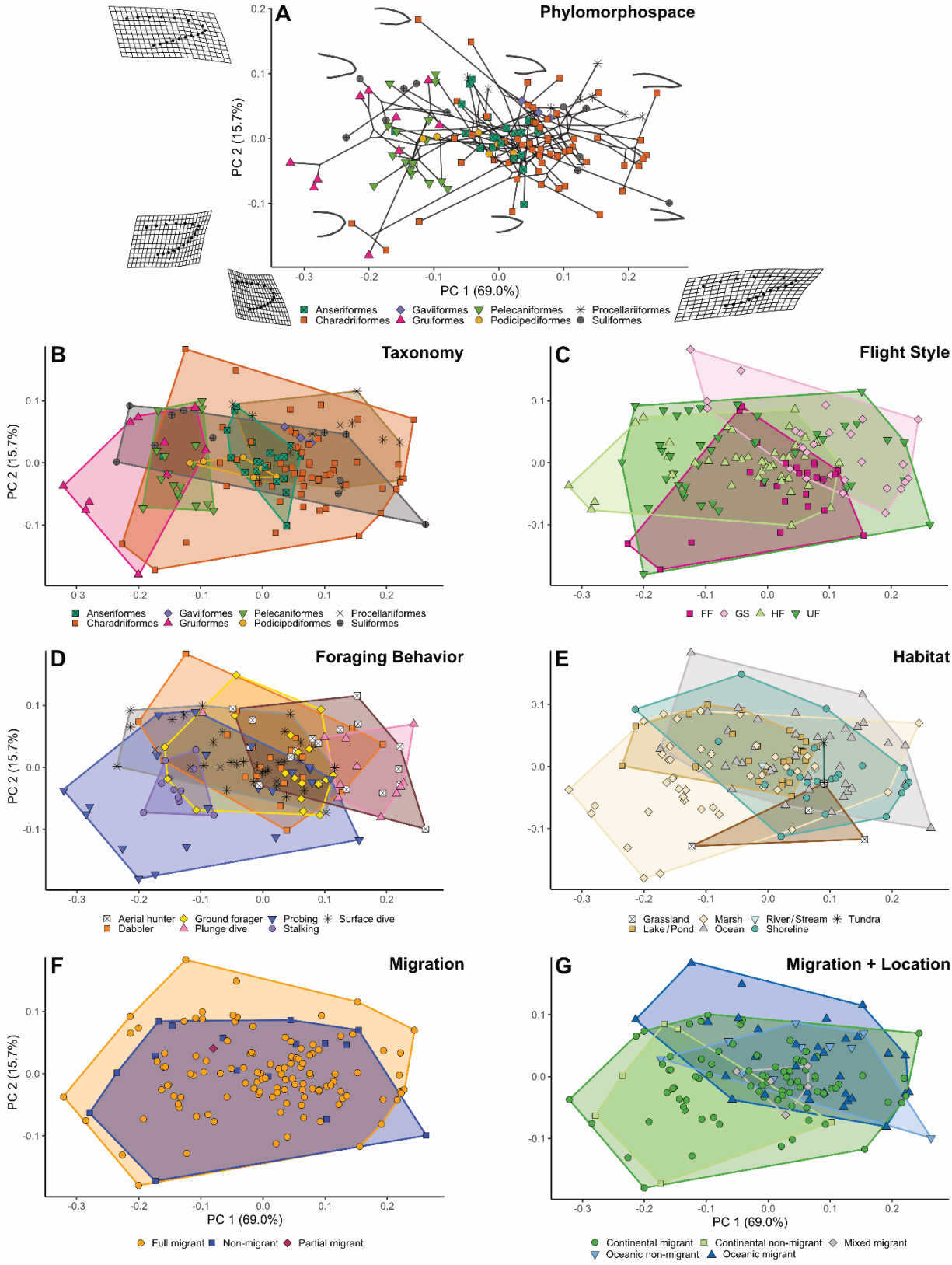

Figure 2.8 Handwing morphospace based on principal components (PC) 1 and 2. (A) Phylomorphospace with warp grids depicting extremes of axes and handwing outlines from

(Figure 2.8 continued) selected specimens. Subsequent morphospaces are colored for (B) major clades, (C) flight style, (D) foraging behavior, (E) habitat, (F) migration, and (G) migration + location. Abbreviations: FF, forward/bounding flight, GS, gliding/soaring flight, HF, high-frequency flapping flight, UF, undulating flapping flight. PC scores available in Suppl. Table. 2.10. Interactive plot in Suppl. Fig. 2.9.

2.4.3 Convergence in waterbird wing shape

When tested with a phylogenetic framework, wing shapes in waterbirds converged at statistically significant levels multiple times. We found significant convergence in whole-wing phylomorphospace among groups of waterbirds with high and with low wing ARs, among clusters of waterbirds with similar foraging behaviors and habitats as well as clusters with a variety of foraging behaviors and habitats (**Table 2.2**).

Table 2.2 Convergence testing in the eleven groups of waterbirds circled in Figure 2.9. C1 represents the amount of convergence in wing shape within a given area of morphospace (1 = high, 0 = low) and whether this value is significant given the phylogenetic relationships of the group. C5 was restricted to clusters of more than 5 species and calculates the number of times lineages represented by the selected cluster invaded the area of morphospace and whether that number is significant with relation to the group's phylogenetic relationships.

Group No.	C1		C5	
	Obs. C	P-value	Obs. C	P-value
1	0.625	< 0.001	6	< 0.001
2	0.458	< 0.001	10	0.009
3	0.625	< 0.001	6	< 0.001
4	0.489	< 0.001	---	---
5	0.501	< 0.001	---	---
6	0.554	< 0.001	---	---
7	0.335	0.018	---	---
8	0.495	0.011	---	---
9	0.340	0.053	---	---
10	0.080	0.385	---	---
11	0.458	0.011	---	---
12	0.391	0.047	---	---

Group 1: *Aramus guarauna*, *Jacana jacana*, *Jacana spinosa*, *Rallus elegans*, *Rallus limicola*, *Rallus longirostris*; **Group 2:** *Alca torda*, *Brachyramphus marmoratus*, *Cerorhinca monocerata*, *Fulmarus glacialis*, *Gavia immer*, *Gavia pacifica*, *Gavia stellata*, *Larus marinus*, *Sula*

(Table 2.2 continued) *dactylatra*, *Sula leucogaster*, *Sula sula*; **Group 3:** *Aechmophorus clarkia*, *Dendrocygna bicolor*, *Egretta rufescens*, *Phalacrocorax auritus*, *Phalacrocorax carbo*, *Podilymbus podiceps*; **Group 4:** *Aechmophorus occidentalis*, *Branta bernicla*, *Pelecanus erythrorhynchos*, *Pelecanus occidentalis*, *Podiceps grisegena*; **Group 5:** *Aethia cristatella*, *Cygnus buccinator*, *Cygnus columbianus*, *Podiceps auritus*, *Podiceps nigricollis*; **Group 6:** *Fregata minor*, *Pterodroma externa*, *Puffinus pacificus*, *Sterna elegans*; **Group 7:** *Aythya valisineria*, *Bucephala clangula*, *Pelecanoides urinatrix*; **Group 8:** *Charadrius vociferus*, *Oceanodroma furcata*; **Group 9:** *Arenaria melanocephala*, *Clangula hyemalis*; **Group 10:** *Anhinga anhinga*, *Bubulcus ibis*; **Group 11:** *Aethia psittacula*, *Branta canadensis*; **Group 12:** *Cerorhinca monocerata*, *Sula sula*.

Most of the groups in **Table 2.2** (circled in **Figure 2.9**) had significant C1 convergence in wing shape, indicating that the maximum phylogenetic distance represented by the clusters was greater than expected under the Brownian motion model of evolution. The larger groups (1-3) also featured highly significant C5 values, a statistic indicating that the selected organisms invaded that area of morphospace a greater number of times than would be expected under the Brownian motion model of evolution.

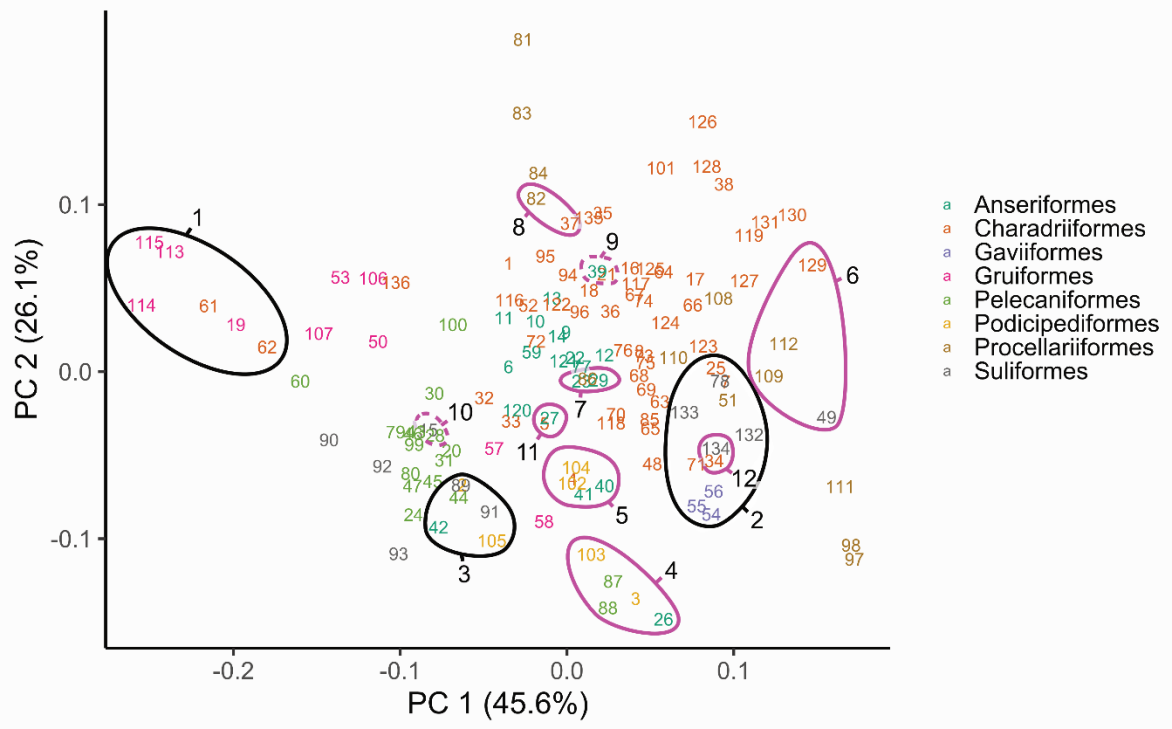

Figure 2.9 Testing wing shape convergence within whole-wing morphospace. Colored numbers refer to index of bird species in Suppl. Table 2.1. Large black numbers refer to group number in Table 2.2. Black lines indicate larger clusters for convergence testing with C1 and C5, magenta

(Figure 2.9 continued) lines indicate smaller clusters for convergence testing with C1. Solid lines indicate significant results, dotted lines indicate insignificant results.

Overall, most groups tested here resulted in significant convergence in wing shape in multiple regions of morphospace. Clusters of species that occupied the regions of morphospace and share similar foraging behaviors and/or habitats had significant convergence (Groups 1, 2, 3, 6, 12). Regions with clusters of species featuring different foraging behaviors and habitats were also significantly convergent (Groups 4, 5, 7, 8, 11) We also located a few pairs that were close in morphospace, but were phylogenetically close enough such that they were not significant in terms of evolutionary convergence (Groups 9, 10): a ground-foraging turnstone and a surface-diving duck have 34.0% convergence on medium aspect ratio wings with a curved leading edge and pointed wings (Group 9: C1 p = 0.053, **Table 2.2**; **Figure 2.9**), and a surface-diving darter and a ground-foraging egret have 8.0% convergence on medium aspect ratio wings with pointed wingtips and a curved leading edge (Group 10: C1 p = 0.385, **Table 2.2**; **Figure 2.9**).

2.5 DISCUSSION

The wings of waterbirds are highly diverse in size and shape. They show a broad range when scored for important functional metrics that characterize their functional diversity and evolutionary history. The central conclusion of this study is that important wing metrics such as aspect ratio, wing areas and wing loading are significantly associated with the trophic ecology and specific habitat traits in waterbird taxa. We also conclude that migratory behavior is not strongly correlated with wing shape in waterbirds from three major avian clades, despite a general correlation between handwing index and migratory behavior among birds (Dawideit et al. 2009; Sheard et al. 2020). Finally, we have identified multiple regions of phylomorphospace

showing convergence in waterbird wing shape. Thus, particular wing shapes appear to be well-suited for survival and reproduction in coastal and aquatic birds.

2.5.1 Trends in waterbird wing shape and ecology

Aspect ratio, a frequently used functional metric when studying flight function (Greenewalt 1962; Norberg 1990), is measured as a single- or double-wing variable, the latter two times the value of the former metric and calculated from the square of total wingspan tip-to-tip divided by sum of the area of both wings (Walker and Westneat 2002). The single-wing AR range among waterbirds (1.8-5.8) is similar to that in other broad-based avian datasets, such as Baliga, Szabo, and Altshuler (2019; AR 1.7-5.4) and Wang and Clarke (2014; AR 2.5-8.1) for wider phylogenetic samples of birds, and those of bats (AR 2.2-4.3; Luo et al. 2019), insects (2.3-8.0; Bhat et al. 2019) and even fishes with flapping underwater flight (AR 1.9-4.3; Thorsen and Westneat 2005). The waterbird ecotypes with the highest aspect ratios are aerial hunters and plunge divers, while those with the lowest AR are the probers. Both procellariiforms and suliforms exhibit a wide range of aspect ratios for a wide range of ecological strategies. Most procellariiforms are ocean-dwelling aerial hunters. They are characterized by a broad range in aspect ratio and whole-wing shape space to accommodate a range of locomotor demands on the wing. Suliformes, in contrast, is divided into two distinct clusters, one with wings of medium aspect ratio (surface-diving cormorants) and another with wings of high aspect ratio (plunge-diving gannets). Procellariiforms exhibit a variety of wing shapes for a given foraging behavior, whereas suliforms have two distinct foraging behaviors and two disparate and extreme areas of wing shape space.

AR slope identifies procellariiforms as having the greatest range in wing shape change along the length of the wing. Some procellariiform wings (petrels) taper much faster than others

(albatrosses), which may be related to the specific aerodynamic requirements for different foraging behaviors (aerial hunting versus dabbling). Most other waterbird clades have a small range of AR slope (excluding charadriiform outliers), suggesting that wing taper is a relatively conservative trait in most birds.

Although the denominator in calculating aspect ratio, wing area can be plotted separately. Waterbirds that spend a lot of time flapping (either forward/bounding or high-frequency) have a narrow range of lesser wing area, suggesting that smaller wings may be an adaptation for less stressful, repetitive movement. Gliding/soaring birds and undulating flappers have a higher average and range of wing areas, underscoring the importance in higher wing area and its variation. Wing area did not differ significantly between gliding/soaring waterbirds and those with undulating flight, and so wingbeat frequency may have less influence over the wing area. No specific wing area seems optimal for any particular variable, as wing area morphospace overlap among variables is substantial. As an example, procellariiforms occupy a very localized region of wing area space, which may be the result of the constraints from aerial hunting or from the long bouts of flight required by their oceanic habitat (Warham 1977). On the other hand, the brent goose (Anseriformes: *Branta bernicla*) and sandhill crane (Gruiformes: *Grus canadensis*), which are relatively large birds with long necks that remain extended in flight and travel long distances during migration (Cornell Lab of Ornithology 2015), seem to converge on wing area distributions at the top of the wing area morphospace (**Figure 2.7**).

Wing loading is another key parameter yielding insight into the structure and function of wings for flight (Vágási et al. 2016). Wing loading is not tied to a particular wing shape (Suppl. Fig 10), but rather to the functional demands of the bird. Within a study examining European species, some birds are found to have a low wing loading that optimizes cost of transport for long

distances, whereas other birds have high wing loading that optimizes speed at the cost of energy efficiency (Vágási et al. 2016). The birds with the highest wing loadings in our waterbird dataset are ducks, loons, and grebes, birds that forage by dabbling and surface diving in lakes/ponds and use high-frequency flapping to get aloft. Loons and grebes are diving birds that have reduced skeletal pneumaticity to increase skeletal density (P. M. O'Connor 2009), which in turn increases wing loading during flight. In contrast, birds that glide and soar have greater skeletal pneumaticity (P. M. O'Connor 2009; Smith 2012), reducing body mass and thus wing loading.

Wing kinematics and wing morphing during flight affects wing loading (Taylor et al. 2012; Harvey et al. 2019), an important frontier in flight biomechanics. Although presented for uniformity in a single outstretched pose, avian wings have a number of components that may be adjusted during flight. Wing shape changes at different flight speeds (D. Lentink et al. 2007; Tobalske 2007). Feathers spread farther apart at slower flight speeds, increasing wing area and vice versa (Tobalske 2007). If one assumes a given bird has a constant body mass, the foregoing necessarily means that wing loading must vary with flight speed. In our study wing shape is static as in the studies we have extensively cited (Lockwood et al. 1998; Wang and Clarke 2015; Pigot et al. 2020). How wing shape varies during flight across birds is an intriguing question for future research.

2.5.2 Wing shape and migration

Most of the birds we sampled (120 species, 88%) are regarded as full migrants; only 15 species are logged as non-migrants and 1 as a partial migrant. We could not distinguish any patterns in wing shape that would distinguish migratory versus non-migratory waterbirds at this scale. The combination variable migration+location , however, shows weak significance with respect to

handwing index (HWI), which is commonly used for wingtip shape (Wilks statistic = 7.278, p = 0.0510). The relationship between migratory behavior, morphology and physiology is complex (Piersma et al. 2005). Migratory patterns are known to vary within genera and sometimes within species (Berthold and Terrill 1991; Lockwood et al. 1998; Fernández and Lank 2007). For example, the rail genus *Rallus* includes the non-migrant *Rallus longirostris* as well as the full migrants *R. elegans* and *R. limicola*. Likewise, the cormorant genus *Phalacrocorax* includes the non-migrants *P. brasilianus* and *P. urile*, the partial migrant (some populations migrate, some do not) *P. carbo*, and the full migrants *P. auritus* and *P. pelagicus*. Despite stark differences in migratory behavior, these birds occupy the same region of morphospace (**Figure 2.6**).

Many aspects of avian biology and behavior influence wing shape, introducing some plasticity in shape at all taxonomic levels. For example, the wing shape of western sandpipers (*Calidris mauri*) varies depending on sex and maturity (Fernández and Lank 2007). Females migrate longer distances than males, and males have to perform aerial displays to attract the females. Therefore, the female wing is longer and more pointed than the wing in males. For rapid escape, immature sandpipers require shorter, rounder wings than adults. Two species of the finch genus *Carduelis* exhibit different wing shapes, the insular non-migrant Corsican finch (*C. corsicanus = C. citrinella corsicanus*) with more rounded wings than the migrant citril finch (*C. citrinella = C. citrinella citrinella*) from the mainland (Förschler et al. 2008; Gill et al. 2020). Although the wing shape differences between these finches match expectations given their migratory patterns, their daily locomotor needs may also explain this difference; the insular *C. corsicanus* must navigate dense foliage compared to its mainland counterpart (Förschler et al. 2008). Among our rail species in the genus *Rallus, R. longirostris* and *R. elegans* are similar in size and wing shape, but the former is non-migratory and the latter migratory (Cornell Lab of

Ornithology 2015; BirdLife International 2020). Some birds alter migratory habits over the course of a few generations (Berthold and Terrill 1991). Our results suggest that migratory behavior is one factor among many that influence wing shape as shown in previous studies (Mönkkönen 1995; Baldwin et al. 2010; Huber et al. 2017).

2.5.3 Evolutionary convergence across phylomorphospace

Four general patterns emerge from our metric consideration of wing form across birds. First, phylomorphospace plots indicate the presence of a significant phylogenetic component to many aspects of avian wing morphology (Wang and Clarke 2015; Pigot et al. 2020). Thus, clade membership has some predictive value with regard to wing morphology.

Second, most sampled waterbirds cluster in the centroid of distribution for a range of wing metrics. These waterbirds are characterized by a wide range of locomotor, foraging and migratory behaviors and ecological habitats. Thus, the sweet spot of wing morphospace among waterbirds is occupied by distantly related taxa with disparate functional, behavioral and ecological traits. Similar to limb morphospace for disparate clades among rodents, outliers in morphospace are limited to extreme morphologies, such as the limbs of fossorial taxa (Hedrick et al. 2020).

Third, a few avian subgroups did plot in relatively extreme wing morphospace, such as the low aspect ratio wings of the probing jacanas and rails and the high aspect ratio wings of aerial and plunge diving specialists (terns, gannets and petrels). In these cases, therefore, wing morphology seems strongly linked to their specialized lifestyles, unlike the vast majority of birds occupying the center of morphospace where aerodynamic factors rather than disparate functional and ecological traits govern wing morphology.

Collectively, these conclusions highlight the prevalence of convergence in wing shape phylomorphospace across waterbirds. We identified and tested 12 likely instances of wing shape convergence. The selected clusters included areas with high and low AR wings in pairs and larger groups of taxa and sampled the majority of waterbird phylomorphospace. Ten out of twelve of these groups were highly significant examples of convergence on similar wing shape from distant ancestral starting points (**Table 2.2**). Convergence in form among flapping appendages is a major evolutionary pattern in organisms as diverse as birds (Norberg 1986; 1990), bats (Norberg 1986), insects (Strauss 1990) and bony fish (Aiello et al. 2017).

Several of the convergent clusters share foraging behavior or habitat, supporting the hypothesis that there is an optimal wing shape for a given behavior or habitat. Jacanas (Charadriiformes), rails and the limpkin (Gruiformes) show an average of 62.5% convergence on very low aspect ratio wings with rounded wingtips and a slightly larger handwing than armwing (Group 1: C1 p = 0; **Figure 2.9**, **Table 2.2**). The species in this cluster transitioned into this space six times, significantly more than would be expected by chance (C5 p = 0, **Table 2.2**). Loons (Gaviiformes) also appear to converge in wing shape with gannets and boobies (Suliformes: Sulidae) (Group 2: **Figure 2.9**, **Table 2.2**) in a region of morphospace shared with a procellariiform (*Fulmarus glacialis*) and a few charadriiforms (*Brachyramphus marmoratus*, *Cerorhinca monocerata*, *Larus marinus*). This group averages 45.8% convergence on high aspect ratio wings with somewhat pointy wingtips, a relatively straight edge and a relatively larger armwing than handwing (C1 p = 0). The species in this cluster transitioned into this morphospace 10 times, significantly more than would be expected by chance (C5 p = 0.009, **Table 2.2**). Within this cluster, the charadriiform, the rhinoceros auklet (*Cerorhinca monocerata*), and red-footed booby (*Sula sula*) share 39.1% convergence (Group 12: C1 p =

0.047, **Table 2.2**; **Figure 2.9**). Another cluster of waterbirds with high aspect ratio wings (Group 6: frigatebird, petrel, shearwater, tern) averaged 55.4% convergence (C1 p = 0, **Figure 2.9**).

Other convergent clusters are composed of waterbirds with a range of behaviors and habitats, suggesting wing shapes may be employed in multiple behaviors and habitats with only extreme wing shapes tied to extreme behaviors and habitats. For example, two pelecaniforms (*Pelecanus erythrorhynchos, Pelecanus occidentalis*), an anseriform (*Branta bernicla*), and two podicipediforms (*Aechmophorus occidentalis, Podiceps grisegena*) averaged 45.8% convergence on medium aspect ratio wings with rounded wingtips and a much larger armwing than handwing (Group 4: C1 p = 0, **Table 2.2**; **Figure 2.9**). Swans, an auklet, and grebes averaged 50.1% convergence on medium aspect ratio wings with a straighter leading edge, a slightly rounded wingtip, and slightly larger armwings than handwings (Group 5: C1 p = 0, **Table 2.2**; **Figure 2.9**). Two anseriforms (*Aythya valisineria* and *Bucephala clangula*) and a procellariiform (*Pelecanoides urinatrix*) averaged 33.5% convergence on medium aspect ratio wings with slightly pointed wingtips and a comparatively similar handwing to armwing (Group 7: C1 p = 0.018, **Table 2.2**; **Figure 2.9**). A ground-foraging charadriiform (*Charadrius vociferus*) and an aerial-hunting procellariiform (*Oceanodroma furcata)* averaged 49.5% convergence on medium aspect ratio wings with very pointed tips and a much larger handwing than armwing (Group 8: C1 p = 0.011, **Table 2.2**; **Figure 2.9**).

Table 2.3 'Group 4' waterbirds showing convergence in wing morphospace.

Species	Taxonomy	Flight Style	Foraging Behavior	Habitat	Body Mass (kg)	Aspect Ratio	Wing loading ($N \cdot m^{-2}$)
Pelecanus erythrorhynchos	Pel.	GS	Surface dive	Lake/Pond	4.970	2.1	87.4
Pelecanus occidentalis	Pel.	GS	Plunge dive	Ocean	3.702	2.4	81.8
Aechmophorus occidentalis	Pod.	HF	Surface dive	Lake/Pond	1.429	1.6	203.5
Podiceps grisegena	Pod.	HF	Surface dive	Lake/Pond	1.023	3.3	167.2
Branta bernicla	Ans.	FF	Dabble	Marsh	1.370	1.7	153.7

Abbreviations: ***Taxonomy*** Pod., Podicipediformes, Ans., Anseriformes, Pel., Pelecaniformes. ***Flight Style*** HF, High-frequency flapping, FF, forward/bounding flight, GS, gliding/soaring flight.

Group 4 waterbirds (**Table 2.3**), which include two pelicans (*Pelecanus),* two grebes (*Aechmophorus occidentalis, Podiceps grisegena)* and the brent goose (*Branta bernicla*), differ markedly in behavior, habitat and overall morphology. This disparate cluster of species is an example of convergence with no basis in the ecological or functional variables examined in this study. The pelicans glide and soar, the grebes use high-frequency flapping, and the brent goose employs forward/bounding flapping flight. Regarding foraging behaviors, the pelicans plunge (*P. occidentalis*) and surface dive (*P. erythrorhynchos*), the grebes surface dive, and the brent goose dabbles. Regarding habitats, pelicans live near lakes and ponds (*P. erythrorhynchos*) and oceans (*P. occidentalis*), the grebes live near lakes and ponds, and the brent goose prefers marshes. In size they range from medium to the high end of body mass range (1-5 kg). Birds with similar wing loading are present across wing morphospace (**Suppl. Figure 2.10**).

Very few regions of whole-wing morphospace are truly dominated by a specific behavior or habitat. The highest aspect ratio wings characterize oceanic birds that glide and soar, and the lowest aspect ratio wings are found in birds that hunt from the ground in more enclosed habitats.

In between these extremes, wing shapes have evolved convergently and are used in a variety of behaviors and habitats. It appears waterbirds are broadly adapted to more open habitats with wing shapes that serve multiple lifestyles and at least partially overlap in morphospace with birds in terrestrial habitats (Wang and Clarke 2015).

2.6 CONCLUSION

Avian wings are appendages of great functional importance to birds and show great shape diversity, ranging from those of high to low aspect ratio and those with rounded or pointed wingtips. Yet it has proved challenging to find significant and regular correlation across birds between wing shape and flight style or various ecological traits. In this study, we examined multiple functional and ecological variables, determining that wing shape and foraging behavior are significantly correlated in waterbirds. In contrast, flight style, habitat and migratory status are not correlated, although combining migratory status and location (continental vs. oceanic) shows weak correlation. Phylogenetic signal, as shown in previous studies, is prevalent, such that wing shape within clades exhibited similarity. Nevertheless, the central morphospace for most traits shows broad overlap of unrelated taxa. This work highlights the complexity in correlating wing shape to aerodynamic performance as well as a number of non-aerodynamic variables. The current study and its forerunners are based on static (spread) wing shape, leaving open for future research considering wing shape as a dynamic variable that changes with flight speed.
(Sibley 2018)

CHAPTER 3

Three-dimensional avian sternum morphology and implications for ecology

In collaboration with Leon P.A.M. Claessens

S.L.B. and L.P.A.M.C. devised the project, L.P.A.M.C. provided the sternum models made by former undergraduate students, S.L.B. wrote the R code and ran the analyses, S.L.B. made the figures, S.L.B. wrote the manuscript with critical feedback from L.P.A.M.C.

3.1 ABSTRACT

The avian sternum, which provides anchor to the main flight muscles, varies greatly in morphology. Some birds have long, narrow sternal plates with deep keels, whereas others have nearly square sternal plates with shallow keels or even a smooth ventral surface. The relationship between sternal shape and ecology has yet to be thoroughly studied. We capture shape in a broad sample of 128 avian sterna using three-dimensional (3D) geometric morphometrics to examine relationship between sternal form and function. General Procrustes Analysis and Principal Component (PC) Analysis were used to examine the sternal plate morphology. PC1 ranges between a square sternal plate and a shallow keel (e.g., pelicans, cormorants) and a long, narrow sternal plate with a deep keel (e.g., turkeys and doves). PC2 is also influenced by the keel and lateral margin, with high PC2 values having short lateral margins (e.g., pigeons) and low PC2 values having long lateral margins (e.g., rails and tinamous) PC3 is most influenced by the keel, and the hoatzin and kiwi have the highest PC3 values. A 3D plot of these PCs shows that phylogeny is the predominant factor driving most of the clustering. Bird sterna have also been found to converge on similar shapes multiple times. These observations suggest that sternal

shape is not rigidly constrained by flight behavior or phylogenetic proximity such that some sternal shapes accommodate different flight behaviors and distant phylogenetic relationship.

3.2 INTRODUCTION

The sternum is a key structure used in powering both flight and respiration (Brocklehurst et al. 2019; Claessens 2009), which should constrain the structure of the sternum to the needs of both major functions. However, the sternum varies greatly in shape throughout Aves, and, paired with a wide range in flight styles and body masses, this variation suggests that biomechanical factors play a role in how birds fly and breathe that influence diversity in sternum shape. Here we focus on the degree to which sternum morphology correlates with flight. We examined the relationship between form and function regarding the avian sternum by exploring the morphospace created by three-dimensional landmarks and compared morphology against flight style data. We hypothesize that sternum shape will be highly influenced by phylogeny but will also correlate with flight style (following terminology of Viscor and Fuster (1987)).

The basic anatomy of an avian sternum is as follows (**Figure 3.1**): in the anterior region of the sternum, a pair of craniolateral processes project anterolaterally. Running ventral and medial to these are a pair of coracoid grooves, the articulation points of the coracoids which make up the ventral supports of the shoulder girdle. At the midline of the anterior margin, a rostral spine juts out. Costal processes line the anterior region of the lateral margin and vary in number from 3-9. The sternal plate can have lateral processes (or trabeculae) which support a cartilaginous membrane between them, reducing bone material in the posterior region of the sternum. Some species have no additional processes and a solid plate of bone, some species have a pair of lateral processes. Some species have two sets of lateral processes, either designated as lateral and medial processes (Baumel and Witmer 1993) or thoracic and abdominal processes

(Ghetie et al. 1976). The processes can sometimes fuse to the sternal plate, creating openings in the plate which are often slightly asymmetric. The keel extends ventrally from the midline of the ventral surface of the sternal plate.

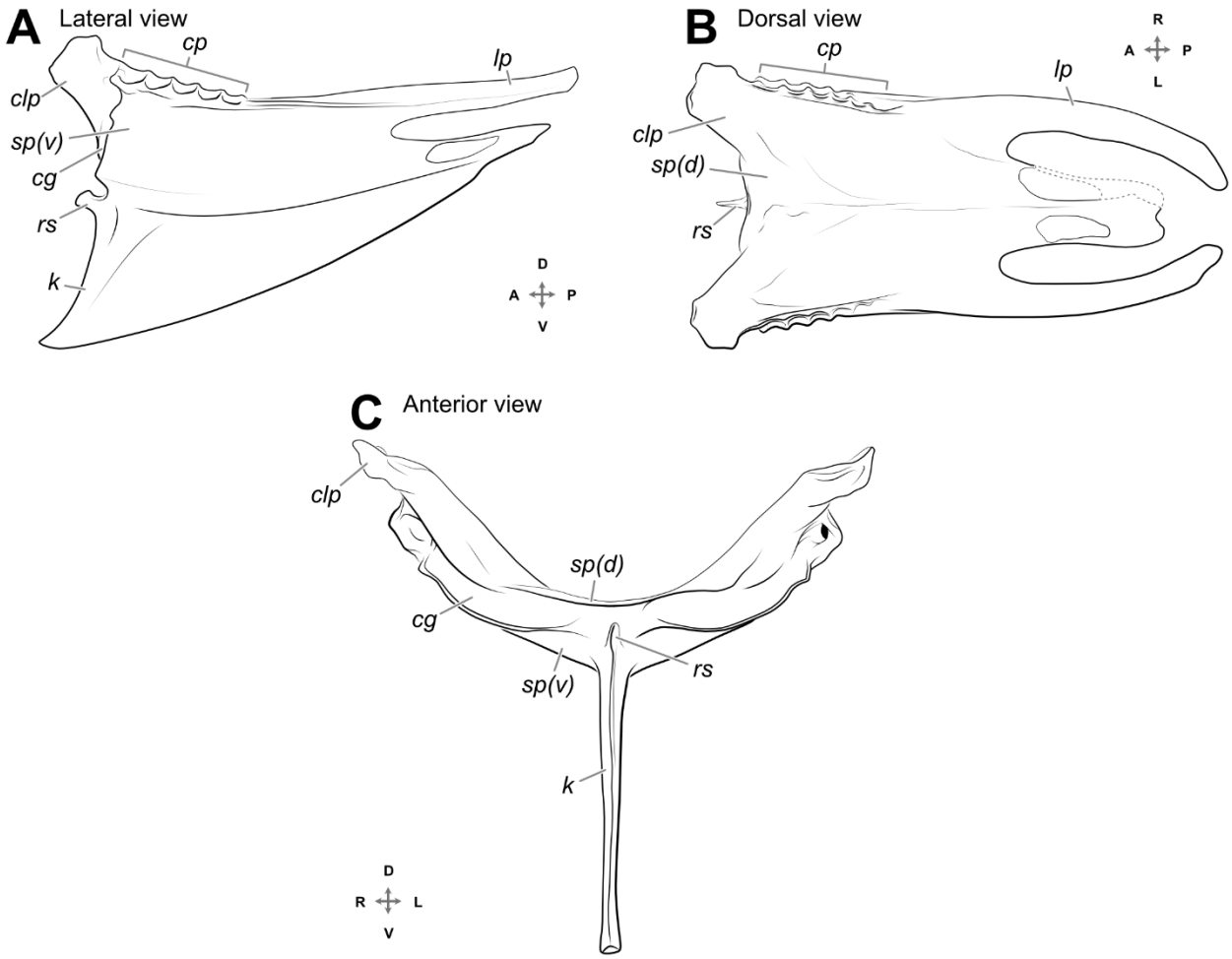

Figure 3.1 Basic anatomy of an avian sternum, as illustrated by the Western Rockhopper Penguin, *Eudyptes crestatus* (MCZ 346428). Abbreviations: cg, coracoid groove; clp, craniolateral process; cp, costal processes; k, keel; lp, lateral process; rs, rostral spine; sp(d), sternal plate, dorsal side; sp(v), sternal plate, ventral side.

The major flight muscles are anchored on the sternum or associated areas. The pectoralis powers the downstroke and originates along the keel of the sternum, the posterior margin of the sternum, the posterior lateral process, the dorsal surface of some ribs, and the furcula (Raikow

1977). The pectoralis inserts on the deltopectoral crest. The supracoracoideus powers the upstroke and originates on the sternum deep to the pectoralis, loops around to the back of the humerus where it inserts on the anteromedial surface of the humerus proximal to the deltopectoral crest (Raikow 1977). The sternocoracoideus connects the coracoid to the craniolateral process of the sternum and is one of the first muscles activated during the downstroke (Dial et al. 1991).

Muscles for respiration and maintaining the structure of the thoracic and abdominal walls are also attached to the sternum. Respiration is controlled by the sternum rocking dorsoventrally (Brocklehurst et al. 2020; Claessens 2009). The costosternalis major originates on the craniolateral process and inserts on the last cervical rib and the sternal ribs (Claessens 2009). Subcostal muscles run between the craniolateral process and the sternal ribs. The external oblique and rectus abdominal muscles attach to the posterior half of the sternum on the lateral margins (Ghetie et al. 1976). If abdominal processes and thoracic processes are present, a membrane runs along their length and connects them to each other and to the lateral margin of the sternal plate, supporting the viscera. During respiration, the sternum moves in either a scissor-like (following the movement of one free blade) or elliptical movement, depending on the timing of the muscle contractions (Brocklehurst et al. 2019; Claessens 2009). The costosternalis major contracts at the beginning of inspiration, tilting the anterior region of the sternum dorsally and sending the posterior region ventrally. The intercostal muscles contract next, and the ribs are pushed up and outward. The differences in rate of contraction of the sternal intercostals versus vertebral intercostals affect the translational motion of the sternum (Claessens 2009). These muscles relax during expiration, returning the sternum and ribcage to their original position.

Sternal shape can also be influenced by tracheal elongation in a few birds (Fitch 1999). In

swans and cranes, the elongated trachea invades the keel (e.g., **Figure 3.2**). In a magpie goose (*Anseranas*), the elongated trachea coils next to the keel. In spoonbills, the elongated trachea loops above the antero-dorsal region of the sternal plate.

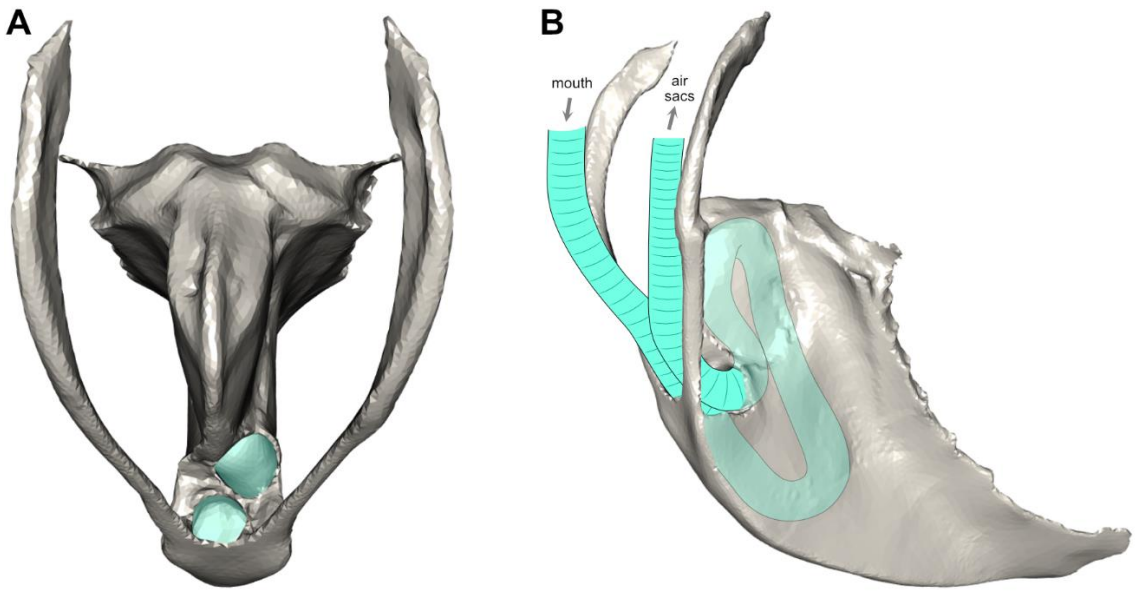

Figure 3.2 Schematic of tracheal invasion of the *Grus antigone* sternum (MCZ 246600). **A)** Anterior view highlighting the openings for the trachea in the anterior margin of the keel, posterior to keel fusion with furcula. **B)** Anterolateral view with the trachea invading the sternum.

3.2.1 Previous morphometric work

Linear morphometrics have linked the locomotor mode or ecological type of the bird (swimming, walking, flying) and the width:height ratio of the avian sternum (Düzler et al. 2006). Linear measurements have been taken, recording height and width at two points of the sterna (Figure 5 of Düzler et al. (2006)), and comparing them in relation to flying, swimming, and walking birds. Another study looked at the diagonal of the keel to measure the depth and length of the keel (Wright et al. 2016). While indicative of flight muscle mass (Wright et al. 2016), these measurements do not reflect the extensive diversity in morphology of the avian sternum or how the sternum morphology relates to the wing that it supports.

More recently, Zhang et al. (2011) expanded on Düzler et al. (2006)'s study by taking the width, height and length of a broad selection of avian sterna to compare changes in proportion across a wider selection of flight ability (flightless to flying) and ecological correlates (see **Table 3.1** for ecological types and examples used). Zhang et al. (2011) used seven ecological types: cursorial/flightless, landfowl, waterbirds, climbing birds, raptors, waders, and perching birds. They found that these measurements of the sternum correlates with flight ability; a deeper, wider sternum indicates a stronger flier. Large flightless birds (Paleognathae) have lost their keel and their sternal plate tapers posteriorly. In climbing birds, raptors, and perching birds, the posterior margin of the sternum widens, the keel extends from the front of the sternal plate to the back completely, and the posterolateral processes are laterally expanded. Raptors tend to have more of the posterior region of the sternum ossified and reduced or fused lateral processes, which is ideal for bursts during flight. This state is in contrast to other birds like landfowl, which have two sets of lateral processes and a cartilaginous membrane to form most of the posterior region of the sternum, which is better suited for rapid take-offs and escape, not sustained flight. This study took major steps in comparing sternum proportions across Aves in relation to ecology, but a landmark-based approach has yet to be used for studying avian sternum morphology in relation to function.

Table 3.1 Ecological types and examples from Zhang et al. (2011). * indicates a non-monophyletic group.

Ecological type	Birds
Walking/flightless fowl	Emu, cassowary
Landfowl*	Pheasant, chicken, sandgrouse, dove, pigeon
Swimming birds*	Anatidae, pelican, penguin
Climbing birds*	Woodpecker, hoopoe, kingfisher, cuckoo, parrot, swift, nighthawk
Raptors*	Owl, eagle, falcon
Waders*	Crane, crake, bustard, snipe, seagull, heron, stork, spoonbill
Perching birds	Passerines (including: swallow, lark, finche, corvid, pipit, oriole, shrike, thrush, starling, babbler, waxwing, tit, bulbul, chaffinch, munia)

3.2.2 This study

Here we use three-dimensional landmark-based geometric morphometrics to measure a broad spectrum of avian sterna and explore relationships between morphology, phylogeny, and ecology. We hypothesize that closely related birds will have sterna of similar shape, as in waterbird wings. We also hypothesize that some bird sterna will have similar shapes due to having similar flight styles. Finally, we hypothesize that bird sterna will converge in shape, due to similar functions.

3.3 Materials and Methods

3.3.1 Source of specimens

Avian sterna were downloaded as .stl files from Aves3D.org, a collection of specimens from the Yale Peabody Museum of Natural History and the Museum of Comparative Zoology at Harvard (Suppl. Table 3.1). An additional specimen came from the Field Museum of Natural History. Specimens used had to have at least one side and a keel in good condition: the lateral processes

must be intact on at least one side, the sternal plate unwarped or minimally warped, and other major anatomical features present. A few specimens had spots too thin for the .stl to render or the sternal plate and/or keel had been damaged by shot, the keel or both, but the landmarking off the specimens was not affected by these imperfections.

3.3.2 Landmarking

The avian sterna were landmarked in Stratovan Checkpoint (2018), protocol seen in **Figure 3.3**. To minimize the effect of warping between the left and right sides of the sternal plate, only the keel and the left side of the sternal plate were landmarked using ten homologous landmarks, six curves and four patches. Landmarking one side also allowed us to mirror the specimen if a lateral process was broken on the left side of the sternal plate, but intact on the right. Patches were created using a 5x5 grid, but not all points were used in the analysis. The removal of some points reduced the influence of the shape of the relatively featureless regions. Many edges of the patches also followed curves of sliding semi-landmarks or other patch edges, so the patch landmarks would essentially be redundant. Patch landmarks that were used in analyses are large and opaque blue, points that were deleted post-landmarking are small and transparent blue.

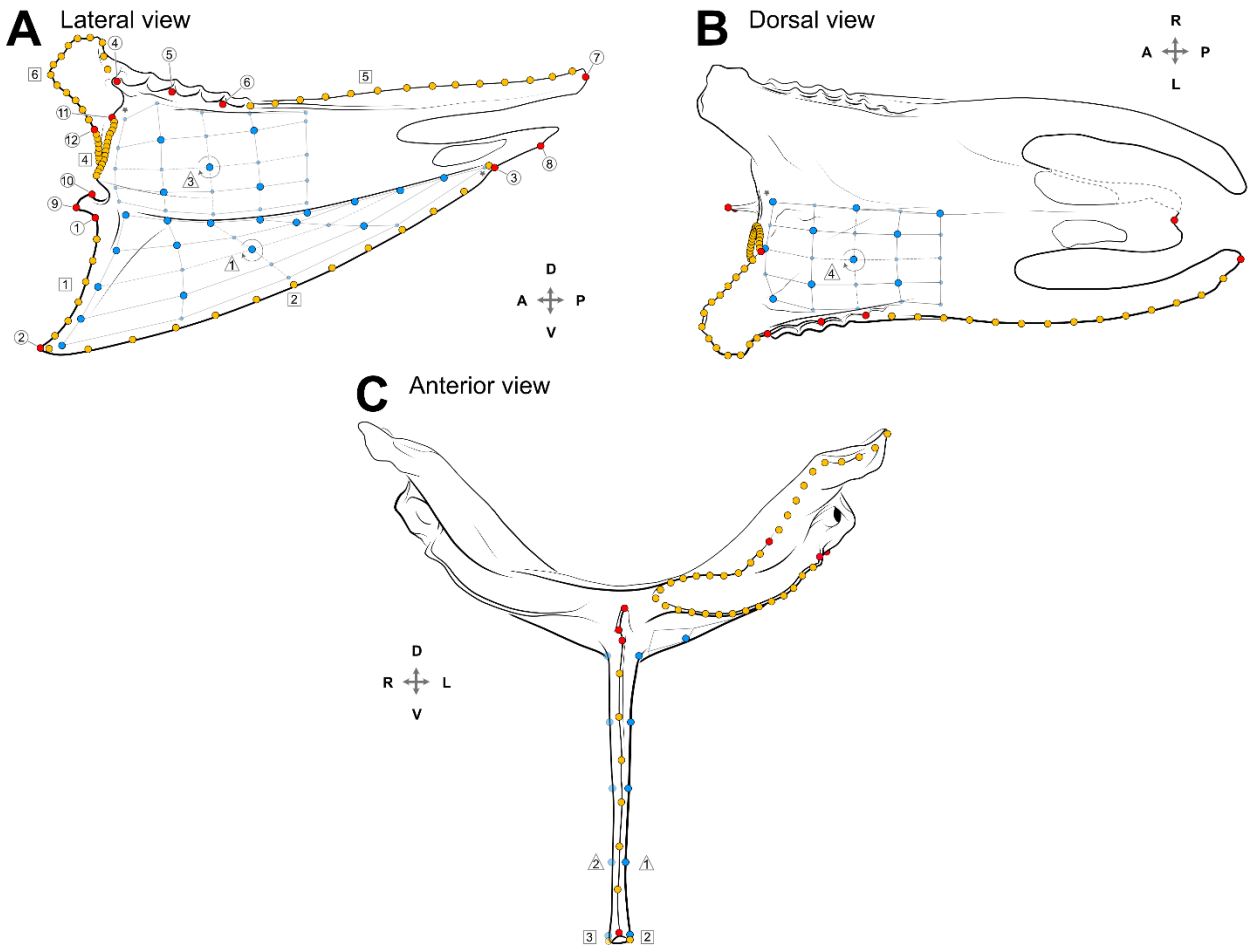

Figure 3.3 Landmarking protocol plotted onto the sternum of *Eudyptes crestatus* (MCZ 346428). Red, circled labels = homologous landmarks; yellow, squared labels = semi-landmarks along curves; blue, triangled labels = pseudo-landmarks in patches. **A)** Left lateral view. **B)** Dorsal view; dotted line indicates missing bone. **C)** Anterior view. Circular arrows indicate Checkpoint patch direction, asterisks indicate Checkpoint patch starting point.

The homologous landmarks are: 1) the dorsalmost point of the anterior margin of the keel, 2) the ventralmost point of the anterior margin of the keel, 3) the posteriormost point of the ventral margin of the keel, 4) the first costal process, 5) the third costal process (or the second in the case of only three costal processes), 6) the last costal process, 7) the posteriormost point on the lateral margin of the lateral process, 8) the posteriormost point of the sternal plate midline, 9) the anteroventral point of the rostral spine, 10) the anterodorsal point of the rostral spine, 11) the lateroventral point of the coracoid groove, and 12) the point at which the coracoid groove margin transitions to the craniolateral process margin (see **Figure 3.3**, red with circle labels).

The curves of landmarks run along: 1) the anterior margin of the keel, 2) the left edge of the ventral surface of the keel, 3) the right edge of the ventral surface of the keel, 4) around the margin of the coracoid groove, 5) along the margin of the lateral process, and 6) around the margin of the craniolateral process (see **Figure 3.3**, yellow with square labels). Curve 3 (indicated in **Figure 3.3**C) is only used in the straightening of the keel, then deleted to avoid any influence from slight left-right asymmetric positioning of landmarks.

The patches of landmarks are placed: 1) on the left side of the keel, 2) on the right side of the keel, 3) on the ventral surface of the sternal plate, and 4) on the dorsal surface of the sternal plate (see **Figure 3.3**, blue with triangle labels). These landmarks are more difficult to place in a homologous manner, and the huge variation in ossified sternal plate morphology make the sternal plate patches extremely difficult to place consistently. All of the patches are reduced to the Checkpoint minimum of 25 landmarks each for exporting, then a subset (small faded blue dots in **Figure 3.3**) are deleted in R to minimize the influence of patch data on the analyses. The second patch on the keel (patch 2, indicated in **Figure 3.3**C) is used only for subsequent calculations to realign the keel and is not used in the analysis to reduce any influence from left-right asymmetric positioning during landmarking.

3.3.3 Correcting the deformation of the ossified keel

Some specimens had keels which warped as they dried out during the skeletonization process. Skeletonized specimens at the Field Museum of Natural History were examined to determine whether a keel with multiple curves down its length was standard or not. These specimens range from very warped keels to straight keels within a given species. Specimens with warped keels were computationally restored to a straight, more natural form (**Figure 3.4**). We assume that the corresponding points in the keel patches are directly opposite from each other.

We also assume that the distance between each pair of landmarks accurately represents the thickness of the keel at that location, and that the midpoint between the landmarks is on the "midsection" of the keel.

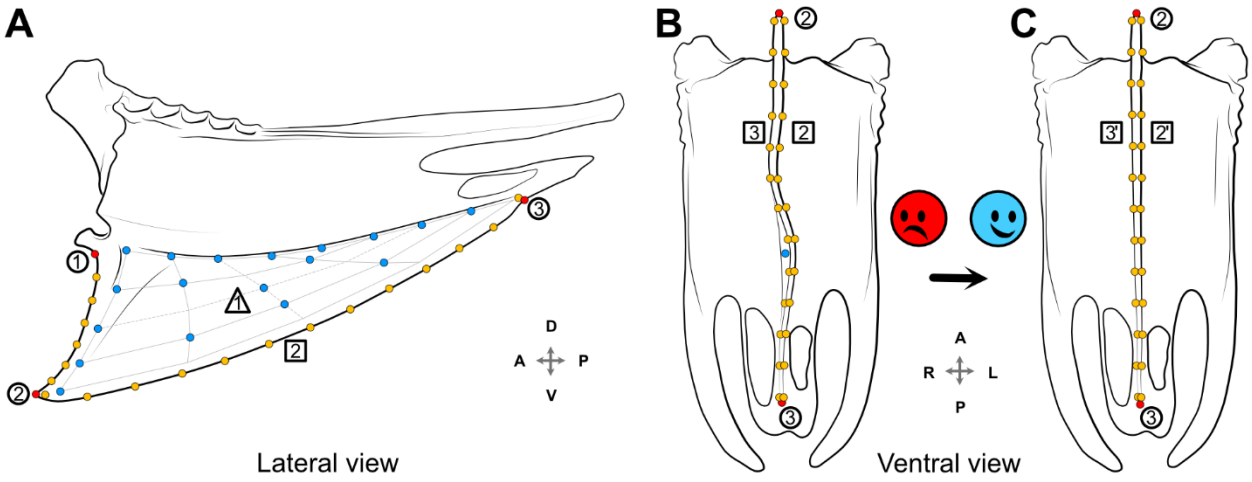

Figure 3.4 The warped keel and its landmarks plotted onto the sternum of *Eudyptes crestatus* (MCZ 346428). **A)** Lateral view of keel landmarks, **B)** ventral view of landmarks on originally warped keel, **C)** ventral view of the representation of a mathematically straightened keel, represented by landmark curves 2' and 3'. Circles = single red points, squares = curves of yellow points, triangles = patches of blue points.

First we found the equation of the plane created by points 1, 2, and 3 in three-dimensions. These points are in relatively stable positions and are minimally affected by the deformation.

Point 1: (0.1235, -2.1229, 51.2183)

Point 2: (-10.5325, -29.5192, 62.6989)

Point 3: (11.4939, 5.2263, 119.9557)

Equation of a plane: $ax + by + cz + d = 0$

$0.1235a - 2.1229b + 51.2183c + d = 0$

$-10.5325a - 29.5192b + 62.6989c + d = 0$

$11.4939a + 5.2263b + 119.9557c + d = 0$

Solve system of equations to get: $0.1994x - 0.08745y - 0.02363z + 1 = 0$

This plane is the corrected midsection of the keel.

Then we started with the first pair of points on curves 1 and 2. We found the midpoint between the points.

Curve 1, point 1: (-10.7779, -28.8184, 63.5632)

Curve 2, point 1: (-9.2144, -29.7163, 63.7765)

$$x_{mid} = -10.7779 - \frac{-10.7779 - (-9.2144)}{2} = -9.9961$$

$$y_{mid} = -28.8184 - \frac{-28.8184 - (-29.7163)}{2} = -29.2674$$

$$z_{mid} = 63.5632 - \frac{63.5632 - 63.7765}{2} = 63.6689$$

Current midpoint: (-9.9961, -29.2674, 63.6689)

The midpoint represents the intersection with the current warped midsection of the keel.

We then calculated point on the plane closest to the current midpoint.

Plane: $0.1994x - 0.08745y - 0.02363z + 1 = 0$

Current midpoint: (-9.9961, -29.2674, 63.6689)

$$-1 = \langle 0.1994, -0.08745, -0.02363 \rangle t + \langle -9.9961, -29.2674, 63.6689 \rangle$$

$$-1 = 0.1994(0.1994t - 9.9961) - 0.08745(-0.08745t - 29.2674) - etc.$$

$$t = 10.4975$$

$$x_{new\_mid} = 0.1994 * 10.4975 - 9.9961 = -7.9029$$

$$y_{new\_mid} = -0.08745 * 10.4975 - 29.2674 = -30.1854$$

$$z_{new\_mid} = -0.02363 * 10.4975 + 63.6689 = 63.4208$$

New midpoint: (-7.9029, -30.1854, 63.4208)

Then we calculated the distance from the current midpoint to the new midpoint, recording that as the distance on each axis (x-distance, y-distance, z-distance).

$$x_{dis} = -9.9961 + 7.9029 = -2.0932$$
$$y_{dis} = -29.2674 + 30.1854 = 0.918$$
$$z_{dis} = 63.6689 - 63.4208 = 0.2481$$

Then we subtracted those distances from the coordinates of each point in the pair to shift the points to the new positions.

Curve 1, point 1: (-10.7779, -28.8184, 63.5632)

Curve 2, point 1: (-9.2144, -29.7163, 63.7765)

$$x_{new\_pt} = -10.7779 + 2.0932 = -8.6847$$
$$y_{new\_pt} = -28.8184 - 0.918 = -29.7364$$
$$z_{new\_pt} = 63.5632 - 0.2481 = 63.3151$$

$$x_{new\_pt} = -9.2144 + 2.0932 = -7.1212$$
$$y_{new\_pt} = -29.7163 - 0.918 = -30.6343$$
$$z_{new\_pt} = 63.7765 - 0.2481 = 63.5284$$

After continuing to do this with all of the landmark points that need to be adjusted, a new keel is created (**Figure 3.5**). From here on, only the left keel patch and curve of the ventral margin of the keel are used in morphometric analyses.

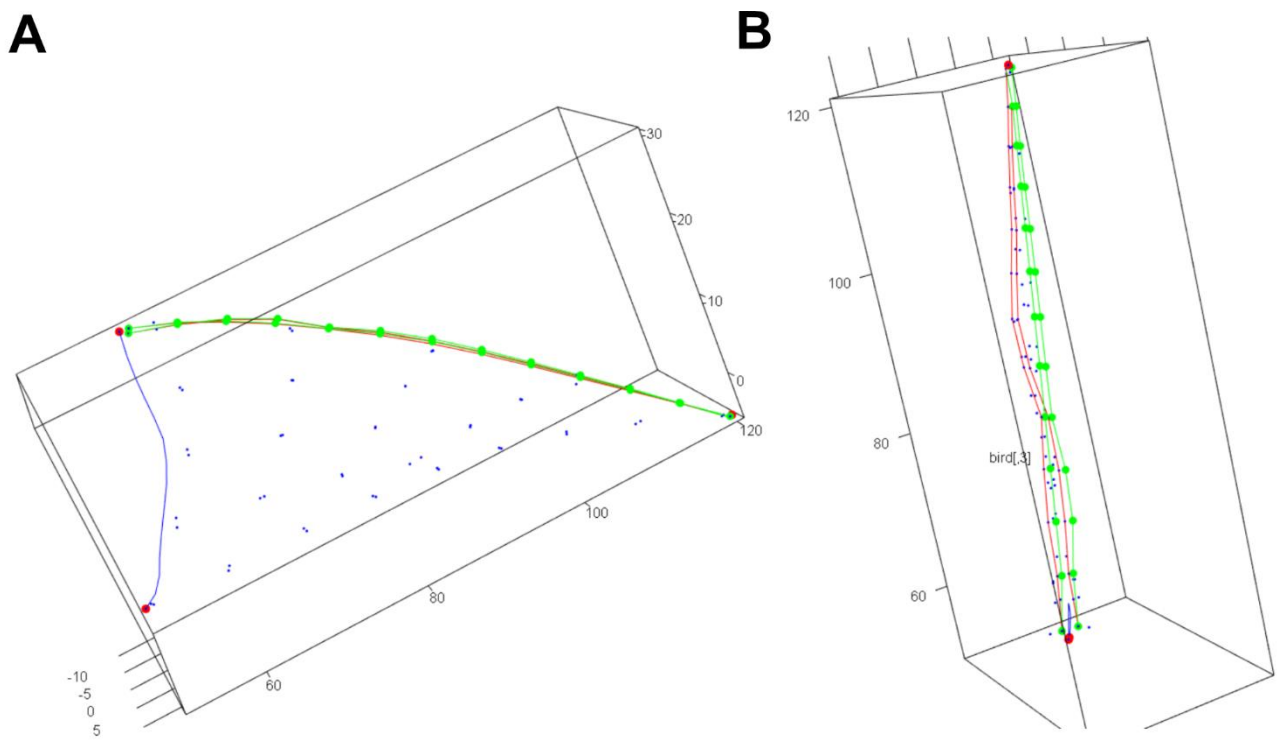

Figure 3.5 Correcting the keel. **A)** right lateral view of keel, **B)** ventral view of keel. Red points = original location, Green points = corrected location.

3.3.4 Analytical techniques and variables

R was used to prepare the data for analysis (e.g., correcting the keel), running the Principal Component (PC) analysis, plotting the morphospaces, phylogenetics, and the "geomorph" R package for modularity analyses. R packages 'ape' and 'geiger' were used to prepare the tree from the Jetz et al. (2012) tree on BirdLife.org (Paradis and Schliep 2019; Harmon et al. 2008). We used the Hackett et al. (2008) backbone for the tree with all 9993 species instead of the tree with the 6670 sequenced species, because some of the species in our dataset have not been sequenced yet. We downloaded 1000 complete trees and used TreeAnnotator with BEAST (Drummond and Rambaut 2007) to obtain a consensus tree based on median node heights. One branch length turned out negative, so we converted it to $1x10^{-6}$. The function *aov.phylo*() from 'geiger' was used for phylogenetically corrected MANOVAs. We used the 'convevol' R package

(Stayton 2015) to test for phylogenetic convergence in several clusters in the phylomorphospace.

'Flight style' as presented by Viscor and Fuster (1987) (see Chapter 2 Appendix, Terminology: Flight Style) describes the kind of flight stroke a given bird uses, therefore it is used to test sternum function. Six of the eight categories of Viscor and Fuster (1987)'s flight style are used in by birds in this dataset: "forward flight," the most common flight pattern; "high frequency flapping flight," similar to forward flight, but the wingbeats tend to be more frequent and better synced with respiration; "undulating flight," which has periods of flapping and gliding, "gliding/soaring," which is used by the most efficient fliers who spend most of their time in the air gliding on wind currents instead of flapping to stay aloft; "hovering flight," used most often by the hummingbird, which is able to stay in one place in the air for a long period of time; and "short flight," which is often used by landfowl for rapid takeoffs and short-distance flights to escape predators. Our categorization was based off the Tables 1 and 2 in Viscor and Fuster (1987), which indicates flight style at both species and family levels. While extensive, these tables are not comprehensive, so flight styles from additional species were extrapolated based on the provided descriptions of flight styles. Viscor and Fuster (1987) only studied flying birds, so we had to add "not flying" for the flightless terrestrial birds like ostriches and "swimming" for penguins which are flightless but often swim with their wings.

3.4 RESULTS

Our analyses of three-dimensional morphometrics of the avian sternum shed new light on the relationship between its morphology and flight style. We used sterna from 128 avian species, one sternum from each species, covering 35 orders and 66 families. Within orders, the species tend to cluster together, but there is substantial convergence between orders. Flight style has a strong influence on sternum morphology, as does whether the taxa are landbirds or waterbirds.

3.4.1 General topology of morphospace

Several patterns in the distribution of sterna in the morphospace are apparent from **Figure 3.6** and **Figure 3.7**. PC 1 (34.8% of the variance) is highly influenced by the keel, particularly the ventral margin and the more ventral portion of the keel, which together describe the depth or inclination of the keel. Species with high PC 1 values have deeper keels with slightly posteriorly inclined keels, whereas low PC 1 values indicate a more shallow keel with an anterior inclination. The keel also extends the full length of the sternum in high PC 1 values, but in low PC 1 values, the posterior end of the keel stops well before the posterior margin. The lateral margin (including costal processes) is also highly influential, with a straighter margin in lower PC 1 values and a more curved or laterally deflected margin in higher PC 1 values. The costal processes also take up the majority of the lateral margin in low PC 1 values, while they are more condensed in the anterior portion in higher PC 1 values (**Figure 3.6**A). The coracoid groove also has some influence, though the specifics of the morphology are unclear. The craniolateral process and sternal plate do not have as much influence, though the sternal plate is a little longer in higher PC 1 values than the lower PC 1 values. PC 2 (21.6% of the variance) has a similar but lessened influence from the keel as PC 1, but greater influence from the lateral margin, especially the last costal process and the posteriormost points. The shape of the whole sternum is proportionally longer and narrower in low PC 2 values, compared to the shorter and wider sterna in high PC 2 values. The keel remains the dominant influence in PC 3 (11.7% of the variance), however, the hoatzin and kiwi are species with the highest PC 3 values and unusual morphologies.

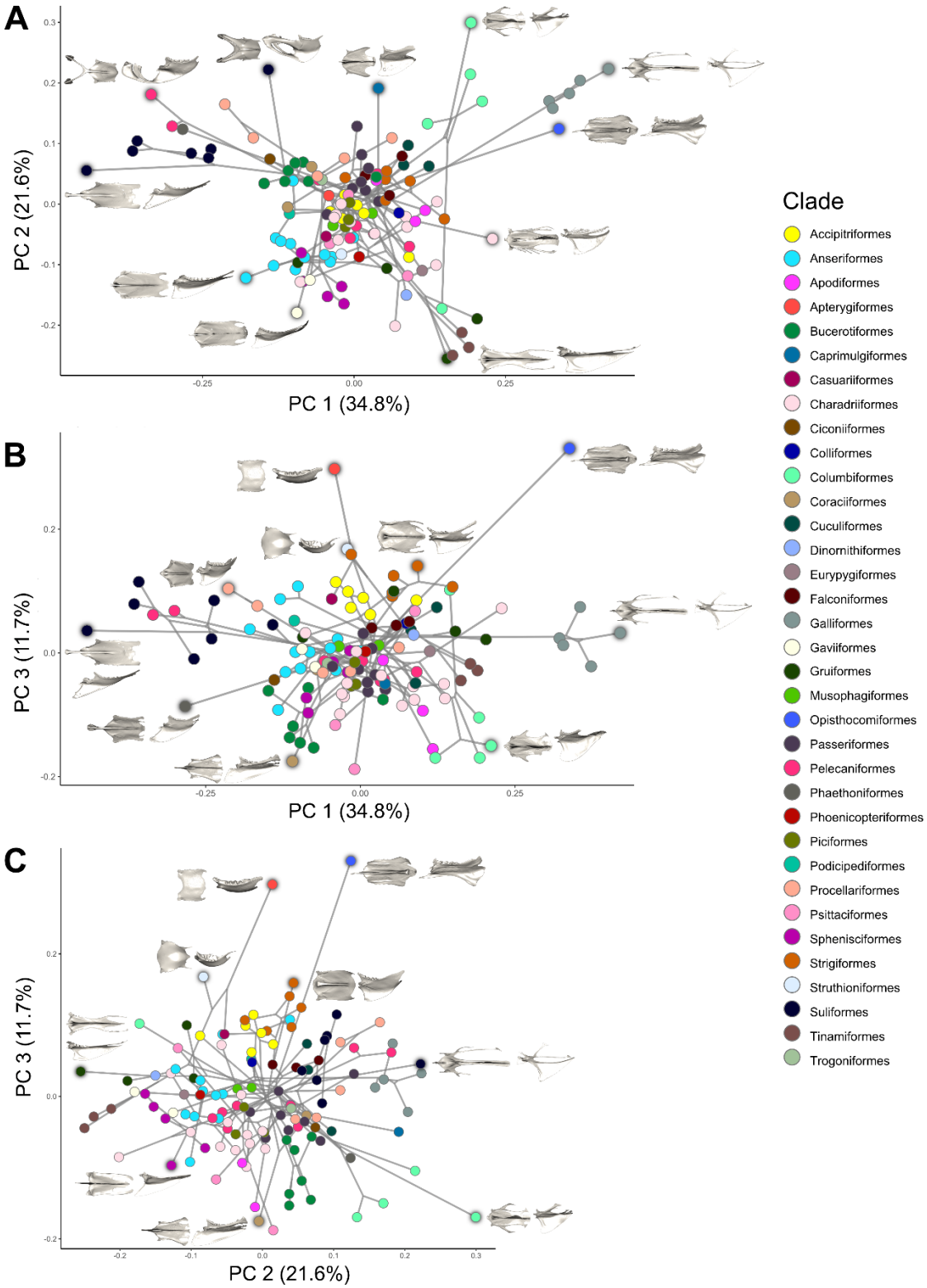

Figure 3.6 Avian sternum phylomorphospace showing PC1 and 2 **(A)**, PC1 and 3 **(B)**, and PC2 and 3 **(C)**. Interactive 3D plot on FigShare for data point identification and flight style, DOI: 10.6084/m9.figshare.15054381.

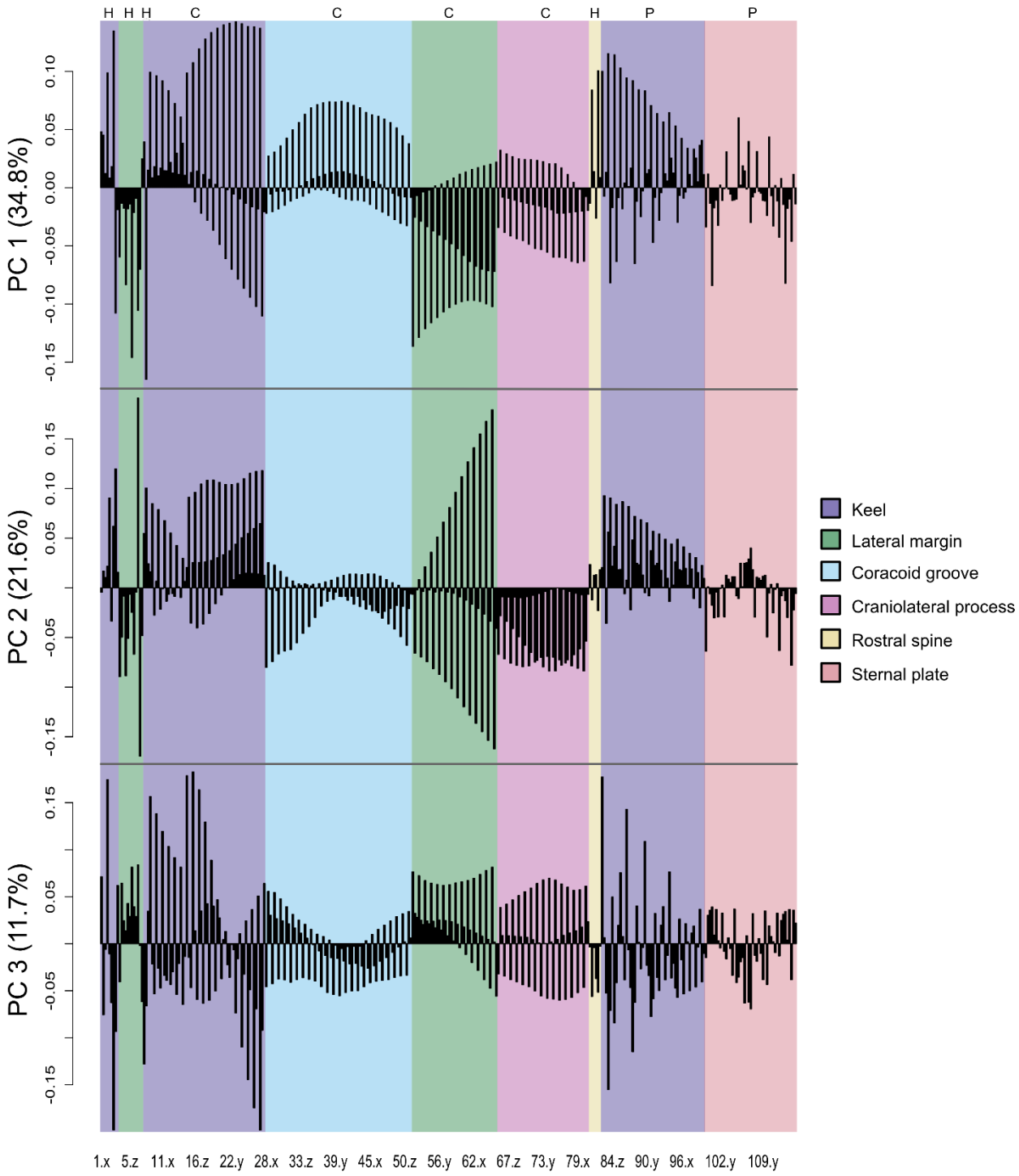

Figure 3.7 Landmark coordinate loadings for PCs 1-3 for the sternum morphospace color-coded by anatomical region. Each of the 114 landmarks has an x, y, and z loading. H, homologous point; C, sliding semi-landmark curve; P, pseudolandmark patch.

The majority of the species are clustered in the middle of the morphospace, but there are

a few clusters that extend into other parts of the morphospace (**Figure 3.6**). Gannets, cormorants, pelicans, frigatebird, and some procellariiforms have low PC 1 values and this relates to the anterior inclination of the keel and wider sternal plate. Hornbills are also extending into that region of morphospace but not to the same extent. With high PC 1 values, Galliformes and the hoatzin have longer sternal plates and more posteriorly positioned and inclined keels. The galliform keel takes up the posterior two-thirds of the keel, and the anterior margin of the keel is perpendicular to the sternal plate. The hoatzin features an extreme morphology in that the keel is positioned in the posterior half of the sternal plate and inclined posteriorly. Rails and tinamous converge in the region defined by high PC 1 and PC 2 values with deep keels and long, narrow sternal plates. The extinct dodo (Columbiformes) converges with the rails and tinamous; the rest of the columbiforms (pigeons) have similar PC 1 values, but low PC 2 values. Waterbirds tend to have positive PC 2 values, ducks, loons, and penguins clustering together with lower PC1 values. Charadriiforms have a larger range in PC 1 values.

The species from many clades cluster together in morphospace indicating a strong influence from evolutionary relationships, but flight style was also found to be a very influential factor (phylo-MANOVA: Wilks, 0.044; p-value < 0.001). Soaring and diving birds (pelicans, cormorants) have low PC 1 values, whereas landfowl with occasional rapid burst takeoffs (turkeys, pheasant) have high PC 1 values. Tinamous and rails are ground-dwelling birds that converge on a similar sternum shape (long, narrow, with a deep keel), as does the flightless dodo. This cluster is a very distinct location in the morphospace from the landfowl, but both clades spend much of their time on the ground, suggesting there are multiple ways a sternum could evolve for a ground-dwelling bird.

3.4.2 Sternum morphology and function

Because the sternum anchors the major flight muscles, the correlation between flight style and sternum morphology was tested. Flight style describes the general frequency and type of wingbeat a bird uses, and we hypothesize this feature might be reflected in the required shape of the sternum. **Figure 3.8** shows a visualization of the sternum morphospace with flight style and waterbird/landbird designation mapped onto the points. A phylo-MANOVA using the first 10 PCs (~90% of the total variance) shows that sternum morphology has a highly significant correlation with flight style (Wilks = 0.040, $p < 0.001$). This relationship can be visualized in the morphospace below (**Figure 3.8**A-B).

Each flight style occupies different trait space (**Figure 3.8**A-B). Birds with undulating flight and gliding/soaring flight overlap the most in all three PCs, clustering towards a short, wide sternal plate with a shallow, anteriorly inclined keel (low PC1 and PC2 values, average to higher PC3 values) or a more anteroposteriorly elongate sternal plate and a less anteriorly inclined keel (average PC1, PC2, PC3 values). Birds with short bursts of flight cluster in two areas: long narrow sterna with long lateral processes (=lateral margin) and deep keels (medium-high PC1 values, high PC2 values, average PC3 values) and long narrow sterna with short lateral processes (=lateral margin), and deep keels (high PC1 values, low PC2 values, average PC3 values).

We also used a phylo-MANOVA to test whether sternum morphology is correlated with the designation as waterbird or landbird. Waterbird wing shapes tend to overlap somewhat with landbird wing shapes (visualized in Fig. 2, Wang and Clarke 2015), but they also each expand into their own region of morphospace. Sternum morphology has a weakly significant correlation

with waterbird/landbird categorization (Wilks = 0.533, p-value = 0.0609), visualized in the morphospace below (**Figure 3.8**C-D).

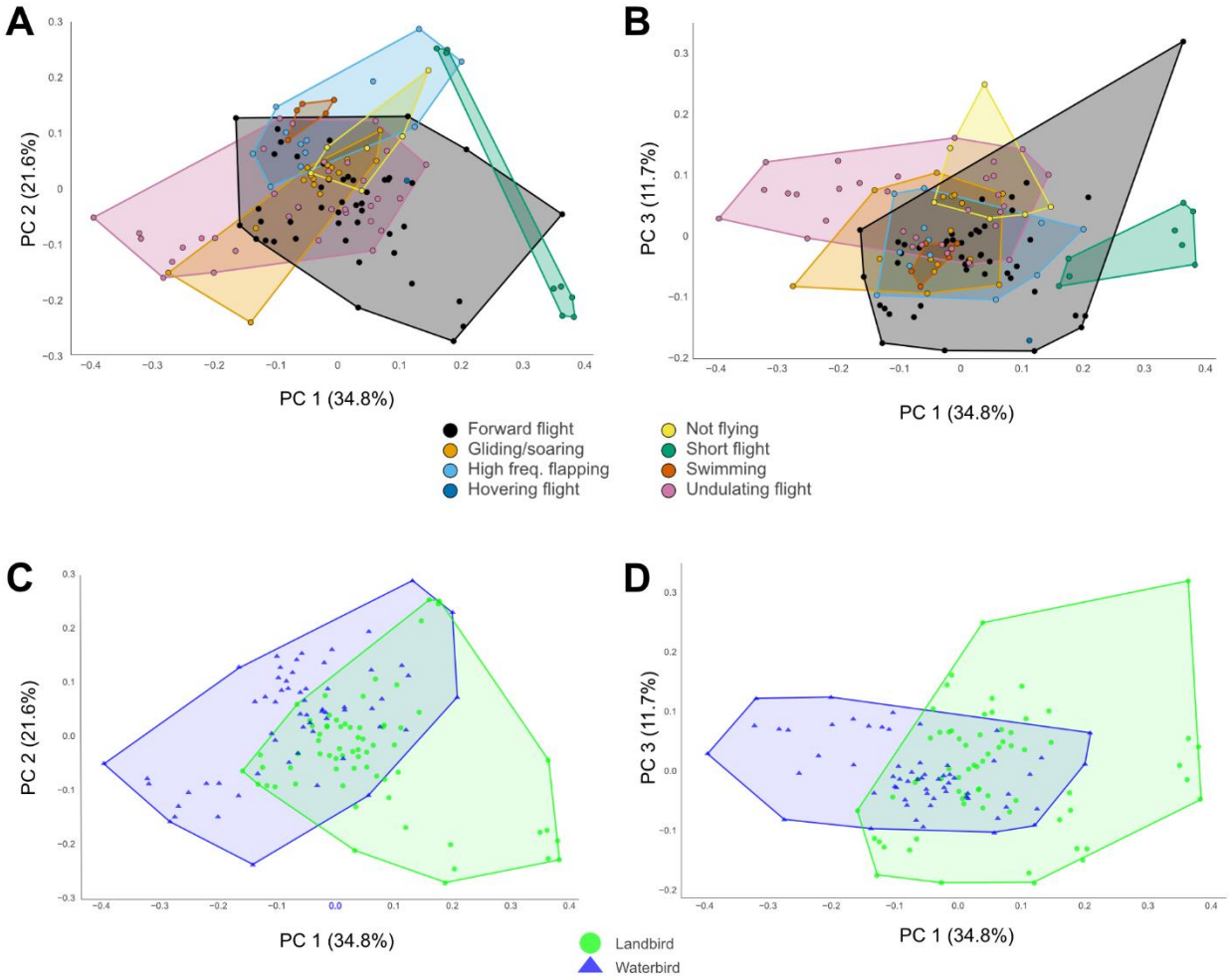

Figure 3.8 Sternum morphospace represented by PCs 1-3 colored by flight style (A-B) and landbird/waterbird designation (C-D). Interactive 3D plots for flight style and for waterbird/landbird on FigShare for data point identification. DOIs: 10.6084/m9.figshare.15054423 and 10.6084/m9.figshare.15054477, respectively.

3.4.3 Convergence in sternum shape

We found repeated convergence in the sternum morphospace. All of the clusters tested had highly significant (p-value < 0.001) C1 values (**Table 3.2**), indicating the maximum phylogenetic distance of clades represented by the clusters is greater than expected under the

Brownian motion model of evolution. The two large clusters (Groups 1 and 2, **Table 3.2**) were also tested with C5, and both clusters invaded the area of morphospace a greater number of times than expected (Group 1 = 6 times, Group 2 = 5 times). Rails, tinamous, and the dodo (Group 1) converged on a relatively long narrow sternal plate with a deep keel (0.674, $p < 0.001$). Frigatebirds, pelicans, and cormorants (Group 2) converged on a relatively square sternal plate and an anteriorly inclined keel in the anterior part of the sternum (0.462, $p < 0.001$). Penguins, geese, and loons (Group 5) have a lower but significant C1 value (0.372, $p < 0.001$), converging on an anteroposteriorly elongate sternum with an anteriorly inclined keel expanding the full length of the sternum.

There are also some interesting pairs that converge. Group 3 contains two waterbirds (a goose and a heron) and two landbirds (a go-away bird and a uropendola). Group 4 (the wading thick-knee and the frequently flying treeswift), show high amounts of convergence (0.811). Group 6 contains a wide range of landbirds: turaco, treeswift, bird-of-paradise, and a sapsucker, with pretty high amounts of convergence (0.732). Group 7 contains a crane and a vulture, and Group 8 has a crow pheasant and a kestrel, both with high amounts of convergence (0.680 and 0.715, respectively).

Table 3.2 Convergence testing of selected clusters in phylomorphospace based on 100 simulations.

Group No.	Species Index No.	C1		C5	
		Obs. C	p-value	Obs. C	p-value
1	16, 42, 81, 103, 105, 123	0.674	<0.001	6	<0.001
2	7, 46, 47, 89, 90, 91	0.462	<0.001	5	<0.001
3	12, 18, 40, 98	0.642	<0.001	---	
4	28, 117	0.811	<0.001	---	
5	22, 62, 111	0.372	<0.001	---	
6	41, 70, 88, 112	0.732	<0.001	---	
7	68, 109	0.680	<0.001	---	
8	30, 58	0.715	<0.001	---	

Group 1: *Aramides cajanea*, *Crypturellus noctivagus*, *Nothura maculosa*, *Rallus elegans*, *Raphus cucullatus*, *Tinamus major*; **Group 2:** *Anhinga anhinga*, *Phoebastria immutabilis*, *Phoebastria nigripes*, *Pelecanus erythrorhynchos*, *Pelecanus occidentalis*, *Phaethon rubricauda*; **Group 3:** *Anseranas semipalmata*, *Ardea herodias*, *Corythaixoides leucogaster*, *Psarcolius angustifrons*; **Group 4:** *Burhinus capensis*, *Streptoprocne zonaris*; **Group 5:** *Branta canadensis*, *Gavia immer*, *Spheniscus humboldti*; **Group 6:** *Crinifer zonurus*, *Hemiprocne mystacea*, *Paradisaea raggiana*, *Sphyrapicus varius*; **Group 7:** *Grus antigone*, *Sarcoramphus papa*; **Group 8:** *Centropus sinensis*, *Falco sparverius*.

3.5 DISCUSSION

The avian sternum is a highly complex structure that is incorporated into multiple organ systems (musculoskeletal, respiratory). Here we conduct the first in-depth phylogenetic analysis on three-dimensional landmark data from avian sterna and find that the sternum is very diverse in shape, with the keel and lateral margin being major influences, sternum shape is tied to flight style and waterbird/landbird designation, and there is repeated convergence within the dataset.

3.5.1 Morphology in relation to flight

The avian sternum has a wide range of shapes which are significantly correlated to flight style. Birds that have undulated flapping and gliding/soaring flight occupy two clusters, but the

cluster in the more extreme region is large-bodied waterbirds (pelicans, cormorants) with medium-high to high aspect ratio wings. The more centralized cluster contain birds like smaller-bodied terns with high aspect ratio wings or medium-large birds of prey with medium aspect ratio wings. These flight styles having two key clusters indicates that there are two ways to build a sternum for a flight style with fewer wingbeats. This result is similar to that of birds with short bursts of flight, there are two ways to make those sterna. High-frequency flappers (ducks, geese and loons) and swimmers (penguins) cluster close together, suggesting convergence in morphology to achieve proper anchoring support for the rapid wingbeats, either in air or water.

The designation as waterbird or landbird is also a significant ecological variable. The morphospace plots are reminiscent of the morphospace seen in Wang and Clarke (2015), with waterbirds and landbirds overlapping but with each also extending into a different area of morphospace. In the sterna, the extension of the landbird morphospace away from the waterbird space is covered by only two flight styles, forward flapping and short flight. These regions are mostly made up of pigeons, galliforms, rails, and tinamous high on the PC 1 axis. The galliforms and tinamous do not fly far, only in short bursts, and the pigeons and rails require intense flapping to take-off. The waterbird-only space is on the low end of the PC 1 axis and occupied by pelicans, cormorants, albatross, tropicbird, and frigatebirds, which all use gliding/soaring or undulating flight.

This particular gradient between rapid takeoffs and soaring, can also be seen in waterbird wings (Baumgart et al. 2021): rails had low aspect ratio wings, albatross had high aspect ratio wings, and aspect ratio was a main influence in PC 1. This would suggest a hypothesis that birds with low aspect ratio wings have a deep keel and either a long or short sternum, and that birds with high aspect ratio wings would have a shallow, anteriorly inclined keel and either a long or

short sternum. Future research should combine wing shape data and sternum shape data to look for such correlations with flight style, because wing shape was not correlated with flight style, but sternum shape was.

Takeoff strategy may be another significant influence on sternum morphology. For example, galliforms (high PC1 values) require a high amount of power to generate lift for their short flights, whereas albatrosses (low PC1 values) tend to catch the headwind in their wings to achieve liftoff. A given bird would have a variety of takeoff strategies depending on the situation they are in. Parrotlets (Psittacidae) were trained to hop or fly a short distance to mimic foraging in a lab setting. Foraging in the trees would be a low-risk situation, and the parrotlets would choose the mechanically efficient technique for a given jump or short flight to another branch depending on the distance and the angle of takeoff and landing (Chin and Lentink 2017). If the birds are in a high-risk situation, like taking off to escape predators, then a rapid, high velocity takeoff is required (Kullberg and Lafrenz 2007). The escape strategy of great tits (Paridae) varies depending on environmental variables: if there is cover around, the birds will make a short dash to the cover, otherwise they will takeoff at a higher angle of ascent and fly faster, though acceleration will be harder (Kullberg and Lafrenz 2007). Different angles of ascent or the velocity of takeoff might be reflected in the inclination or depth of the keel, depending on how much mechanical energy is required in which direction. Further exploration of how the sterna are positioned within the thorax would yield critical information on the angles of the muscles and how exactly the sternum shape and position translates into a biomechanically optimal structure for a given takeoff or flight style.

3.5.2 Repeated convergence in sternum morphology

We also found instances of convergence in the morphospace, indicating similar function or one structure for multiple functions. A few examples are discussed. Rails and tinamous tend to be smaller birds that live in forested areas or near marshes. They typically eat invertebrates or plant material and fly very little, often short distances. These birds have long narrow sterna with deep keels and a set of long thin lateral processes. The dodo also converges with this group and lived in forested areas, but it is a much larger, flightless bird that existed on islands, and possibly used its wings for balance while walking or running. Island habitats do influence "flightedness" in birds, with island populations evolving reduced flight muscle volume and longer hindlimbs compared to their continental counterparts (Wright et al. 2016). The dodo does not have lateral processes on the sternum like the rails and tinamous, but the overall shape captured by the keel and lateral margin show that they all have long, narrow sterna with deep keels, and the costal processes clustered tightly together in the anterior portion of the lateral margin. This group represents one cluster of birds with the "short flight" flight style. Galliforms also have short bursts of flight, and have long, narrow sterna with deep keels. Galliforms have two sets of lateral processes, the lateralmost is shorter and more laterally deflected than the medialmost process which is almost as long as the sternal plate.

Another sternum morphology that several birds converge on is the short, wide sternum with a shallow, anteriorly inclined keel. Birds that fall into this category include albatrosses (*Phoebastria immutabilis* and *P. nigripes*), pelicans (*Pelecanus erythrorhynchos* and *P. occidentalis*), the anhinga/darter (*Anhinga anhinga*), and the tropicbird (*Phaethon rubricauda*). These are larger seabirds on the opposite spectrum as the birds with short bursts of flight, and they tend to fly long distances, either for food or migration. The albatrosses are based out of

islands in the Pacific, but they cover a wide range hunting for food on the wing. The pelicans do not hunt over the ocean, *P. erythrorhynchos* preferring hunting on the surface of more inland waters than *P. occidentalis* which will hunt by plunge diving near oceanic coasts. The anhinga hunts by foot-propelled diving and only the populations at the northern and southern ends of the geographic range will migrate. Like the albatrosses, the tropicbird nests on islands in the Pacific and Indian Oceans, and they also tend to go out on long-distance foraging trips and have a number of aerial maneuvers in their repertoire. The pelicans and tropicbird also fuse their furcula to the anteroventral point of the keel which would reduce bone material required to build the girdle. (The landmark curves were placed dorsal to the keel-furcula fusion site to account for this particular configuration, the end result comparable to other avian sterna with unfused furculae.) The sternum shape that these birds share seems related to distance flight and use either undulating flight or gliding/soaring and are related to aquatic habitats.

3.5.3 Fossil data and the potential for comparisons

Taking a step back in time, theropod fossils indicate that the sterna started elaborating in Paraves. There is currently no evidence for ossified sternal elements in *Mei*, *Anchiornis*, *Archaeopteryx*, and *Sapeornis*, and cartilage is rarely preserved in fossils from the localities of these specimens (Zheng et al. 2014). The clade represented by Confuciusornithiformes + Ornithothoraces shows the evolution of the more modern avian sternum. The evolution of the sternum is not straightforward, because there is quite the variation in quantity and bilateral versus midline placement of ossification centers (**Figure 3.9**A; O'Connor et al. 2015). Developmentally, tetrapod sternal elements have been found to expand from bilateral ossification centers (Hanson 1919), but there is a lot of variation in ossification center configuration throughout in the fossil record of stem birds, either bilateral or midline (O'Connor et al. 2015),

so perhaps the developmental pathways for maniraptoran sterna have changed or become more labile. Even with the arrival of modern Aves, it is not clear whether the paleognath clade lost flight and tinamous regained it, or the ancestral condition was flighted and then there were several losses of flight throughout the clade (**Figure 3.9**B; Sackton et al. 2019). Examining the sterna used in this dissertation (**Figure 3.9**B), the flighted tinamous have long narrow sterna with deep keels whereas the flightless moa and ostrich have shorter, wider sterna and lack the keel entirely. (The moa also completely lost the forelimb, and so its sternum also lacks the coracoid groove.)

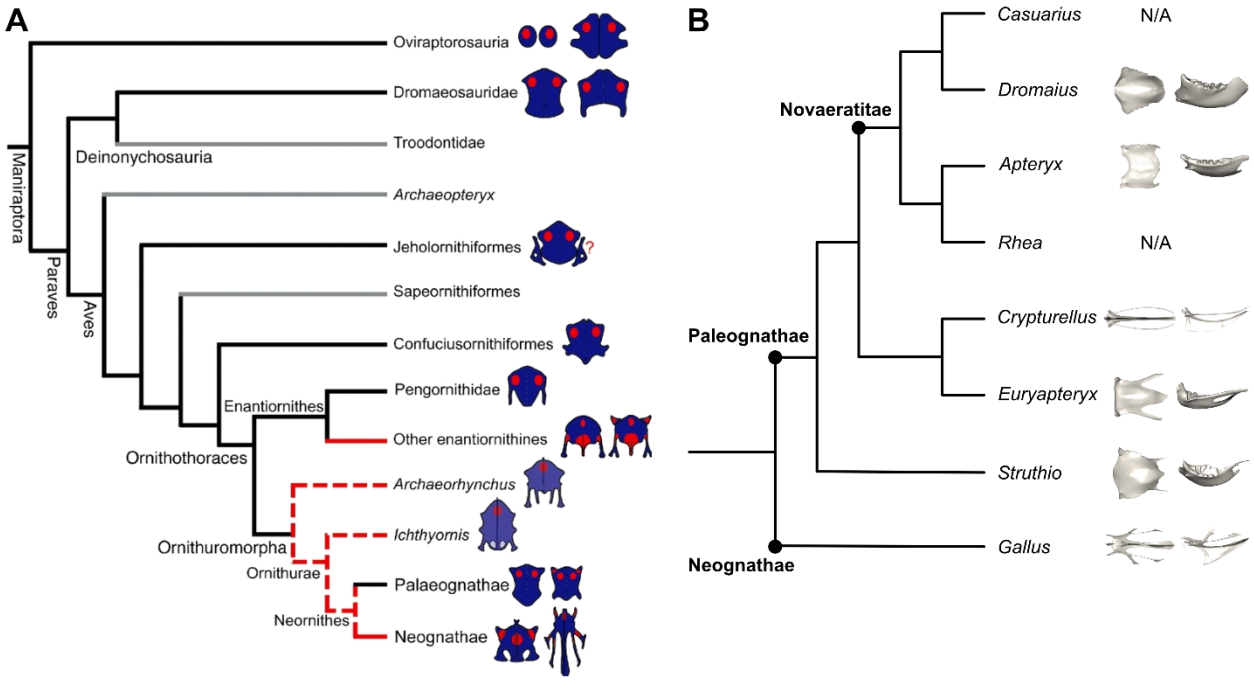

Figure 3.9 A) Evolution of the sternum in maniraptorans. Icons: red, ossification centers; blue, chondral regions. Branches: grey, lost sterum; red, midline ossification present; dashed, uncertainty regarding midline ossification. Reproduced from O'Connor et al. 2015 with permission from John Wiley and Sons publishing. B) Paleognath phylogeny following the results of Sackton et al. 2019 with genus names and sterna from this dataset. Neither *Rhea* nor *Casuarius* were represented in my dataset, so they are marked with 'N/A.'

As many fossil avian sterna are preserved in slabs, comparisons between extant taxa and extinct taxa would likely have to be two-dimensional. Avian fossils from the Jehol Biota represent a promising source of fossils to investigate. Those with well-preserved sternal elements tend to have a ventral surface exposed (O'Connor et al. 2015), so comparing those against photographs of extant sterna from the ventral view would provide key information regarding the early evolution of the avian sternum. Avian fossils from the Green River Formation are much younger (Lower Eocene, 56–47.8 Mya), plentiful, and some have well-ossified sterna preserved in either lateral view or ventral view, so these would provide additional specimens for comparison (Weidig 2010).

3.6 CONCLUSION

The sternum is the anchor for the major flight muscles and is therefore a critical structure for powered flight. The avian sternum has a large range in morphology, yet the patterns of morphology in relation to lifestyle has barely been studied. In this study, we created a landmarking protocol to capture the three-dimensional morphology and computationally unwarp distorted keels which would otherwise skew the results. After running morphometric analyses, we found that species of the same order did tend to cluster together, but there are also many instances of convergence. Flight style was also a significant influence, indicating that the sternum is influenced by the various biomechanical requirements of different kinds of powered flight. Waterbird sterna show a similar relationship with landbird sterna as seen in their wing shape, so continuing down this avenue of inquiry regarding the forces and experiences faced by waterbirds versus landbirds would be intriguing future research.

CHAPTER 4

Comparative pneumaticity in the avian humerus and implications for pterosaurs

4.1 ABSTRACT

Air-filled, or pneumatized, bones are a key adaptation that have allowed several vertebrate lineages with powered flight to evolve large body sizes. These air-filled spaces are connected via diverticula to air sacs within the body cavity and redistribute bone tissue within the skeleton, resulting in reduced body mass. Birds and pterosaurs evolved pneumatized skeletons and larger body size, whereas bats are without this pneumatization. Bats have achieved a wingspan up to 1.5m, birds up to 6.4m and pterosaurs up to 11m. In birds, little is known about how the degree of pneumatization is related to body mass or flight function. This study examines avian humeri using computed-tomography (CT) scans, allowing non-invasive exploration of exterior and interior bone structure. The humerus is typically pneumatized in birds, with more distal wing bones pneumatized only among specialized fliers. The taxonomic sampling in this study incorporates birds across four orders of magnitude of body mass (8g-11300g) assigned to 12 orders to determine how the degree of pneumatization changes with body mass and by clade, many of which are characterized by particular flight functions or lifestyles. I found that body mass has a weak but significant relationship with air space proportion (ASP) in a phylogenetic regression. No combination of pneumaticity, body mass or cortical thickness predicted flight style, though body mass and pneumaticity did have a significant relationship with whether the bird was a landbird or a waterbird. The addition of data from comparable and larger-sized pterosaurs indicate that the largest of the flying extant birds has not achieve as high pneumaticity

or cortical thickness values as pterosaurs, but pterosaurs may be reaching their maximum values before reaching maximum body size due to structural or biomechanical constraints.

4.2 INTRODUCTION

Pterosaurs and birds independently evolved an elaborate pneumatic air sac system within the bones of their postcranial skeleton, allowing them to reach body sizes many times greater than bats which have apneumatic postcrania. Detailed work on postcranial skeletal pneumatization proportions has covered sauropod vertebrae, pterosaur wing bones, avian vertebrae, and a few avian long bones (Wedel 2003; 2005; 2013; Martin-Silverstone and Palmer 2014; Moore 2020; Gutzwiller et al. 2013; Fajardo et al. 2007; O'Connor 2009; Smith 2012), but an extensive comparison of pneumatic spaces in wing bones across Aves has yet to be conducted. The wing is a morphologically and functionally plastic structure that is a main locomotive propeller for most birds (Baumgart et al. 2021), so the structure of the wing has to be responsive to its environment and how it is used to maximize efficiency. Skeletal pneumatization of the wing is hypothesized to be one of those characteristics that is modified according to body mass and behavior, and some work has shown this (O'Connor 2009; Cubo and Casinos 2000; Smith 2012; Currey and Alexander 1985). This study combines the features of these works while looking in depth at the humerus. I used species across Aves and calculated the proportion of cavity to bone and the cortical thickness. Then I used phylogenetic comparative methods to test for correlations and how these variables relate to flight style and body mass, two possible factors that could influence humerus structure of birds with wing-propelled locomotion.

4.2.1 Pneumatic air sac system among volant archosaurs

Air-sacs have evolved at least three times in archosaurs (pterosaurs, sauropod dinosaurs, and theropod dinosaurs), and are not present in mammals, except the paranasal sinuses (O'Connor 2003). The thoracic and abdominal air sacs in the body cavity are used to move air through the comparatively immobile lungs. Diverticulae from these air sacs can invade the skeleton through pneumatic foramina, openings in the bones at the articulating ends. In most birds, a number of dorsal and cervical vertebrae are pneumatized by these air-sacs, as well as the humeri. In large soaring birds, the skeleton becomes hyperpneumatized with most of the bones being pneumatized. Subcutaneous air-sacs are also found in these birds, most notably on the ventral surface of their body and their wings (Picasso et al. 2014; O'Connor 2009; Lovvorn and Jones 1991). On the other hand, diving birds decrease or lose pneumatic air-sacs to decrease their buoyancy and dive more efficiently (Lovvorn and Jones 1991). Hyperpneumatization and reduced pneumatization have both evolved multiple times throughout the avian clade (O'Connor 2009).

Pterosaurs also are thought to have additional air-sacs due to the presence of pneumatic foramina of similar morphology as those in the avian skeletons. Earlier pterosaurs do not have pneumatic foramina, while the later pterosaurs do have the foramina and are larger in body size (Claessens et al. 2009). Numerous studies have used a variety of techniques attempting to model the body mass of different pterosaurs (Witton 2008), particularly *Quetzalcoatlus northropi*. The results of these analyses are overall inconclusive, however, as the body mass estimate for *Q. northropi* ranges from 75kg to 250kg (Witton 2008). One study calculated the maximum size for a soaring bird was a wingspan of 5.1m and a mass of 41 kg, and concluded that larger pterosaurs may not have been able to fly (Sato et al. 2009). However, some extinct birds grew up to

wingspans of 6.1-7.9m with mass estimates of 70-80 kg (Vizcaíno and Fariña 1999; Ksepka 2014) and researchers have yet to doubt that they were successful soarers.

4.2.2 Avian postcranial pneumaticity and cortical thickness

Pneumaticity index. Pneumatized bones and air-sacs have typically been studied as a character present or absent in various bones across the avian skeleton. Researchers have used a pneumaticity index based on presence or absence of pneumatic foramina on skeletonized bones, a higher index indicating more bones have pneumatic foramina, a lower index indicating fewer pneumatic foramina (Wedel 2003; O'Connor 2004; Smith 2012; O'Connor 2009). O'Connor (2009) calculated the pneumaticity index for a range of birds across Aves and noted that both hyperpneumatization (high percentage of bones with pneumatic foramina) and reduced pneumatization (low percentage of bones with pneumatic foramina) appeared multiple times independently. The pneumaticity scores were plotted against log-transformed body mass and a positive correlation was found, with consistent differences discriminating between large soaring birds, generalized fliers, and specialized divers (P. M. O'Connor 2009). This regression did not take phylogeny into account, so Smith (2012) calculated the pneumaticity scores for a selection of waterbirds and found that pneumaticity and body mass had a weak but significant positive correlation, a relationship that also held up in a smaller subset of taxa (n=22).

This pneumaticity index would suggest that large soaring birds, like vultures and albatrosses, are pneumatized to the same extent, because both have the same index scores. On the other end of the spectrum, penguins and loons are diving birds which have no pneumatization, a feature thought to help reduce buoyancy as both groups are diving birds. But a vulture, a static soarer traveling via thermals off the land, and an albatross, a dynamic soarer using the wind currents over the water, have different biomechanical requirements and different skeletal

morphologies despite sharing similar pneumaticity indices. The penguin does not fly at all, but the loon has not given up flight and dives, but these two birds also share the same pneumaticity index. These examples suggest that there may be more to explore with regards to pneumatization and bone structure to understand potential driving factors of different wing bone structure.

Vertebral volume. Recent studies on skeletal pneumaticity in vertebrae seems to indicate that variation in skeletal pneumaticity may be due to behavior and function. Fajardo et al. (2007) compared the centrum of the third thoracic vertebrae of a non-diving duck (*Aix sponsa*) to a dedicated diving duck (*Oxyura jamaicensis*) around the same size (several specimens of each) and found that the diving duck's centrum is 48% bone (=52% air), and the non-diving duck centrum has 36% bone (=64% air). Gutzwiller et al. (2013) examined vertebrae from apneumatic divers and pneumatized non-divers in both Pelecaniformes and Charadriiformes and compared a sphere of trabecular bone volume/total volume of a mid-cervical to an anterior dorsal. They noted that their calculations were higher than those of Fajardo et al. (2007), but that could be due to the way they sampled: Fajardo et al. (2007) sampled the full centrum; in Gutzwiller et al. (2013), they sampled a spherical section of the anterior centrum with trabecular bone. Pelecaniforms supported the expectation that cortical bone was thicker in diving birds than non-diving birds (same with anseriforms from Fajardo et al. (2007)), but there was, however, no relationship between pneumaticity and diving/not diving behavior in charadriiforms (Gutzwiller et al. 2013).

Cervical and thoracic vertebrae are also structured slightly differently: charadriiforms often had thicker cortical bone in cervicals compared to thoracic vertebrae, but there was no difference in the pelecaniforms (Gutzwiller et al. 2013). The authors suggest that this may be due to the different stresses the vertebrae are under. Cervical vertebrae are much more mobile and

therefore are under greater varieties of stress and require more bone to safely absorb the stress compared to the thoracic vertebrae which are much more stable (Gutzwiller et al. 2013). In contrast to sampling subsections of vertebrae, Moore (2020) calculated bone and air volumes for several whole cervical vertebrae in storks (=Pelecaniformes), conducted 3d morphometrics on the bones, and compared the proportion (ASP) against morphology. The ASP dips around C7 and is highest at the base of the neck and changes in vertebra morphology were correlated with the ASP (Moore 2020). Together, these studies indicate that structure varies depending on differences in local function, not just whether a bird dives or not. As of writing this, there are yet to be any volumetric studies that analyze the composition of the whole humerus, a key bone in for wing-propelled locomotion, so I aim to fill this gap in knowledge.

Long bone cortical thickness. Another variable that is related to pneumaticity is cortical thickness of long bones and how much of the total radius is devoted to bone versus the cavity. This information is often presented as K, which is the portion of the radius devoted to the cavity and runs between 0 and 1 (Currey and Alexander 1985). The higher the value of K, the thinner the shaft walls. For example, an alligator femur has a very thick wall with a K of 0.35, and a pterosaur (*Pteranodon*) has a very thin wall with a K of 0.91 (Currey and Alexander 1985). Swartz, Bennett, and Carrier (1992) suggest that reduction of cortical thickness may be convergent in powered fliers, because bat long bones have relatively thinner walls compared to other small mammals, as do birds and pterosaurs. As a bone becomes more hollow, the bending strength decreases, but the torsional strength increases, which is believed to help with the torsional stresses experienced during downstrokes of powered flight (Cubo and Casinos 2000; De Margerie et al. 2005; Swartz et al. 1992).

4.2.3 This study

I hypothesize that even with phylogenetic signal taken into account, there will still be a strong relationship between quantitative variables (K, ASP) with functional variables (flight style) on a larger scale across Aves. The humeri experience stresses of flight in general and, with different kinds of flight styles (for instance, flapping more during take off or less frequently once in the air), there should be different structural responses, either in the overall volume of bone to air in the humerus or within the cortical thickness of the bone. By sampling species across Aves and comparing statistics relating to whole bone structure as well as shaft structure against functional and ecological variables using phylogenetic comparative methods, I bring key elements in previous literature together in one study to make large-scale comparisons regarding the structure of the archosaurian powered-flier humerus.

4.3 METHODS

4.3.1 Taxonomic sample and variables

In order to compare avian specimens across a range of body masses and behaviors, scan data were downloaded from MorphoSource. Eighteen specimens (one per species) were chosen across 16 families and 14 orders (per IOC World Bird List v10.2, (Gill et al. 2020)) at a range of body masses (from Dunning Jr. 2007) and the highest scanning resolution available (metadata from MorphoSource) (Suppl. Table 4.1). I included a penguin, auk, and loon in the dataset even though their humeri are marrow-filled (Smith 2012), because they would represent different kinds of diving birds and expand the ecological representation in the analyses. The measurement variables used in this chapter are air space proportion (ASP), log-transformed body mass (BM),

and K (ratio of cavity radius to total radius in a long bone shaft (Currey and Alexander 1985)). The functional or ecological variables used are flight style (FS) and category (Cat.) which indicates whether a bird is considered a landbird or a waterbird. Waterbird wing shapes and sternum shapes occupy distinct regions of avian morphospace from landbirds (Baumgart et al. (2021), Chapter 3), so I test for patterns associated with that relationship in pneumaticity. Flight style was tabulated for the study species following Bruderer et al. (2010) and Viscor and Fuster (1987) data, and interpolating within clades for species included here but not in those studies.

4.3.2 Humeral segmentation, volumes and cross-sections

Computed tomography (CT) scans were loaded into Mimics 22.0 and the humerus was segmented out in two volumes, the air volume (**Figure 4.1**, top) and the bone volume (cortical and trabecular; **Figure 4.1**, bottom). I then recorded the volumes of each as quantified by the program. These volumes were used to calculate the whole-bone air space proportion (ASP) calculated as $ASP = \frac{air\ volume}{air\ volume + bone\ volume}$ (Fajardo et al. 2007; Gutzwiller et al. 2013; Moore 2020; Martin-Silverstone and Palmer 2014; Wedel 2005). Previous research used the equation for whole-bone volumes, volumes from sections of bones, and two-dimensional cross-sections, so this method would be useful for drawing comparisons between vertebrate clades.

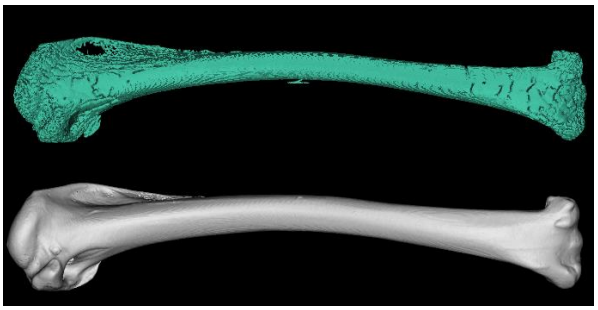

Figure 4.1 Volumes derived from the humerus of *Gavia immer*. Top: air volume (2776.9mm^3), Bottom: bone volume (1820.1mm^3), for an ASP of 60.4.

I also calculated a simple pneumaticity index (PI) for the bird wings, following O'Connor (2009). If the humerus did not have a large pneumatic foramen at the proximal end, the species received a PI of 0.0. If that foramen was present in the humerus, but there was no indication that the distal wing elements were pneumatized, the species received a PI of 0.5. If both humerus and distal wing elements had pneumatic foramina, the species received a PI of 1.0.

In addition to volumetric ASP ratios, I also measured the cross-sectional air space proportion in eight slices down the length of the humerus (**Figure 4.2**). This variable changes along the length of pterosaur wing bones (Martin-Silverstone and Palmer 2014) but has yet to be quantified for bird wing bones. Comparing these trends between different species would indicate how bone distribution may vary between animals of different sizes, clades or behaviors. This dataset permits interesting comparisons with the pterosaur wing bone data, because both birds and pterosaurs have developed an extensive pneumatic system beneficial for more efficient powered flight. Cross-sectional measurements were quantified in ImageJ2 (Rueden et al. 2017).

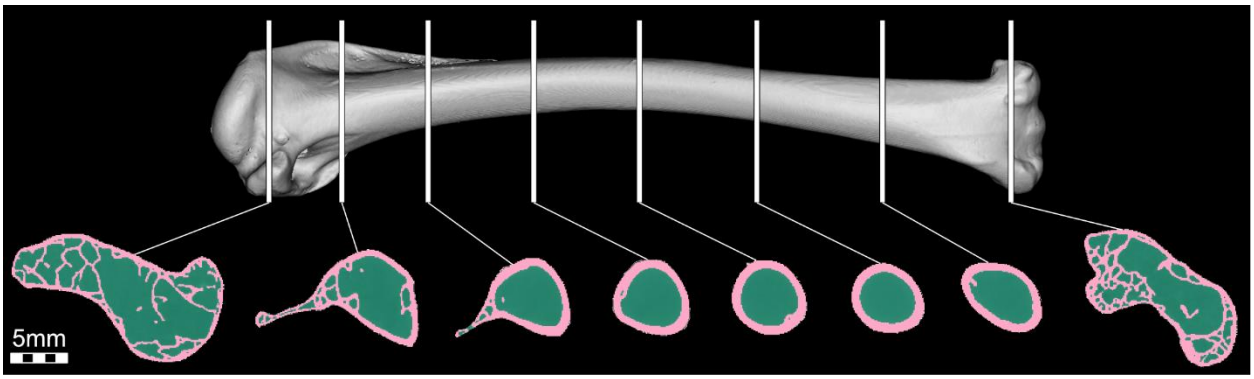

Figure 4.2 Eight cross-sections through the humerus of *Gavia immer* used to calculate volume distributions across the length of the humerus. Pink = bone, turquoise = air.

4.3.3 Analytical techniques

The phylogeny in this chapter was created with the Jetz et al. (2012) molecular phylogeny with the Hackett et al. (2008) backbone. A consensus tree was generated using TreeAnnotator in BEAST (Drummond and Rambaut 2007) with median node heights from 1000 full trees downloaded from BirdTree.org. The tree was pruned, ladderized and branch lengths calibrated using the 'ape' package in R (Paradis and Schliep 2019). Phylogenetic independent contrasts were calculated using *pic*() in the 'ape' package. The contrasts were tested for correlation using the Spearman's test and a linear model plotted using the base stats package (R Core Team 2020). The function *aov.phylo*() from the geiger package was used to calculate the (M)ANOVAs between the measurement variables and the functional variables (Harmon et al. 2008).

4.4 RESULTS

4.4.1 Volumetric pneumaticity

Volumetric pneumaticity (as measured by ASP) in the avian species tested here ranges from 21.6 in the penguin (*Spheniscus mendiculus*) to 71.3 in the shoebill (*Balaeniceps rex*), with the average at 58.0 (Suppl. Table 4.2, **Figure 4.3**). There is not a strong pattern in this selection of species as to what might be influencing the differences in ASP (adj. $R^2 = 0.04$, **Figure 4.4**A). The Andean condor (*Vultur gryphus*) is the heaviest bird tested (11,300g) and it has the same pneumaticity value as a bald eagle (*Haliaeetus leucocephalus*), a medium-weight bird (4740g) with similar behavior. The albatross (*Phoebastria irrorata*) is a large soaring bird, which should have a higher ASP value, yet it falls in the lower end of the range at 55.3, 10% lower than the brown pelican (*Pelecanus occidentalis*, 65.3). Within Anseriformes (*Chauna torquata*, *Aix sponsa*, *Cygnus cygnus*, *Branta hutchinsii*), there does appear to be a slight correlation between

body mass and ASP. When tested for phylogenetic signal, ASP does not have a significant signal (lambda=7.3E-5, p=1).

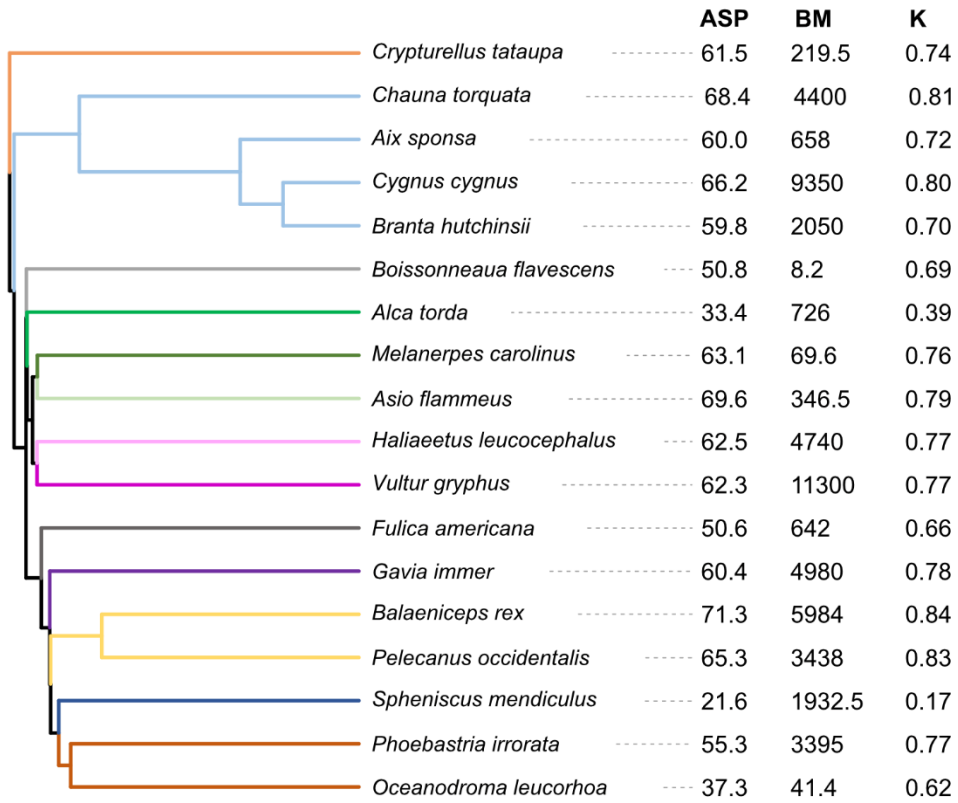

Figure 4.3 Humeral pneumaticity (ASP), body mass (BM, g), and cortical thickness (K) mapped onto the phylogeny.

The linear regression of ASP against log-transformed body mass shows a weak positive correlation between the variables (**Figure 4.4**A), made statistically significant once the penguin is removed from the dataset (**Figure 4.4**C). The regression of the phylogenetic independent contrasts supports this relationship, again with a weak positive correlation between ASP and body mass (**Figure 4.4**B) which becomes significant after removed the penguin (**Figure 4.4**D).

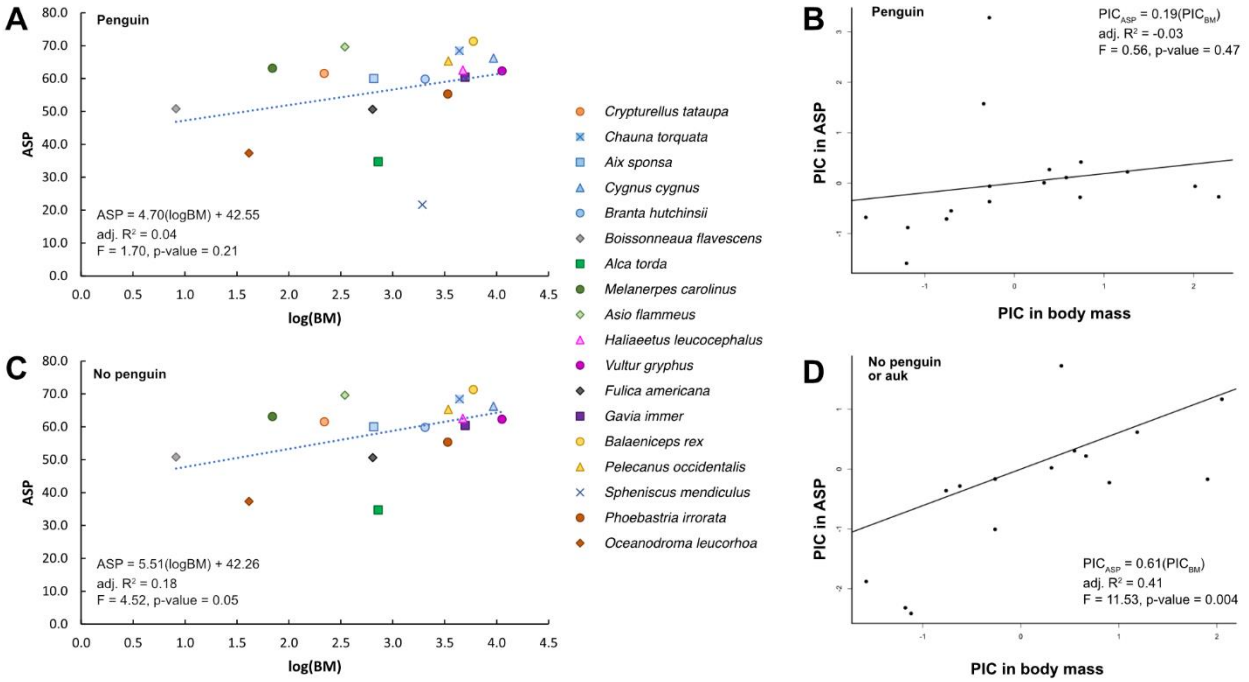

Figure 4.4 Traditional regression (A, C) and phylogenetic independent contrast regression (B, D) of ASP against log-transformed body mass with (A-B) and without (C-D) the penguin, *Spheniscus mediculus*. The auk, *Alca torda*, was also removed in (D), because it was an outlier.

4.4.2 Pneumaticity index as compared to humeral cross-sections

The pneumaticity index shows that most of the birds in this study have a pneumatized humerus but not distal wing elements (**Figure 4.5**A). A few species (*Vultur gryphus* and *Pelecanus occidentalis*, and *Boissonneaua flavescens*) are highly pneumatic with both humerus and distal wing elements pneumatized. Five species do not have a pneumatized wing skeleton: *Gavia immer*, *Alca torda*, *Spheniscus mendiculus*, *Oceanodroma leucorhoa*, and *Fulica americana*.

Like the volumetric approach, cross-sectional ASP data shows that there is a huge range in ASP (averaged across slices), but no strong explanations. Most of the humeral cross-sections are between 50 and 80, with a median of 60.6 (Suppl. Table 4.3, **Figure 4.5**B). The shaft of the American coot (*Fulica americana*) humerus has a relatively high cortical thickness. Interestingly, the petrel (*Oceanodroma leucorhoa*) has relatively high cortical thickness as well,

though as an avid flier, it would be expected to have a lower cortical thickness. The penguin (*Spheniscus mendiculus*) has a really thick humeral shaft, ASP less than 10, though both articular ends have ASPs in the 40s. The albatross (*Phoebastria irrorata*) has an ASP a little lower than the median (55.8 and 60.6 respectively) and a relatively low ASP in the shaft, low 50s. The pelecaniforms have the higher ASP scores of the waterbirds, followed by anseriforms, then the procellariforms. Averaging cross-sectional areas to get an ASP yields very similar results to those calculated from whole volumes (**Figure 4.6**), so this comparison is valid.

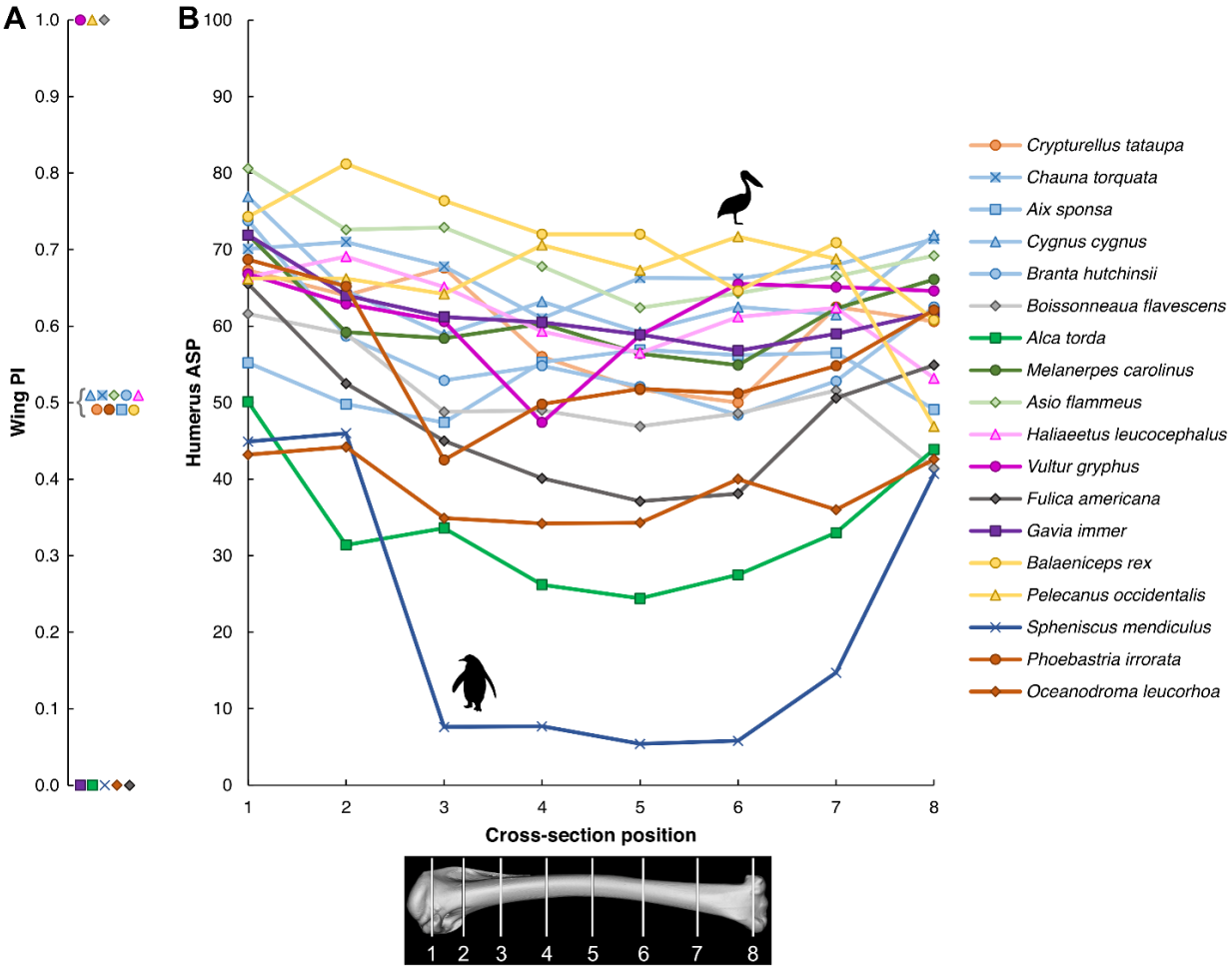

Figure 4.5 Different measures of pneumaticity. A) Pneumaticity index (PI) in the wing: 0, no wing elements pneumatized; 0.5, humerus pneumatized; 1, humerus and distal elements pneumatized. B) ASP plotted at each of the cross-sections for the specimens in this analysis, positions depicted in the image below the x-axis. The penguin and pelican icons were created by Steven Traver and Ferran Sayol respectively, both available on phylopic.org.

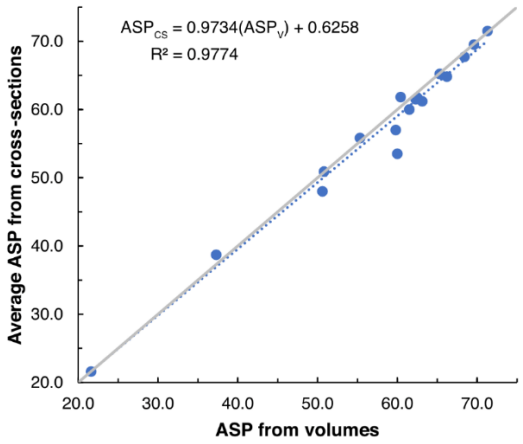

Figure 4.6 Comparing the two methods of calculating ASP in the avian humeri. Grey line indicates x=y.

4.4.3 Covariance of pneumaticity, cortical thickness and flight function

Many relationships regarding structure and function tested with this dataset remained insignificant, though cortical thickness did influence most of the significant ones (**Table 4.1**). The penguin was an outlier, so these analyses were done both with and without the penguin. The combination of ASP and BM was weakly significant in terms of whether the bird was categorized as a waterbird or a landbird when corrected for phylogenetic relationships, with and without the penguin ($p = 0.072$ and $p = 0.087$ respectively). Cortical thickness (K) was highly significant with flight style until the penguin was removed ($p = 2.0E\text{-}3$ and $p = 0.381$, respectively). Both MANOVAs with ASP, BM, K against flight style and category were significant with the penguin ($p = 5.0E\text{-}3$ and $p = 0.090$ respectively), but lost significance without the penguin ($p = 0.381$ and 0.173, respectively). These results show that the penguin is a highly influential data point and should not be considered further without additional species to make the analyses more robust against the penguin. The main result of these analyses indicates that there is no strong relationship between the measurement variables and functional variables used in this study, except for the relationship of pneumaticity and body mass with bird category (waterbird vs. landbird).

Table 4.1 Phylogenetically corrected (M)ANOVAs correlating different measurement variables against functional variables. Abbreviations: ASP, air space proportion; BM, log-transformed body mass; K, cortical thickness ratio; FS, flight style; Cat., category (waterbird vs. landbird).

	With penguin and auk				Without penguin and auk			
	F	Wilks	p	p w/phylo	F	Wilks	p	p w/phylo
ANOVA: ASP, FS	1.88	--	0.172	0.166	0.23	--	0.941	0.935
MANOVA: BM, ASP, FS	--	0.16	0.036	0.042	--	0.37	0.367	0.399
ANOVA: ASP, Cat.	1.27	--	0.277	0.213	0.23	--	0.638	0.638
MANOVA: BM, ASP, Cat.	--	0.70	0.071	0.065	--	0.69	0.088	0.087
ANOVA: K, FS	4.37	--	0.017	0.018	0.40	--	0.836	0.838
MANOVA: ASP, BM, K, FS	--	0.073	0.033	0.030	--	0.21	0.389	0.381
ANOVA: K, Cat.	0.87	--	0.365	0.326	2.6E-5	--	0.996	0.998
MANOVA: ASP, BM, K, Cat.	--	0.64	0.092	0.060	--	0.68	0.187	0.173

I conducted a phylogenetic multiple regression with ASP, BM, and K to determine if multiple interacting predictor variables are able to represent the relationship between them better than pairwise comparisons (**Table 4.2**). The best supported interaction is that K is predicted by the interaction between BM and ASP, because this interaction had the lowest AIC (-46.98) and the highest log-likelihood (28.49) out of the combinations tested. The ASP term is not a significant contributor to the model, but because the higher-order interaction term BM*ASP is significant, the ASP term should remain in the model.

Table 4.2 Multiple PGLS regression of different combinations of ASP, BM, and K for the avian species using the Brownian correlation structure and the maximum likelihood model. Int = intercept.

	Coefficients		p-values	AIC	Log-likelihood
ASP ~ BM*K	Int:	-110.31	0.0067	100.43	-45.21
	BM:	36.69	0.0004		
	K:	226.64	0.0043		
	BM*K:	-47.93	0.0061		
BM ~ ASP*K	Int:	6.43	0.0224	47.98	-18.99
	ASP:	-0.11	0.0440		
	K:	-8.22	0.3227		
	ASP*K:	0.200	0.0677		
K ~ BM*ASP	Int:	0.74	0.0029	-56.42	33.21
	BM:	-0.25	0.0023		
	ASP:	8.1E-5	0.9828		
	BM*ASP:	0.004	0.0039		

4.5 DISCUSSION

4.5.1 Humeral pneumaticity across Aves

Several pairwise comparisons show that, even though a bird may have the same pneumaticity score, there are structural differences between the humeri of different species. For example, even though both the penguin (*Spheniscus mendiculus*) and the loon (*Gavia immer*) are pursuit divers (Smith 2012), the loon has much thinner cortical bone than the penguin, placing the loon with the rest of the flying birds. Being flighted, loons retain a more circular humerus (**Figure 4.7**M) like other fliers to better resist torsional stresses of the aerial downstroke, whereas penguins (**Figure 4.7**P) have adapted to the demands of aquatic locomotion by dorsoventrally compressing the wing bones into a flipper, allowing locomotor mechanics similar to the Surf perch, *Cymatogaster aggregata* (Clark and Bemis 1979). The auk (*Alca torda*) also has a dorsoventrally compressed humerus (**Figure 4.7**G), though not quite to the degree of the penguin and it is still able to fly. Furthermore, as the largest and heaviest soaring bird, the Andean condor

(*Vultur gryphus*) does not have an unusually large ASP, the trend of its cross-sectional areas and K indicate that it is not that structurally different from the bald eagle (*Haliaeetus leucocephalus*), which exhibits similar soaring behavior. The pelecaniforms are lighter soaring birds but are more pneumatized and have thinner cortical walls. This comparison between large soaring landbirds and large soaring waterbirds may suggest that waterbirds did something structurally different to allow for a thinner skeleton than landbirds.

The wing PI also illuminated a very interesting cluster for comparison, the three species with the highest index. The Andean condor (*Vultur gryphus*) is the largest, heaviest species included in this dataset and is considered a landbird, using thermals to glide around inland regions at relatively high altitudes. The brown pelican (*Pelecanus occidentalis*) is a large coastal bird that has periods of flapping and gliding then will plunge dive to stun and catch prey, The buff-tailed coronet (*Boissonneaua flavescens*) is a tiny hummingbird that flits around flowers, drinking the nectar. The first two are large soaring birds and fit with the narrative relating pneumaticity to body mass. The hummingbird is the smallest bird in the dataset, yet pneumatic foramina were found on both proximal and distal ends of the humerus as well as distal wing bones like the ulna. Perhaps the unique aerial capabilities of the hummingbird and extreme wingbeat frequency require as little bone as possible in the wing skeleton. It would be interesting to further study the hummingbird skeleton and see if the rest of the skeleton is extensively pneumatized or not.

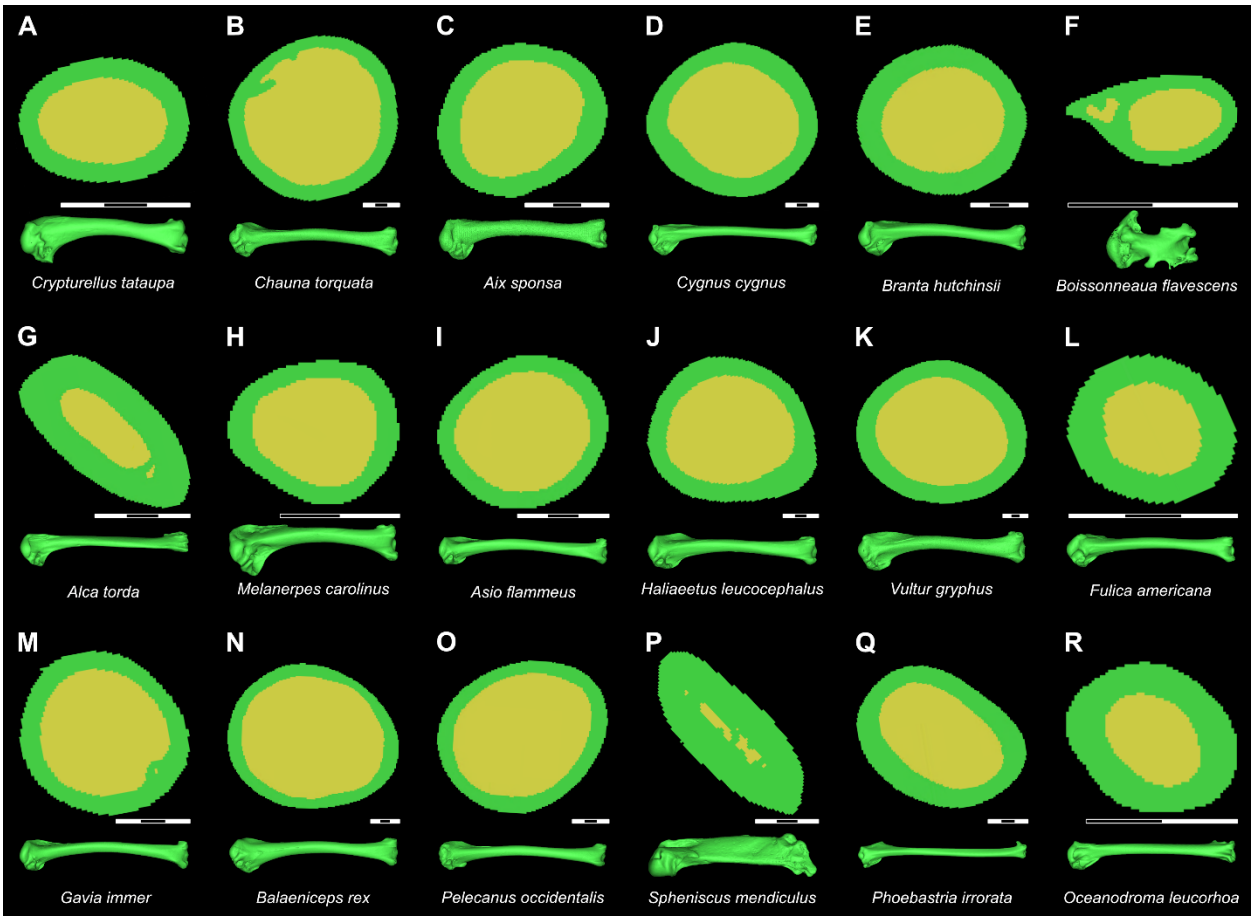

Figure 4.7 Mid-shaft (5th) cross-sections of the humerus. Cross-section scale bar is 3mm except for F, H, and R which are 2mm scale bars. Anterior is at the bottom of the cross-section, posterior is at the top. Whole humerus renderings are not to scale, posterior view. Humeri are positioned with proximal on the left. Created from CT scan data available on Morphosource.org.

Humeral morphology may also be coming into play regarding the ASP differences. The albatross is often lauded as built for efficiency and has extremely long narrow wings which would be energetically costly if they were flapped frequently or weighed too much. The albatross humerus is narrow, straight, and the shaft changes little in diameter (**Figure 4.7**Q). However, the humeri that are most hollow are proportionally wider in diameter and have a bit of a sinusoidal curve to their shaft (**Figure 4.7**N) Perhaps the thicker shaft walls in the albatross humerus are a way to provide additional strength to the straight bone. Further study of skeletal morphology in

relation to flight patterns, both take-off and horizontal travel, may yield further insights into the relationship between pneumaticity and different humeral shaft shapes.

Cross-sectional geometry of the humerus yields additional information about the primary use of the bone. Simons et al. (2011) examined the wing bones of a few pelecaniform species wtih at CT scans and comparing cross-sectional geometry between birds and down the wing (humerus, ulna, carpometacarpus. They found that gliding birds tend to have more circular humeral and carpometacarpus cross-sections, which are key for resisting torsional loads, whereas birds that flap more frequently have more elliptical shapes, which are key for resisting bending loads. The diving species also had thicker cortical bone which is key for resisting compression loads. Diving birds in this study include the auk and the penguin, which show highly elliptical and very thick cortical bone, indicating they are very well adapted for resisting both bending and compression, ideal for long deep dives, "flying" through the more viscous water.

However, the loon, another diving bird, still has a fairly circular cross-section and the cortical bone is not abnormally thick, indicating that its wings are still highly adapted for flight in air. The procellariiforms (albatross **Figure 4.7**Q, petrel **Figure 4.7**R) have slightly elliptical cross-sections with cortical bone on the thicker side, indicating their bones are also under higher amounts of bending stress, even though the albatross is predominantly a glider and therefore should have more circular cross-sections. As high-frequency flappers, the anseriforms (**Figure 4.7**B-E) should have more elliptical cross-sections to resist bending. Instead, they are mostly circular (*Aix sponsa* having a slight elliptical shape, **Figure 4.7**C) with thicker cortical bone compared to the pelecaniforms in this study. More specimens need to be included in these sorts of studies to better track the wide range of cross-sectional geometry across birds in association with biomechanical properties and flight.

4.5.2 Implications for Pterosauria

Pterosaurs are the other major lineage of vertebrates with powered flight that evolved a pneumatized skeleton. Previous work shows that the K and ASP of various pterosaur wing bones overlaps with birds, but also expands into higher ranges; for example, the K of the *Pteranodon* first wing phalanx is 0.91 (Currey and Alexander 1985; Martin and Palmer 2014). The ASP data for the pterosaur *Bennettazhia* was added to the cross-section plot (**Figure 4.9**) to compare the bird data with a 3-4m wingspan pterosaur, which is on par with the condor wingspan. The ASP for *Bennettazhia* is the highest, with a large difference between itself (average CSs = 80.9) and the condor (*Vultur gryphus*, average CSs = 61.5, volumetric ASP = 62.3). The average ASP of the single *Bennettazhia* humerus is 80.9 (Martin and Palmer 2014), whereas the highest ASP for avian humeri tested here is 71.3 in the shoebill stork (*Balaeniceps rex*), the waterbird with the longest wingspan (~3m (Fletcher 1979)) and heaviest body mass (~6kg) in this dataset. The landbird with the largest wingspan is the Andean condor (*Vultur gryphus*) at 3.2m (Myers et al. 2020), ASP of 62.3, and weighs around 11.3kg which is the highest overall mass in this dataset. *Bennettazhia* is estimated to have a wingspan of 3-4m (pers. comm. Michael Habib), but pterosaur body mass is very difficult to predict due to uncertainty regarding soft tissue reconstruction (ex: Witton 2008). Even with this information, the range in ASP is striking for three animals with similar wingspans. I calculated K for the *Bennettazhia* humeral shaft using CT scan data provided by Michael Habib and Evan Garofalo and got 0.889. Martin-Silverstone and Palmer (2014) state that ASP tends to be equivalent to K^2, which would yield a *Bennettazhia* humerus K of 0.89, so our data are in agreement. This K is also similar to that calculated by Currey and Alexander (1985) for a *Pteranodon* first wing phalanx, 0.91. The square of 0.91 yields an estimated ASP of 0.828, which I can multiply by 100 to match the scale of my other

ASP values. If I add the pterosaurs to a plot of K vs. ASP in birds, they fit right in line with the rest of the data (**Figure 4.10**).

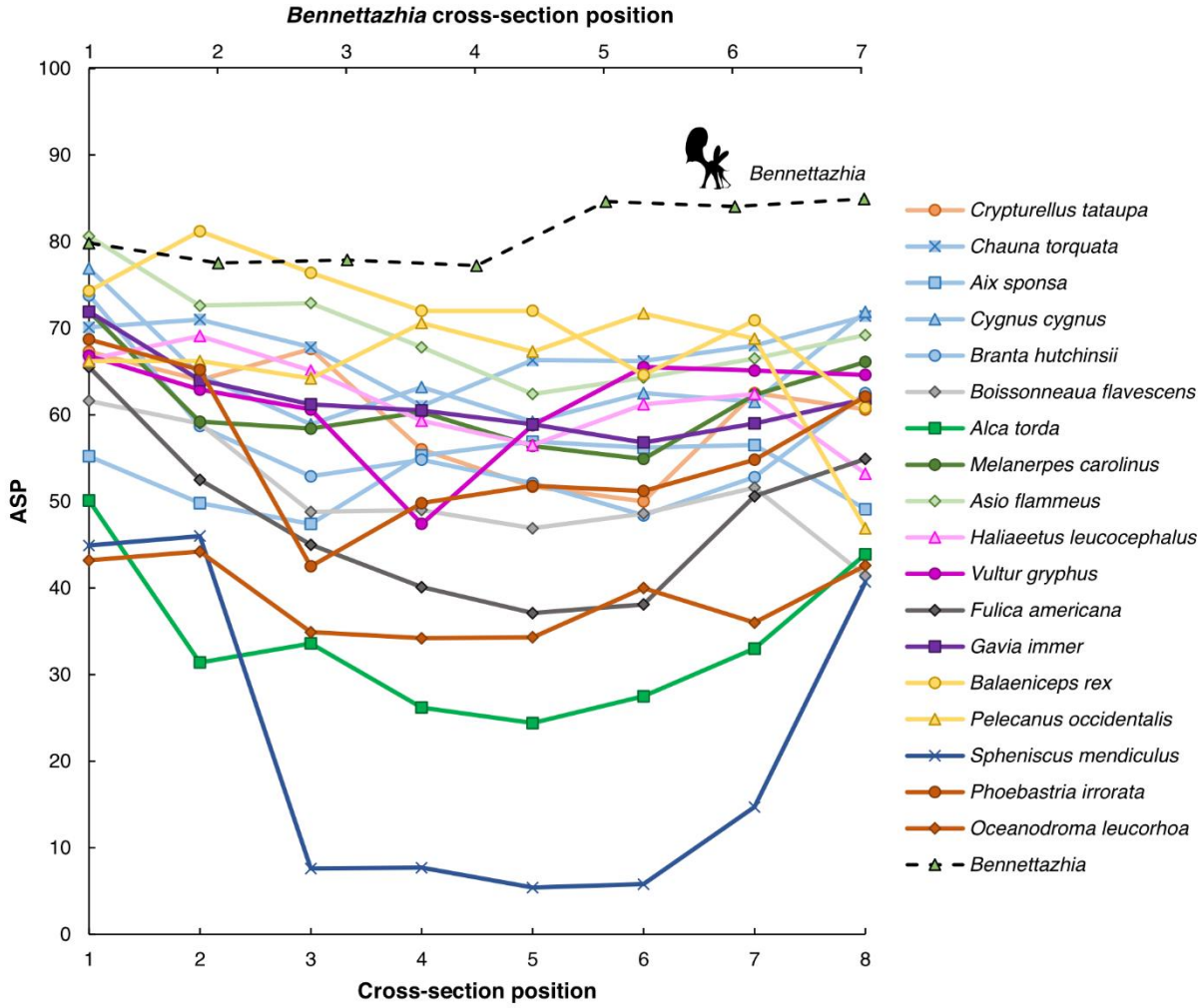

Figure 4.8 Cross-sectional ASP with *Bennettazhia oregonensis*. Solid lines, birds. Dotted line, pterosaur. Data for the *Bennettazhia* humerus was acquired from Martin and Palmer (2014). The icon is *Tapejara* (another tapejaromorph like *Bennettazhia*) created by Jaime Headden and shared on phylopic.org under the CC By 3.0 license.

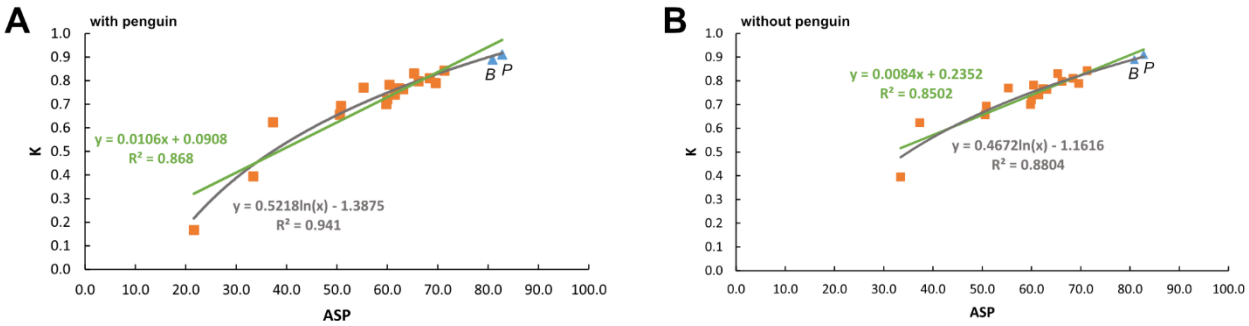

Figure 4.9 Plots of K vs. ASP with (A) and without (B) the penguin. Squares = birds, triangles = pterosaurs. B = *Bennettazhia oregonensis* humerus, P = *Pteranodon ingens* first wing phalanx.

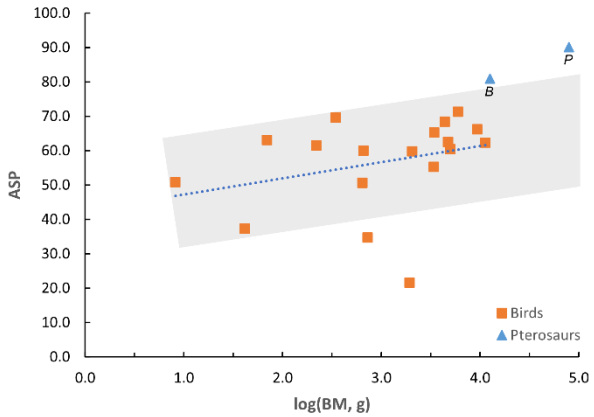

Figure 4.10 ASP vs. log-transformed body mass of birds and pterosaurs. B, *Bennettazhia oregonensis*; P, *Pteranodon ingens*. Pterosaur body masses estimated using the calculation $M_{bm} = 0.519b^{2.550}$ from Witton (2008), where M_{bm} is body mass and b is wingspan. Wingspan estimates were 3.5m (*B*) and 7m (*P*). Grey box represents an interval that contains most of the birds, centered around the regression, to contextualize the pterosaur data.

This result suggests that some of the larger pterosaurs do have higher ASP and K than modern birds, but the clade may be approaching the maximum values before maxing out on wingspan. As mentioned earlier, *Bennettazhia* is about 3-4m wingspan. The *Pteranodon ingens* wingspan for that specimen is almost 7m (Bramwell and Whitfield 1974). The largest pterosaur, *Quetzalcoatlus northropi* has a wingspan estimate of over 10m (Witton 2008; Martin and Palmer 2014). Cross-sectional data from *Quetzalcoatlus* are not currently available, but structurally, a pterosaur wing bone, especially that of the largest pterosaurs, would need to maintain a certain cortical thickness in order to resist torsion during flight and bending stress from any impacts the bone may have during day-to-day life. Currey and Alexander (1985) propose that the *Pteranodon*

is pneumatized with the goal of weight-saving, whereas birds optimized for sturdier bones as "adaptations for the fairly rough-and-tumble lifestyle most birds lead." As an interesting counterpoint, pterosaurs have also been hypothesized to be quadrupedal animals when on the ground, and even launch into the sky quadrupedally (Habib 2008), so the pterosaur humerus would also be experiencing compression stresses pivoting around the bone as well, which is not a stress experienced by bird humeri.

Calculating pterosaur mass estimates and plotting them onto the avian ASP versus body mass plot, pterosaurs fall above what the avian trend would likely predict (**Figure 4.11**). Pterosaur body masses are estimated using the derived equation for calculating pterodactyloid body mass from wingspan, $M_{bm} = 0.519b^{2.55}$, from Witton (2008) and estimated wingspans of 3.5m and 7m for *Bennettazhia* and *Pteranodon* respectively. This equation yields a body mass estimate of 12.7kg for *Bennettazhia* and 74.2kg for *Pteranodon*. A wingspan of 3.5m is a bit larger than any birds used in the dataset, so *Bennettazhia* being a bit heavier than the heaviest bird would be reasonable. Even if the mass estimates were off, they would have to be off by an extreme amount, almost an order of magnitude, to fall within the grey interval extrapolated from the bird data. Additional pterosaur specimens would be critical for solidifying this point, but the preliminary data suggests pterosaurs were doing something a little bit different in their wing bone structure to adapt with extra pneumatic bones compared to birds.

4.6 CONCLUSION

In summary, there is a weak but significant correlation between log-transformed body mass and avian ASP, indicating that birds generally increase in ASP as they get larger, though extant birds seem to reach a limit of low 70s. Most of the measurement variables tested in this study did not yield strong predictive relationships with flight style or landbird-waterbird

categorization, except the combination of body mass and ASP had a weakly significant relationship with whether a bird was a landbird or a waterbird. Birds highly adapted for diving have highly compressed humeri, procellariforms have slightly elliptical humeri, and others have mostly circular humeri, which opens up avenues for further research on correlations between cross-sectional geometry and flight behavior. When comparable or larger pterosaurs are added to the avian data, the ASP and K values are higher than those that would be predicted by extant birds, suggesting pterosaurs were structuring their bones under different constraints than birds.

CHAPTER 5

Conclusion

In this work I examined three components of the avian flight apparatus— wing shape, sternum shape and humeral pneumaticity. These relate, respectively to flight performance, the form of the primary anchor for flight muscles, and structure (degree of pneumatic hollowing) of the proximate and principal bone of the wing. I compiled quantitative measurements and landmarks to search within each of these components for correlations with known functional or ecological variables in birds.

Each of these three foci include the construction of a dataset of broad scope among avians. The first includes 136 waterbirds and investigates how wing shape varies in relation to function and ecology. That sampling includes many, but not all, of the birds in Wang and Clarke (2015) landmark pan-avian study on wing shape. I selected a subset of birds, an assemblage referred to as waterbirds, which was particularly suited to questions of form and function given their functional and ecological diversity. The second study includes 128 birds across Aves and investigates how sternum shape varies, as captured by a set of three-dimensional landmarks. Previous work was limited to analysis of select linear measurements in a smaller sampling of birds without broader comparative analysis. The third study involves 18 birds and used CT scans to look at the internal structure of the humerus in avians across a wide range of body masses, ecological niches and flight styles.

5.1 MAJOR CONCLUSIONS

Convergence of form is widespread in the avian flight apparatus. Wing shapes, both high and low aspect ratio wings, are convergent in birds of similar and distinctive ecologies. The same

holds for sternal morphology, for which there are convergent groups with similar flight styles, (birds with short bursts of flight versus gliding/soaring birds) as well as birds with disparate flight styles and ecologies. Sample size requires expansion for reliable convergence testing in humeral pneumaticity, although volume and cross-sectional shape data suggest that the auk and the penguin have convergent structure for deep, sustained diving. Future work could combine wing shape and sternal shape in the same species to search for convergent patterns involving both parts of the flight apparatus.

Morphology correlates with flight function and ecology to different degrees in the different parts of the avian flight apparatus. As wings are used to navigate through, and interact with, the environment, more ecological variables were tested with this study. Foraging behavior and habitat were significant, but flight style and migration were not. The sternum does not interact with the environment directly, but anchors flight muscles, and its morphology is correlated with flight style. Humeral pneumaticity (ASP) is a structural feature that helps redistribute mass and would strengthen the bone against torsional stresses, but it is not correlated with flight style and only weakly correlated with body mass. These results are not necessarily saying form is not linked to function, but that perhaps the current set of variables and categorizations with data available for many species do not fully capture the complexities of the flight apparatus's function and behavioral repertoire. Many-to-one mapping may also be a factor: a single structure or shape could be sufficient for multiple behaviors and therefore there is no additional selective pressures to evolve further in a specific direction.

Waterbirds and landbirds extend into different areas of morphospace, suggesting further avenues of research. My study on waterbirds did not incorporate landbirds, but the morphospace in Wang and Clarke (2015) shows that waterbirds and landbirds overlap slightly in the center,

and then waterbirds expand into lower PC 1 values and landbirds into higher PC 1 values. My sternum data show a similar pattern, with more of an overlap in the center and waterbirds expanding into lower PC 1 values and landbirds into higher PC 1 values. The only significant phylo-MANOVA for humeral pneumaticity was predicting waterbird/landbird designation using the interaction of body mass and ASP. For the sternum, the main groups of waterbirds separating out were the large soaring birds and cormorants on one end, and the landbirds that use short bursts of flight and the hoatzin on the other. Rails converge on the short burst flight with the tinamous, but it would seem this variety of fast escape behavior is not found as often in waterbirds as landbirds. Both waterbirds and landbirds have gliding/soaring species, but the waterbird soarers have lower PC 1 and PC2 values than the landbird soarers which have a more central location in the morphospace. More work would have to be done to determine whether this is evolution of two different solutions to the same flight needs or evolution of two solutions for two different kinds of needs. Air density is known to affect wingbeat frequency (Pennycuick 2008) which is part of flight style, so perhaps taking off at sea level vs higher inland altitudes would require different sternal structures to yield similar behavioral results in different air densities. Humeral pneumaticity is more difficult, because bird humeri face rapidly changing stresses from many different directions during flight. Both the highest ASP (pelecaniforms) and lowest ASP (auk and penguin) are found in waterbirds, whereas landbirds have a smaller range in ratios.

5.2 PLASTICITY IN BIRD MORPHOLOGY AND BEHAVIOR

One of the other considerations in looking at this data is plasticity exhibited by birds and how it affects representation of their ecology and function. Liem's paradox describes the situation in which what is evolutionarily expected - a tight link between morphology and ecology, for

example - does not seem to be upheld by the data. One might expect that bird wings should be in very discrete areas of morphospace given the different uses each kind of wing would have. Yet, only extreme morphs separate out, leaving a centralized cluster that includes a wide variety of behaviors and characteristics with a more generalized wing shape. The same generalist vs extremist distribution was seen in bird sterna.

Functional and biomechanical metrics are influenced by many factors, and values are often studied using a single point within a range of possible values. For example, wing area and wing loading vary depending on flight speed. The faster the bird flies, the tighter the feathers are together, reducing wing area and increasing wing loading (**Figure 5.1**). Flight speed and wingbeat frequency is also dependent on air density: the denser the air, the slower the flight speed and wingbeat.

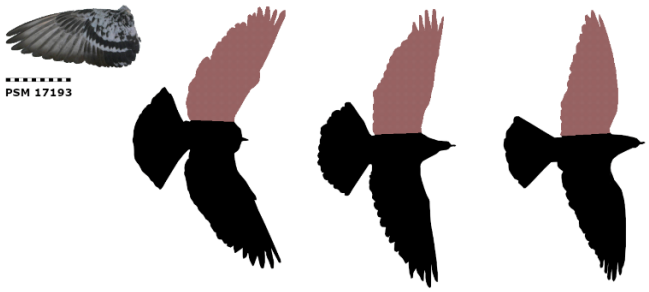

	Slow ($6\ ms^{-1}$)	Intermediate ($10\ ms^{-1}$)	Fast ($16\ ms^{-1}$)
Wing area	$306.7\ cm^2$	$278.4\ cm^2$	$255.3\ cm^2$
Wing loading	$12.0\ kg/m^2$	$13.2 kg/m^2$	$14.4 kg/m^2$

Figure 5.1 Schematic illustrating variation in wing shape at different flight speeds. Silhouettes based on pigeon outlines in Figure 3A from Tobalske (2007), adapted with permission from The Company of Biologists, Ltd. Wing image with scale bar scaled to silhouettes to help estimate wing area and calculate wing loading. Wing image from University of Puget Sound's Slater Museum of Natural History's online Wing and Tail Image Collection.

Body mass and composition are constantly changing too. Eating food increases body mass, and birds ingest even more if they have to feed hungry chicks. Long-distance migrants cycle between hypertrophied flight muscles with atrophied nutritional organs (viscera, liver,

kidneys) during the migratory phase and atrophied flight muscles with hypertrophied nutritional organs during the non-migratory phase (Weber and Hedenström 2001). Before the migration, nutritional organs are reduced via autophagy by at least 50% to make room for lightweight energy-rich fat stores and the heart and flight muscles are enlarged. Upon arrival, the organs are built up again, and the heart and flight muscles are reduced. The black-necked grebe (*Podiceps nigricollis*) takes this to the extreme, reducing flight muscles to the point where these birds become flightless during their stay (**Figure 5.2**; Jehl 1997). Their hindlimbs also fluctuate in size, becoming larger during their non-migratory phases, and reduced during their migratory phases.

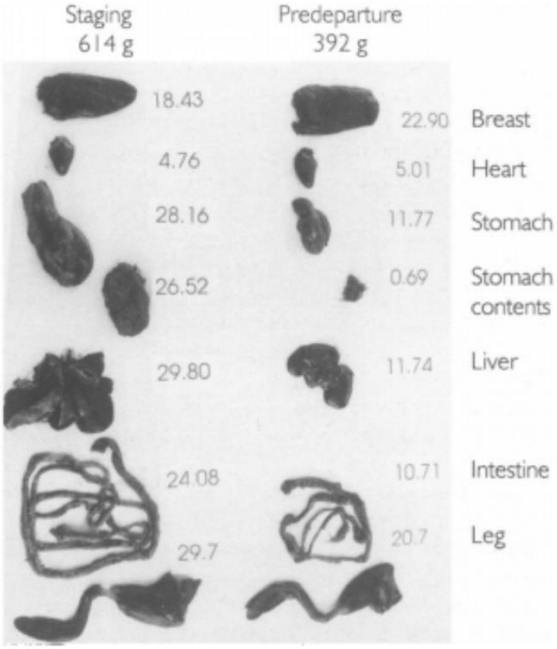

Figure 5.2 Mass and size of different organs in *Podiceps nigricollis* at the non-migratory phase (left) and just before migrating (right). Reproduced from Figure 3 in Jehl (1997) with permission from John Wiley and Sons publishing.

Birds also have plasticity with regards to their behavior. The flight style categories as defined by Viscor and Fuster (1987) are descriptive yet limited, as an analysis with those variables captures one kind of flight, and birds often exhibit multiple kinds of flight.

Hummingbirds are noted as having “hovering flight,” indicating they are highly capable and specialized for hovering, but they also have to travel between food and nest sites, some migrating, so they would also exhibit “forward/bounding flight.” Birds marked as “short flight,” tend to stay on the ground most often, but have short bursts of flight to escape predators or travel short distances. While this description is attributed to galliforms, rails, and tinamous, one could argue that passerines with “forward/bounding flight” also must execute a “short flight” escape response, suddenly leaping off tree branches and making a beeline for the closest cover or safe haven. The angle and acceleration of a particular escape response is modified based on how close the predator is (how eminent the danger), whether there is cover close by or not, and the properties of the takeoff and landing perches (Kullberg and Lafrenz 2007).

Availability of food resources and nutritional requirements also influences a bird’s behavior. Ducks will vary their diet, either for opportunistic reasons or needing different things before or after migration (Janke et al. 2019). Sometimes the weather patterns result in different food sources being available (Janke et al. 2019), so they must be open to a sufficiently large range of food or they will starve. Parrots have also been known to either chose different food sources when their preferred food is scarce or fly farther away to find their preferred food (Renton et al. 2015).

All of these examples of structural and behavioral plasticity indicate that trying to classify birds using single variables for any of these categories is inherently difficult. Currently available categories, like those used in this dissertation, assume a static state of being, even though it is apparent that there are primary flight styles and secondary flight styles, or a range of physical compositions throughout a given year. The studies conducted here establish comparisons between clades, behaviors, etc. using a single snapshot of morphology and the latest

techniques to learn more about the range of adaptations in Aves, but the next step would necessarily be looking at the ranges of these variables across Aves.

5.3 TRADE-OFFS IN FORM AND FUNCTION

Discussions regarding evolution often focus on trade-offs – an organism specializes for one thing and reduces its capability to do something else. These trade-offs are often compared between species, comparing different wing aspect ratios, sternum dimensions, or the proportion of air to bone. But, as illustrated above with the grebe, an individual can undergo significant morphological and physiological changes within a given migration cycle. An individual bird has the potential for adjusting its morphology to optimize for different functions, either long-distance flying or eating lots of food and building up its stores of energy; the extent it can vary likely depending on the species and its particular requirements. Robinson and Wilson (1998) proposed a resolution to Liem's paradox by showing cichlids adapt to new feeding niches but retain the ability to use alternate niches when their preferred food is scarce. Looking at the bird data and analyses presented here, this thinking can be applied not just to feeding adaptations, but locomotion as well – birds specialize, but they also need to be flexible in terms of how they move within different environments, in changing weather conditions, and with regards to goals that change across an annual cycle (migrating, breeding, etc.).

Recalling Louis Sullivan's statement in the introduction, he also said "where function does not change form does not change." The amount of plasticity seen in individual birds indicates that the relationship between form and function is indeed very tight: birds are constantly changing their bodies and how they use them to match constantly changing needs throughout their lives. Wings are much easier to change shape than sterna or pneumaticity once

fully developed, which may be part of why it was more difficult to track the relationship between form and function in the wings.

5.4 FUTURE WORK

The elements I focused on (spread wing image, isolated sterna and humeri) are in isolation from the rest of the bird. As discussed briefly in the previous section, a bird wing goes through a huge range of configurations, and a static spread wing does little to capture that range. It would be worth digging into this further, to try and determine which phase during flight a spread wing is most similar to, if any. A middle portion of the downstroke or a gliding position would be likely candidates, because the wing is outstretched to the side at these times, not unlike a spread wing. This would have to be studied using multiple cameras to record flight of live birds in a wind tunnel, and landmark wing joints and feather positions in a similar fashion as the wing shape study, but in three dimensions to capture the range of a bird's wing shape during steady flight.

Sternum morphology was studied in isolation, so studying sternum morphology in relation to the ribcage, shoulder girdle, vertebrae and overall posture would give more information about other possible influences on sternum morphology relating to flight. An informative analysis would involve conducting a larger scale 3D geometric morphometric study using fluid-preserved whole specimens and landmarks placed throughout the pectoral girdle, ribs, and vertebrae.

Sternum morphology also cannot be studied without looking at the muscles, their mass, cross-sectional geometry, and fiber direction to truly understand how this system works together to power different kinds of flight and navigate through a variety of air conditions. The methodology to do some of this muscle work has been developed using European starlings

(*Sternus vulgaris*) with digital renderings of the pectoral muscles including fiber length and direction (S. P. Sullivan et al. 2019), and combining this sort of muscle data with morphometric skeletal data would strengthen comparisons across a wide range of taxa with a wide range of functional and ecological variables.

Analyzing pneumaticity in the humerus yielded some interesting results, but extending the techniques to look at whole-volume ASP and ASP from cross-sections down the length of the remainder of the wing bones would show how this tract of air sacs continues to influence wing bone geometry and properties. A case study in Pelecaniformes indicates that there are biomechanical changes across the wing that would result in different cross-sectional geometries (Simons et al. 2011). Expanding my dataset to include the ulna and the carpometacarpus and to more avian species would help enhance our understanding of the variation of pneumaticity across Aves and would be an even stronger foundation for comparing avian skeletal pneumaticity to pterosaur skeletal pneumaticity. Additional research would involve building a dataset with a single selection of species featuring wing shape, sternum shape, and humeral pneumaticity data. With such integrated data, I would be able to test hypotheses of co-evolution and trade-offs between these three features within birds. Studying the sternum morphology in relation to its position in the thorax and to the additional bones in the pectoral girdle (coracoid, scapula, furcula) *in situ* would also be valuable for understanding the full complexity of pectoral girdle morphology and morphological trade-offs. Using CT data to quantify pneumaticity and bone structure in the other main wing bones (ulna, radius, carpometacarpus) in relation to ecology across Aves would be critical for tracking how those variables change along the bird wing. Simons et al. (2011) began part of this work using a small number of pelecaniform species, finding there were correlations between bone cross-sectional shape and flapping or gliding, but

scaling these sorts of studies up to all of Aves would further complete the picture and help better establish large scale patterns of bone morphology.

Going even further, I can adapt and expand these techniques and create datasets that compare the three groups of volant vertebrates: birds, bats, and pterosaurs. I can examine bird wings, bat wings, and pterosaur wing estimates using landmark-based morphometrics to make direct comparisons in the degrees of change across the wing and the shapes of the morphospaces. All three clades have keeled sterna, so comparing sternum shape across birds and bats to capture the degree of variation within clades in three dimensions would be valuable when comparing that to either reconstructed pterosaur sterna or two-dimensional images of the ventral view (for example specimens, see: Jiang et al. 2016). Some work has been done on pneumaticity in pterosaur wing bones (Martin and Palmer 2014) and cross-sectional geometry in bats (López-Aguirre et al. 2021), but adding that data to my data in birds, adding fossil birds where possible, and adding volumetric data from bats would show overall trends in pneumaticity throughout flying vertebrates.

REFERENCES

Adams, Dean C., Michael L. Collyer, and Antigoni Kaliontzopoulou. 2020. *Geomorph: Software for Geometric Morphometric Analyses. R Package Version 3.2.1*. https://cran.r-project.org/package=geomorph.

Aiello, Brett R., Mark W. Westneat, and Melina E. Hale. 2017. "Mechanosensation Is Evolutionarily Tuned to Locomotor Mechanics." *Proceedings of the National Academy of Sciences* 114 (17): 4459–64. https://doi.org/10.1073/pnas.1616839114.

Alexander, David. 2015. *On the Wing: Insects, Pterosaurs, Birds, Bats and the Evolution of Animal Flight*. New York, NY: Oxford University Press.

Bahlman, Joseph W., Sharon M. Swartz, and Kenneth S. Breuer. 2013. "Design and Characterization of a Multi-Articulated Robotic Bat Wing." *Bioinspiration & Biomimetics* 8 (1): 016009. https://doi.org/10.1088/1748-3182/8/1/016009.

Baldwin, M. W., H. Winkler, C. L. Organ, and B. Helm. 2010. "Wing Pointedness Associated with Migratory Distance in Common-Garden and Comparative Studies of Stonechats (*Saxicola torquata*)." *Journal of Evolutionary Biology* 23 (5): 1050–63. https://doi.org/10.1111/j.1420-9101.2010.01975.x.

Baliga, V. B., I. Szabo, and D. L. Altshuler. 2019. "Range of Motion in the Avian Wing Is Strongly Associated with Flight Behavior and Body Mass." *Science Advances* 5 (10): eaaw6670. https://doi.org/10.1126/sciadv.aaw6670.

Barr, Andrew. 2017. "Ggphylomorpho." GitHub: Ggphylomorpho. 2017. https://github.com/wabarr/ggphylomorpho/.

Baumel, J.J., and L.M. Witmer. 1993. "Osteologica." In *Handbook of Avian Anatomy: Nomina Anatomica Avium*, 45–90. Cambridge, Massachusetts: Nuttall Ornithological Club.

Baumgart, Stephanie L, Paul C Sereno, and Mark W Westneat. 2021. "Wing Shape in Waterbirds: Morphometric Patterns Associated with Behavior, Habitat, Migration, and Phylogenetic Convergence." *Integrative Organismal Biology* 3 (1). https://doi.org/10.1093/iob/obab011.

Bennett, S. Christopher. 2003. "Morphological Evolution of the Pectoral Girdle of Pterosaurs: Myology and Function." *Geological Society, London, Special Publications* 217 (1): 191–215. https://doi.org/10.1144/GSL.SP.2003.217.01.12.

Berthold, P, and S B Terrill. 1991. "Recent Advances in Studies of Bird Migration." *Annual Review of Ecology and Systematics* 22 (1): 357–78. https://doi.org/10.1146/annurev.es.22.110191.002041.

Bhat, S. S., J. (赵季生) Zhao, J. Sheridan, K. Hourigan, and M. C. Thompson. 2019. “Aspect Ratio Studies on Insect Wings.” *Physics of Fluids* 31 (12): 121301. https://doi.org/10.1063/1.5129191.

BirdLife International. 2020. “IUCN Red List for Birds.” 2020. http://www.birdlife.org/.

Bramwell, Cherrie D., and G. R. Whitfield. 1974. “Biomechanics of Pteranodon.” *Philosophical Transactions of the Royal Society of London B: Biological Sciences* 267 (890): 503–81. https://doi.org/10.1098/rstb.1974.0007.

Brewer, Michael L., and Fritz Hertel. 2007. “Wing Morphology and Flight Behavior of Pelecaniform Seabirds.” *Journal of Morphology* 268 (10): 866–77. https://doi.org/10.1002/jmor.10555.

Brocklehurst, Robert J., Sabine Moritz, Jonathan Codd, William I. Sellers, and Elizabeth L. Brainerd. 2019. “XROMM Kinematics of Ventilation in Wild Turkeys (*Meleagris gallopavo*).” *Journal of Experimental Biology* 222 (jeb209783). https://doi.org/10.1242/jeb.209783.

Brocklehurst, Robert J., Emma R. Schachner, Jonathan R. Codd, and William I. Sellers. 2020. “Respiratory Evolution in Archosaurs.” *Philosophical Transactions of the Royal Society B: Biological Sciences* 375 (1793): 20190140. https://doi.org/10.1098/rstb.2019.0140.

Bruderer, Bruno, Dieter Peter, Andreas Boldt, and Felix Liechti. 2010. “Wing-Beat Characteristics of Birds Recorded with Tracking Radar and Cine Camera.” *Ibis* 152 (2): 272–91. https://doi.org/10.1111/j.1474-919X.2010.01014.x.

Butler, Richard J., Paul M. Barrett, and David J. Gower. 2012. “Reassessment of the Evidence for Postcranial Skeletal Pneumaticity in Triassic Archosaurs, and the Early Evolution of the Avian Respiratory System.” *PLoS ONE* 7 (3): e34094. https://doi.org/10.1371/journal.pone.0034094.

Chin, Diana D., and David Lentink. 2017. “How Birds Direct Impulse to Minimize the Energetic Cost of Foraging Flight.” *Science Advances* 3 (5): e1603041. https://doi.org/10.1126/sciadv.1603041.

Claessens, Leon P. A. M. 2009. “The Skeletal Kinematics of Lung Ventilation in Three Basal Bird Taxa (Emu, Tinamou, and Guinea Fowl).” *Journal of Experimental Zoology Part A: Ecological Genetics and Physiology* 311A (8): 586–99. https://doi.org/10.1002/jez.501.

Claessens, Leon P. A. M., Patrick M. O’Connor, and David M. Unwin. 2009. “Respiratory Evolution Facilitated the Origin of Pterosaur Flight and Aerial Gigantism.” *PLoS ONE* 4 (2): e4497. https://doi.org/10.1371/journal.pone.0004497.

Claramunt, Santiago, Elizabeth P. Derryberry, J. V. Remsen, and Robb T. Brumfield. 2012. “High Dispersal Ability Inhibits Speciation in a Continental Radiation of Passerine

Birds." *Proceedings of the Royal Society B: Biological Sciences* 279 (1733): 1567–74. https://doi.org/10.1098/rspb.2011.1922.

Clark, Brian D., and Willy Bemis. 1979. "Kinematics of Swimming of Penguins at the Detroit Zoo." *Journal of Zoology* 188 (3): 411–28. https://doi.org/10.1111/j.1469-7998.1979.tb03424.x.

Collyer, Michael L., and Dean C. Adams. 2018. "RRPP: An R Package for Fitting Linear Models to High-Dimensional Data Using Residual Randomization." *Methods in Ecology and Evolution* 9 (2): 1772–79. https://doi.org/10.1111/2041-210X.13029.

———. 2020. *RRPP: Linear Model Evaluation with Randomized Residuals in a Permutation Procedure. R Package Version 0.5.2*. https://cran.r-project.org/package=RRPP.

Combes, S. A., and T. L. Daniel. 2001. "Shape, Flapping and Flexion: Wing and Fin Design for Forward Flight." *Journal of Experimental Biology* 204 (12): 2073–85.

Cornell Lab of Ornithology. 2015. "All About Birds." 2015. https://www.allaboutbirds.org/.

Cubo, Jorge, and Adrià Casinos. 2000. "Incidence and Mechanical Significance of Pneumatization in the Long Bones of Birds." *Zoological Journal of the Linnean Society* 130 (4): 499–510. https://doi.org/10.1111/j.1096-3642.2000.tb02198.x.

Currey, J. D., and R. McN. Alexander. 1985. "The Thickness of the Walls of Tubular Bones." *Journal of Zoology* 206 (4): 453–68. https://doi.org/10.1111/j.1469-7998.1985.tb03551.x.

Da Vinci, Leonardo. 1505. *The Codex on the Flight of Birds*. Turin, Italy. https://airandspace.si.edu/exhibitions/codex/codex.cfm#page-1.

Dalla Vecchia, Fabio M. 2019. "*Seazzadactylus venieri* Gen. et Sp. Nov., a New Pterosaur (Diapsida: Pterosauria) from the Upper Triassic (Norian) of Northeastern Italy." *PeerJ* 7 (July): e7363. https://doi.org/10.7717/peerj.7363.

Darwin, Charles R. 1845. *Journal of Researches into the Natural History and Geology of the Countries Visited during the Voyage of H.M.S. Beagle Round the World.* 2nd ed. London: John Murray. http://darwin-online.org.uk/content/frameset?viewtype=text&itemID=F14&pageseq=392.

Dawideit, Britta A., Albert B. Phillimore, Irina Laube, Bernd Leisler, and Katrin Böhning-Gaese. 2009. "Ecomorphological Predictors of Natal Dispersal Distances in Birds." *Journal of Animal Ecology* 78 (2): 388–95. https://doi.org/10.1111/j.1365-2656.2008.01504.x.

De Margerie, Emmanuel, Sophie Sanchez, Jorge Cubo, and Jacques Castanet. 2005. "Torsional Resistance as a Principal Component of the Structural Design of Long Bones: Comparative Multivariate Evidence in Birds." *The Anatomical Record Part A: Discoveries in Molecular, Cellular, and Evolutionary Biology* 282A (1): 49–66. https://doi.org/10.1002/ar.a.20141.

Dial, Kenneth P., G. E. Goslow, and Farish A. Jenkins. 1991. “The Functional Anatomy of the Shoulder in the European Starling (*Sturnus vulgaris*).” *Journal of Morphology* 207 (3): 327–44. https://doi.org/10.1002/jmor.1052070309.

Drummond, Alexei J., and Andrew Rambaut. 2007. “BEAST: Bayesian Evolutionary Analysis by Sampling Trees.” *BMC Evolutionary Biology* 7 (1): 214. https://doi.org/10.1186/1471-2148-7-214.

Dunning Jr., John B. 2007. *CRC Handbook of Avian Body Masses*. 2nd ed. New York, NY: CRC Press.

Düzler, Ayhan, Özcan Özgel, and Nejdet Dursun. 2006. “Morphometric Analysis of the Sternum in Avian Species.” *Turkish Journal of Veterinary and Animal Sciences* 30 (3): 311–14.

Dyke, G. J., R. L. Nudds, and J. M. V. Rayner. 2006. “Limb Disparity and Wing Shape in Pterosaurs.” *Journal of Evolutionary Biology* 19 (4): 1339–42. https://doi.org/10.1111/j.1420-9101.2006.01096.x.

Ehrlich, Paul, David S. Dobkin, and Darryl Wheye. 1988. *The Birder’s Handbook: A Field Guide to the Natural History of North American Birds*. New York, NY: Simon and Schuster Inc.

Ellington, Charles Porter. 1984. “The Aerodynamics of Hovering Insect Flight. II. Morphological Parameters.” Edited by Michael James Lighthill. *Philosophical Transactions of the Royal Society of London. B, Biological Sciences* 305 (1122): 17–40. https://doi.org/10.1098/rstb.1984.0050.

Fajardo, R. J., E. Hernandez, and P. M. O’Connor. 2007. “Postcranial Skeletal Pneumaticity: A Case Study in the Use of Quantitative MicroCT to Assess Vertebral Structure in Birds.” *Journal of Anatomy* 211 (1): 138–47. https://doi.org/10.1111/j.1469-7580.2007.00749.x.

Fernández, Guillermo, and David B. Lank. 2007. “Variation in the Wing Morphology of Western Sandpipers (*Calidris mauri*) in Relation to Sex, Age Class, and Annual Cycle.” *The Auk* 124 (3): 1037–46. https://doi.org/10.1093/auk/124.3.1037.

Findley, James S., Eugene H. Studier, and Don E. Wilson. 1972. “Morphologic Properties of Bat Wings.” *Journal of Mammalogy* 53 (3): 429–44. https://doi.org/10.2307/1379035.

Fitch, W. T. 1999. “Acoustic Exaggeration of Size in Birds via Tracheal Elongation: Comparative and Theoretical Analyses.” *Journal of Zoology* 248 (1): 31–48. https://doi.org/10.1111/j.1469-7998.1999.tb01020.x.

Fletcher, K. C. 1979. “Repair of Bilateral Mandibular Fractures in a Shoebill Stork (*Balaeniceps rex*).” *The Journal of Zoo Animal Medicine* 10 (2): 69–72. https://doi.org/10.2307/20094421.

Förschler, M. I., Karl-Heinz Siebenrock, and T Coppack. 2008. “Corsican Finches Have Less Pointed Wings than Their Migratory Congeners on the Mainland.” *Vie et Milieu* 58 (3–4): 277–81.

Ghetie, Vasile, Stefan Chitescu, Vasile Cotofan, and A Hillebrand. 1976. *Anatomical Atlas of Domestic Birds*. Bucharest, Romania: Editura Academiei Republicii Socialiste Romania.

Gill, Frank, David Donsker, and Pamela Rasmussen. 2020. “IOC World Bird List.” *(V10.2)* 2020. https://www.worldbirdnames.org/new/ioc-lists/crossref/.

Gómez-Bahamon, Valentina, Diego Tomás Tuero, María Isabel Castaño, John M. Bates, and Christopher J. Clark. 2020. “Non-Vocal Acoustic Signals in Fork-Tailed Flycatchers (*Tyrannus savana*).” *Integrative and Comparative Biology*.

Greenewalt, Crawford H. 1962. “Dimensional Relationships for Flying Animals.” *Smithosonian Miscellaneous Collections* 144 (2): 89.

———. 1975. “The Flight of Birds: The Significant Dimensions, Their Departure from the Requirements for Dimensional Similarity, and the Effect on Flight Aerodynamics of That Departure.” *Transactions of the American Philosophical Society* 65 (4): 1–67. https://doi.org/10.2307/1006161.

Gutzwiller, Sarah C., Anne Su, and Patrick M. O’Connor. 2013. “Postcranial Pneumaticity and Bone Structure in Two Clades of Neognath Birds.” *The Anatomical Record* 296 (6): 867–76. https://doi.org/10.1002/ar.22691.

Habib, Michael B. 2008. “Comparative Evidence for Quadrupedal Launch in Pterosaurs.” *Zitteliana*, 159–66.

Hackett, Shannon J., Rebecca T. Kimball, Sushma Reddy, Rauri C. K. Bowie, Edward L. Braun, Michael J. Braun, Jena L. Chojnowski, et al. 2008. “A Phylogenomic Study of Birds Reveals Their Evolutionary History.” *Science* 320 (5884): 1763–68. https://doi.org/10.1126/science.1157704.

Hansen, James R. 2003. *The Bird Is on the Wing: Aerodynamics and the Progress of the American Airplane*. Centennial of Flight 6. College Station, TX: Texas A&M University Press.

Hanson, Frank Blair. 1919. “The Ontogeny and Phylogeny of the Sternum.” *American Journal of Anatomy* 26 (1): 40–115. https://doi.org/10.1002/aja.1000260104.

Harmon, Luke J., Jason T. Weir, Chad D. Brock, Richard E. Glor, and Wendell Challenger. 2008. “GEIGER: Investigating Evolutionary Radiations.” *Bioinformatics* 24 (1): 129–31. https://doi.org/10.1093/bioinformatics/btm538.

Hartman, Frank A. 1961. “Locomotor Mechanisms of Birds.” *Smithsonian Miscellaneous Collections* 143 (1): 95.

Harvey, C., V. B. Baliga, P. Lavoie, and D. L. Altshuler. 2019. “Wing Morphing Allows Gulls to Modulate Static Pitch Stability during Gliding.” *Journal of The Royal Society Interface* 16 (150): 20180641. https://doi.org/10.1098/rsif.2018.0641.

Hedrick, Brandon P., Blake V. Dickson, Elizabeth R. Dumont, and Stephanie E. Pierce. 2020. “The Evolutionary Diversity of Locomotor Innovation in Rodents Is Not Linked to Proximal Limb Morphology.” *Scientific Reports* 10 (1): 1–11. https://doi.org/10.1038/s41598-019-57144-w.

Hermanson, John W., and J. Scott Altenbach. 1983. “The Functional Anatomy of the Shoulder of the Pallid Bat, *Antrozous pallidus*.” *Journal of Mammalogy* 64 (1): 62–75. https://doi.org/10.2307/1380751.

Higham, Timothy E. 2007. “The Integration of Locomotion and Prey Capture in Vertebrates: Morphology, Behavior, and Performance.” *Integrative and Comparative Biology* 47 (1): 82–95. https://doi.org/10.1093/icb/icm021.

Hone, D. W. E., M. K. Van Rooijen, and M. B. Habib. 2015. “The Wingtips of the Pterosaurs: Anatomy, Aeronautical Function and Ecological Implications.” *Palaeogeography, Palaeoclimatology, Palaeoecology* 440 (December): 431–39. https://doi.org/10.1016/j.palaeo.2015.08.046.

Huber, Gernot H., Sheela P. Turbek, Kimberly S. Bostwick, and Rebecca J. Safran. 2017. “Comparative Analysis Reveals Migratory Swallows (Hirundinidae) Have Less Pointed Wings than Residents.” *Biological Journal of the Linnean Society* 120 (1): 228–35. https://doi.org/10.1111/bij.12875.

Janke, Adam K., Michael J. Anteau, and Joshua D. Stafford. 2019. “Extreme Climatic Variability during Migration Invokes Physiological and Dietary Plasticity among Spring Migrating Ducks.” *Canadian Journal of Zoology* 97 (4): 340–51. https://doi.org/10.1139/cjz-2018-0075.

Jehl, Joseph R. 1997. “Cyclical Changes in Body Composition in the Annual Cycle and Migration of the Eared Grebe *Podiceps nigricollis*.” *Journal of Avian Biology* 28 (2): 132–42. https://doi.org/10.2307/3677306.

Jenkinson, Lloyd, Paul Simpkin, and Darren Rhodes. 1999. *Civil Jet Aircraft Design*. Great Britain: Arnold Publishers. https://www.academia.edu/41166598/Civil_Jet_Aircraft_Design.

Jetz, W., G. H. Thomas, J. B. Joy, K. Hartman, and A. O. Mooers. 2012. “The Global Diversity of Birds in Space and Time.” *Nature* 491 (November): 444–48.

Jiang, Shunxing, Xin Cheng, Yingxia Ma, and Xiaolin Wang. 2016. “A New Archaeopterodactyloid Pterosaur from the Jiufotang Formation of Western Liaoning, China, with a Comparison of Sterna in Pterodactylomorpha.” *Journal of Vertebrate Paleontology* 36 (6): e1212058. https://doi.org/10.1080/02724634.2016.1212058.

Kipp, F.A. 1959. “Der Handflügel-Index Als Flugbiologisches Maß.” *Vogelwarte* 20 (2): 77–86.

Ksepka, Daniel T. 2014. “Flight Performance of the Largest Volant Bird.” *Proceedings of the National Academy of Sciences* 111 (29): 10624–29. https://doi.org/10.1073/pnas.1320297111.

Kullberg, Cecilia, and Maria Lafrenz. 2007. “Escape Take-off Strategies in Birds: The Significance of Protective Cover.” *Behavioral Ecology and Sociobiology* 61 (10): 1555–60.

Lentink, D., U. K. Müller, E. J. Stamhuis, R. de Kat, W. van Gestel, L. L. M. Veldhuis, P. Henningsson, A. Hedenström, J. J. Videler, and J. L. van Leeuwen. 2007. “How Swifts Control Their Glide Performance with Morphing Wings.” *Nature* 446 (7139): 1082–85. https://doi.org/10.1038/nature05733.

Lentink, David, and Andrew A. Biewener. 2010. “Nature-Inspired Flight—beyond the Leap.” *Bioinspiration & Biomimetics* 5 (4): 040201. https://doi.org/10.1088/1748-3182/5/4/040201.

Lockwood, Rowan, John P. Swaddle, and Jeremy M. V. Rayner. 1998. “Avian Wingtip Shape Reconsidered: Wingtip Shape Indices and Morphological Adaptations to Migration.” *Journal of Avian Biology* 29 (3): 273–92. https://doi.org/10.2307/3677110.

López-Aguirre, Camilo, Laura A. B. Wilson, Daisuke Koyabu, Vuong Tan Tu, and Suzanne J. Hand. 2021. “Variation in Cross-Sectional Shape and Biomechanical Properties of the Bat Humerus under Wolff’s Law.” *The Anatomical Record* n/a (n/a). https://doi.org/10.1002/ar.24620.

Lovvorn, James R., and David R. Jones. 1991. “Body Mass, Volume, and Buoyancy of Some Aquatic Birds, and Their Relation to Locomotor Strategies.” *Canadian Journal of Zoology* 69 (11): 2888–92. https://doi.org/10.1139/z91-407.

Luo, Bo, Sharlene E. Santana, Yulan Pang, Man Wang, Yanhong Xiao, and Jiang Feng. 2019. “Wing Morphology Predicts Geographic Range Size in Vespertilionid Bats.” *Scientific Reports* 9 (1): 4526. https://doi.org/10.1038/s41598-019-41125-0.

Martin, Elizabeth, and Colin Palmer. 2014. “Air Space Proportion in Pterosaur Limb Bones Using Computed Tomography and Its Implications for Previous Estimates of Pneumaticity.” *PLOS ONE* 9 (5): e97159. https://doi.org/10.1371/journal.pone.0097159.

Martin-Silverstone, Elizabeth, Michael B. Habib, and David W. E. Hone. 2020. “Volant Fossil Vertebrates: Potential for Bioinspired Flight Technology.” *Trends in Ecology & Evolution*. https://doi.org/10.1016/j.tree.2020.03.005.

Minias, Piotr, Wlodzimierz Meissner, Radoslaw Wlodarczyk, Agnieszka Ozarowska, Anna Piasecka, Krzysztof Kaczmarek, and Tomasz Janiszewski. 2015. “Wing Shape and Migration in Shorebirds: A Comparative Study.” *Ibis* 157 (3): 528–35.

Mönkkönen, Mikko. 1995. “Do Migrant Birds Have More Pointed Wings?: A Comparative Study.” *Evolutionary Ecology* 9 (5): 520–28. https://doi.org/10.1007/BF01237833.

Moore, Andrew J. 2020. “Vertebral Pneumaticity Is Correlated with Serial Variation in Vertebral Shape in Storks.” *Journal of Anatomy*. https://doi.org/10.1111/joa.13322.

Mosimann, James E. 1970. “Size Allometry: Size and Shape Variables with Characterizations of the Lognormal and Generalized Gamma Distributions.” *Journal of the American Statistical Association* 65 (330): 930–45. https://doi.org/10.1080/01621459.1970.10481136.

Mulvihill, Robert S, and C Ray Chandler. 1990. “The Relationship between Wing Shape and Differential Migration in the Dark-Eyed Junco.” *Auk* 107 (3): 490–99.

Myers, P., R. Espinosa, C.S. Parr, T. Jones, G.S. Hammond, and T.A. Dewey. 2020. “The Animal Diversity Web (Online).” University of Michigan. https://animaldiversity.org.

Norberg, Ulla M. 1986. “Evolutionary Convergence in Foraging Niche and Flight Morphology in Insectivorous Aerial-Hawking Birds and Bats.” *Ornis Scandinavica (Scandinavian Journal of Ornithology)* 17 (3): 253–60. https://doi.org/10.2307/3676835.

———. 1990. *Vertebrate Flight: Mechanics, Physiology, Morphology, Ecology and Evolution*. Vol. 27. Zoophysiology. Berlin, Heidelberg: Springer.

———. 1995. “How a Long Tail and Changes in Mass and Wing Shape Affect the Cost for Flight in Animals.” *Functional Ecology* 9 (1): 48–54. https://doi.org/10.2307/2390089.

Norberg, Ulla M., and J. M. V. Rayner. 1987. “Ecological Morphology and Flight in Bats (Mammalia; Chiroptera): Wing Adaptations, Flight Performance, Foraging Strategy and Echolocation.” *Philosophical Transactions of the Royal Society B: Biological Sciences* 316 (1179): 335–427. https://doi.org/10.1098/rstb.1987.0030.

O’Connor, Jingmai K., X.-T. Zheng, C. Sullivan, C.-M. Chuong, X.-L. Wang, A. Li, Y. Wang, X.-M. Zhang, and Z.-H. Zhou. 2015. “Evolution and Functional Significance of Derived Sternal Ossification Patterns in Ornithothoracine Birds.” *Journal of Evolutionary Biology* 28 (8): 1550–67. https://doi.org/10.1111/jeb.12675.

O’Connor, Patrick M. 2003. “Pulmonary Pneumaticity in Extant Birds and Extinct Archosaurs.” PhD, New York: Stony Brook University.

———. 2004. “Pulmonary Pneumaticity in the Postcranial Skeleton of Extant Aves: A Case Study Examining Anseriformes.” *Journal of Morphology* 261 (2): 141–61. https://doi.org/10.1002/jmor.10190.

———. 2009. “Evolution of Archosaurian Body Plans: Skeletal Adaptations of an Air-Sac-Based Breathing Apparatus in Birds and Other Archosaurs.” *Journal of Experimental Zoology Part A: Ecological Genetics and Physiology* 311A (8): 629–46. https://doi.org/10.1002/jez.548.

Olsen, Aaron M., and Annat Haber. 2017. “StereoMorph: Stereo Camera Calibration and Reconstruction Manual. Version 1.6.1.” https://CRAN.R-project.org/package=StereoMorph.

Olsen, Aaron M., and Mark W. Westneat. 2015. “StereoMorph: An R Package for the Collection of 3D Landmarks and Curves Using a Stereo Camera Set-Up.” *Methods in Ecology and Evolution* 6 (3): 351–56. https://doi.org/10.1111/2041-210X.12326.

Palmer, Colin, and Gareth Dyke. 2012. “Constraints on the Wing Morphology of Pterosaurs.” *Proceedings: Biological Sciences* 279 (1731): 1218–24.

Paradis, Emmanuel, and Klaus Schliep. 2019. “Ape 5.0: An Environment for Modern Phylogenetics and Evolutionary Analyses in R.” *Bioinformatics* 35 (3): 526–28. https://doi.org/10.1093/bioinformatics/bty633.

Pennycuick, C. J. 2008. *Modelling the Flying Bird*. Elsevier.

Picasso, Mariana BJ, MC Mosto, R Tozzi, FJ Degrange, and CG Barbieto. 2014. “A Peculiar Association: The Skin and the Subcutaneus Diverticula of the Southern Screamer (*Chauna torquata*, Anseriformes).” *Vertebrate Zoology* 64: 245–49.

Piersma, Theunis, Javier Pérez-Tris, Henrik Mouritsen, Ulf Bauchinger, and Franz Bairlein. 2005. “Is There a ‘Migratory Syndrome’ Common to All Migrant Birds?” *Annals of the New York Academy of Sciences* 1046 (1): 282–93. https://doi.org/10.1196/annals.1343.026.

Pigot, Alex L., Catherine Sheard, Eliot T. Miller, Tom P. Bregman, Benjamin G. Freeman, Uri Roll, Nathalie Seddon, Christopher H. Trisos, Brian C. Weeks, and Joseph A. Tobias. 2020. “Macroevolutionary Convergence Connects Morphological Form to Ecological Function in Birds.” *Nature Ecology & Evolution* 4: 230–39. https://doi.org/10.1038/s41559-019-1070-4.

Price, S A, S T Friedman, K A Corn, C M Martinez, O Larouche, and P C Wainwright. 2019. “Building a Body Shape Morphospace of Teleostean Fishes.” *Integrative and Comparative Biology* 59 (3): 716–30. https://doi.org/10.1093/icb/icz115.

Prum, Richard O., Jacob S. Berv, Alex Dornburg, Daniel J. Field, Jeffrey P. Townsend, Emily Moriarty Lemmon, and Alan R. Lemmon. 2015. “A Comprehensive Phylogeny of Birds (Aves) Using Targeted next-Generation DNA Sequencing.” *Nature* 526 (7574): 569–73. https://doi.org/10.1038/nature15697.

R Core Team. 2020. *R: A Language and Environment for Statistical Computing. Version 3.6.3* (version 3.6.3). Vienna, Austria: R Foundation for Statistical Computing. https://www.R-project.org/.

Raikow, Robert J. 1977. “Pectoral Appendage Myology of the Hawaiian Honeycreepers (Drepanididae).” *The Auk* 94 (2): 331–42.

Renton, Katherine, Alejandro Salinas-Melgoza, Miguel Ángel De Labra-Hernández, and Sylvia Margarita de la Parra-Martínez. 2015. “Resource Requirements of Parrots: Nest Site Selectivity and Dietary Plasticity of Psittaciformes.” *Journal of Ornithology* 156 (S1): 73–90. https://doi.org/10.1007/s10336-015-1255-9.

Revell, Liam J. 2012. “Phytools: An R Package for Phylogenetic Comparative Biology (and Other Things).” *Methods in Ecology and Evolution* 3 (2): 217–23. https://doi.org/10.1111/j.2041-210X.2011.00169.x.

Robinson, Beren W, and David Sloan Wilson. 1998. “Optimal Foraging, Specialization, and a Solution to Liem’s Paradox.” *The American Naturalist* 151 (3): 223–35.

Rueden, Curtis T., Johannes Schindelin, Mark C. Hiner, Barry E. DeZonia, Alison E. Walter, Ellen T. Arena, and Kevin W. Eliceiri. 2017. “ImageJ2: ImageJ for the next Generation of Scientific Image Data.” *BMC Bioinformatics* 18 (1): 529. https://doi.org/10.1186/s12859-017-1934-z.

Sackton, Timothy B., Phil Grayson, Alison Cloutier, Zhirui Hu, Jun S. Liu, Nicole E. Wheeler, Paul P. Gardner, et al. 2019. “Convergent Regulatory Evolution and Loss of Flight in Paleognathous Birds.” *Science* 364 (6435): 74–78. https://doi.org/10.1126/science.aat7244.

Sato, Katsufumi, Kentaro Q. Sakamoto, Yutaka Watanuki, Akinori Takahashi, Nobuhiro Katsumata, Charles-André Bost, and Henri Weimerskirch. 2009. “Scaling of Soaring Seabirds and Implications for Flight Abilities of Giant Pterosaurs.” *PLOS ONE* 4 (4): e5400. https://doi.org/10.1371/journal.pone.0005400.

Schachner, Emma R., John R. Hutchinson, and Cg Farmer. 2013. “Pulmonary Anatomy in the Nile Crocodile and the Evolution of Unidirectional Airflow in Archosauria.” *PeerJ* 1 (March): e60. https://doi.org/10.7717/peerj.60.

Sheard, Catherine, Montague H. C. Neate-Clegg, Nico Alioravainen, Samuel E. I. Jones, Claire Vincent, Hannah E. A. MacGregor, Tom P. Bregman, Santiago Claramunt, and Joseph A. Tobias. 2020. “Ecological Drivers of Global Gradients in Avian Dispersal Inferred from Wing Morphology.” *Nature Communications* 11 (1). https://doi.org/10.1038/s41467-020-16313-6.

Sibley, David. 2018. “Wing Basics by David Sibley.” BirdWatching. 2018. https://www.birdwatchingdaily.com/birds/david-sibleys-id-toolkit/wing-basics-by-david-sibley/.

Sievert, Carson. 2020. *Interactive Web-Based Data Visualization with R, Plotly, and Shiny*. Chapman and Hall/CRC. https://plotly-r.com.

Simons, Erin L. R., Tobin L. Hieronymus, and Patrick M. O’Connor. 2011. “Cross Sectional Geometry of the Forelimb Skeleton and Flight Mode in Pelecaniform Birds.” *Journal of Morphology* 272 (8): 958–71. https://doi.org/10.1002/jmor.10963.

Slater Museum of Natural History. 2011. “Wing & Tail Image Collection.” Wing & Tail Image Collection. 2011. http://digitalcollections.pugetsound.edu/cdm/landingpage/collection/slaterwing.

Smith, Nathan D. 2012. “Body Mass and Foraging Ecology Predict Evolutionary Patterns of Skeletal Pneumaticity in the Diverse ‘Waterbird’ Clade.” *Evolution* 66 (4): 1059–78. https://doi.org/10.1111/j.1558-5646.2011.01494.x.

Stayton, C. Tristan. 2015. “The Definition, Recognition, and Interpretation of Convergent Evolution, and Two New Measures for Quantifying and Assessing the Significance of Convergence.” *Evolution* 69 (8): 2140–53. https://doi.org/10.1111/evo.12729.

Stratovan Corporation. 2018. *Stratovan Checkpoint* (version 2018.08.07). https://www.stratovan.com/products/checkpoint.

Strauss, Richard E. 1990. “Patterns of Quantitative Variation in Lepidopteran Wing Morphology: The Convergent Groups Heliconiinae and Ithomiinae (Papilionoidea: Nymphalidae).” *Evolution* 44 (1): 86–103. https://doi.org/10.1111/j.1558-5646.1990.tb04281.x.

Sullivan, Louis H. 1896. “The Tall Office Building Artistically Considered.” *Lippincott’s Magazine*.

Sullivan, S. P., F. R. McGechie, K. M. Middleton, and C. M. Holliday. 2019. “3D Muscle Architecture of the Pectoral Muscles of European Starling (*Sturnus vulgaris*).” *Integrative Organismal Biology* 1 (1). https://doi.org/10.1093/iob/oby010.

Swaddle, John P., and Rowan Lockwood. 2003. “Wingtip Shape and Flight Performance in the European Starling *Sturnus vulgaris*.” *Ibis* 145 (3): 457–64. https://doi.org/10.1046/j.1474-919X.2003.00189.x.

Swartz, Sharon M., Michael B. Bennett, and David R. Carrier. 1992. “Wing Bone Stresses in Free Flying Bats and the Evolution of Skeletal Design for Flight.” *Nature* 359 (6397): 726–29. https://doi.org/10.1038/359726a0.

Taylor, Graham K., Anna C. Carruthers, Tatjana Y. Hubel, and Simon M. Walker. 2012. “Wing Morphing in Insects, Birds and Bats: Mechanism and Function.” In *Morphing Aerospace Vehicles and Structures*, 13–40. Texas: John Wiley & Sons, Ltd. https://doi.org/10.1002/9781119964032.

Thorsen, Dean H., and Mark W. Westneat. 2005. “Diversity of Pectoral Fin Structure and Function in Fishes with Labriform Propulsion.” *Journal of Morphology* 263 (2): 133–50. https://doi.org/10.1002/jmor.10173.

Tobalske, Bret W. 2007. “Biomechanics of Bird Flight.” *Journal of Experimental Biology* 210 (18): 3135–46. https://doi.org/10.1242/jeb.000273.

Tokita, Masayoshi, Hiroya Matsushita, and Yuya Asakura. 2020. “Developmental Mechanisms Underlying Webbed Foot Morphological Diversity in Waterbirds.” *Scientific Reports* 10 (1): 8028. https://doi.org/10.1038/s41598-020-64786-8.

Vágási, Csongor I., Péter L. Pap, Orsolya Vincze, Gergely Osváth, Johannes Erritzøe, and Anders Pape Møller. 2016. “Morphological Adaptations to Migration in Birds.” *Evolutionary Biology* 43 (1): 48–59. https://doi.org/10.1007/s11692-015-9349-0.

Viscor, G, and J. F Fuster. 1987. “Relationships between Morphological Parameters in Birds with Different Flying Habits.” *Comparative Biochemistry and Physiology Part A: Physiology* 87 (2): 231–49. https://doi.org/10.1016/0300-9629(87)90118-6.

Vizcaíno, Sergio F., and Richard A. Fariña. 1999. “On the Ftight Capabilities and Distribution of the Giant Miocene Bird Argentavis Magnificens (Teratornithidae).” *Lethaia* 32 (4): 271–78. https://doi.org/10.1111/j.1502-3931.1999.tb00546.x.

Walker, Jeffrey A., and Mark W. Westneat. 2002. “Performance Limits of Labriform Propulsion and Correlates with Fin Shape and Motion.” *Journal of Experimental Biology* 205 (2): 177–87.

Wang, Xia, and Julia A. Clarke. 2014. “Phylogeny and Forelimb Disparity in Waterbirds.” *Evolution* 68 (10): 2847–60. https://doi.org/10.1111/evo.12486.

———. 2015. “The Evolution of Avian Wing Shape and Previously Unrecognized Trends in Covert Feathering.” *Proc. R. Soc. B* 282 (1816): 20151935. https://doi.org/10.1098/rspb.2015.1935.

Warham, John. 1977. “Wing Loadings, Wing Shapes, and Flight Capabilities of Procellariiformes.” *New Zealand Journal of Zoology* 4 (1): 73–83. https://doi.org/10.1080/03014223.1977.9517938.

Webb, P. W. 1984. “Body Form, Locomotion and Foraging in Aquatic Vertebrates.” *American Zoologist* 24 (1): 107–20. https://doi.org/10.1093/icb/24.1.107.

Weber, Thomas, and Anders Hedenström. 2001. “Long-Distance Migrants as a Model System of Structural and Physiological Plasticity.” *Evolutionary Ecology Research* 3 (3): 255–71.

Wedel, Mathew John. 2003. “Vertebral Pneumaticity, Air Sacs, and the Physiology of Sauropod Dinosaurs.” *Paleobiology* 29 (2): 243–55.

———. 2005. “Postcranial Skeletal Pneumaticity in Sauropods and Its Implications for Mass Estimates.” In *The Sauropods: Evolution and Paleobiology*, 201–28. Berkeley, CA: University of California Press.

———. 2013. “Postcranial Pneumaticity in Dinosaurs and the Origin of the Avian Lung.” *ArXiv:1302.3267 [q-Bio]*, February. http://arxiv.org/abs/1302.3267.

Weidig, Ilka. 2010. “New Birds from the Lower Eocene Green River Formation, North America.” *Records of the Australian Museum* 62 (1): 29–44.

West, J. B., R. R. Watson, and Z. Fu. 2007. “The Human Lung: Did Evolution Get It Wrong?” *European Respiratory Journal* 29 (1): 11–17. https://doi.org/10.1183/09031936.00133306.

Wickham, Hadley. 2016. *Ggplot2: Elegant Graphics for Data Analysis. R Package Version 3.3.2* (version 3.3.2). Springer-Verlag New York. https://ggplot2.tidyverse.org.

Witton, M.P. 2008. “A New Approach to Determining Pterosaur Body Mass and Its Implications for Pterosaur Flight.” *Zitteliana* B28: 143–58.

Wright, Natalie A., David W. Steadman, and Christopher C. Witt. 2016. “Predictable Evolution toward Flightlessness in Volant Island Birds.” *Proceedings of the National Academy of Sciences* 113 (17): 4765–70. https://doi.org/10.1073/pnas.1522931113.

Zhang, Yu-guang, Zhi-heng Li, Di Liu, Qing-guo Liu, and Li-ya Fu. 2011. “The Diversity of Morphology of the Avian Sternum and Its Relationship with Flight Ability.” *Sichuan Journal of Zoology* 30 (5): 677–86.

Zheng, Xiaoting, Jingmai O’Connor, Xiaoli Wang, Min Wang, Xiaomei Zhang, and Zhonghe Zhou. 2014. “On the Absence of Sternal Elements in *Anchiornis* (Paraves) and *Sapeornis* (Aves) and the Complex Early Evolution of the Avian Sternum.” *Proceedings of the National Academy of Sciences* 111 (38): 13900–905. https://doi.org/10.1073/pnas.1411070111.

CHAPTER 2 APPENDIX

TERMINOLOGY

Flight Style

Flight style terminology is taken from (Viscor and Fuster 1987). Data used in this paper collected from Viscor and Fuster (1987), (Bruderer *et al.* 2010), and from (Wang and Clarke 2015). The first four flight styles were the only ones reported for the species used in Chapter 2. The last two were used in Chapter 3.

> *Forward/bounding flapping flight* – "the majority of avian species are forward flapping birds which use a sustained horizontal flight, with an elevated energetic cost. A great number of species of passerines perform an intermittent bounding flight style with short and continuous ascending and descending periods resulting in an oscillatory flight path" Viscor and Fuster (1987), p1
>
> *Gliding/soaring* – "need large wing areas to sustain the body weight during prolonged flights without flapping their wings and so at relatively little energy cost." Viscor and Fuster (1987), p1
>
> *High-frequency flapping flight* – "elevated respiration frequency which is coordinated to their wing beat at a ratio 4-5:1, and a strong pectoral musculature that allows them to perform long migration flights. Many of these birds are associated with the aquatic medium, so these species are morphologically adapted to diving or plunging, like ducks, grebes and loons." Viscor and Fuster (1987), p1

Undulating flapping flight – "enhance their muscular performance operating at conditions of optimum thermodynamic efficiency… period of powered flight, during which height is gained, followed by a period of conventional gliding flight." Viscor and Fuster (1987), p1

Short flight – "relatively large mass, a high frequency pectoral musculature, short broad wings and a small wing area that deprives them of extended flight; they are usually adapted to short bursts of activity." Viscor and Fuster (1987), p1

Hovering flight – "stationary flight in still air represents a specialization from an evolutionary point of view… hummingbirds for example" Viscor and Fuster (1987), p1

The additional flight styles below were created for use in Chapter 3, because Viscor and Fuster (1987) did not consider non-volant birds in their study.

Non-flying – terrestrial flightless birds

Swimming – flightless birds that swim

Foraging behavior

Foraging behavior is a set of terms mostly defined by the Cornell Lab of Ornithology on their website, allaboutbirds.org (Cornell Lab of Ornithology 2015) and *The Birder's Handbook* (Ehrlich, Dobkin and Wheye 1988). "Aerial hunter" was defined in this paper to better capture the behavior of the selection of birds in this dataset.

Aerial hunter – This term is defined in this paper as birds that acquire food on the wing. Either petrels that are flying over the water surface and dip their heads in the water to catch a fish, or jaegers that attack other birds in the air to steal their food.

Dabbler – These birds float on the water surface and pivot down to grab food under the water.

Ground forager – Ground foragers hunt along the shoreline, either chasing prey or pulling invertebrates off of rocks.

Plunge dive – These birds will fly high above the water and dive down into the water to hunt for prey.

Probing – These birds probe the sand or mud to find food, either on the shore or in the shallow water.

Stalking – Stalking birds hunt by standing still at the edge of the water and spear their prey.

Surface dive – These birds will float on the water surface, then dive (wing-propelled or foot-propelled) down into the water for prey.

Habitat

Habitat is taken from the species pages on The Cornell Lab of Ornithology's allaboutbirds.org (Cornell Lab of Ornithology 2015), which reports the primary habitat frequented by the species. The habitats used by the birds in this study include: grassland, lake/pond, marsh, ocean, river/stream, shoreline, and tundra. Note: "grassland" refers to shorebirds that have moved more inland to grassy plains and mudflats.

Migration

Migration is adapted from the Bird Life International: http://datazone.birdlife.org/species/spchabalt (BirdLife International 2020)

Full migrant – the majority of the species' populations makes regular, cyclical movements to locations outside their breeding range

Non-migrant – the populations do not migrate, but stay in one location

Partial migrant – For this paper, this term encompasses includes species with some of the populations migrating and other do not, as well as nomadic species (those who congregate at unpredictable times or locations).

Migration + Location

This compound term encompasses the species' migratory pattern and the location of their complete range as provided by Bird Life International (2020). This variable would expand the migration variable to include whether the bulk of the bird's time is spent over the ocean and dealing with oceanic wind currents or more over large land masses like continents and dealing with varying topology and land-based wind currents. See **Suppl. Figure 2.1** as an example of the different categories.

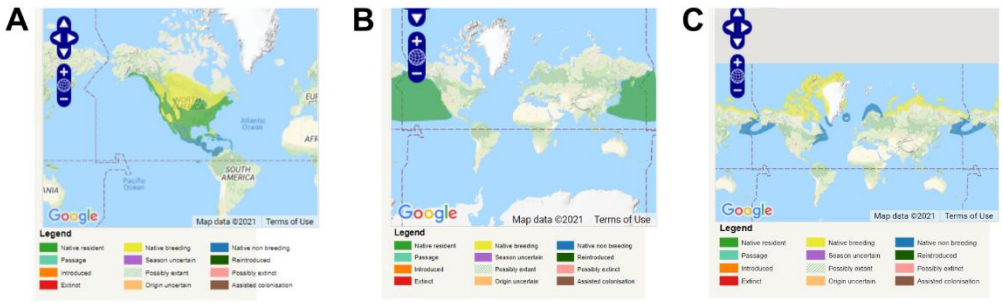

Ardea herodias
Continental

Phoebastria immutabilis
Oceanic

Somateria spectabilis
Mixed

Suppl. Figure 2.1 Range maps of different species considered A) continental, B) oceanic, and C) mixed.

Continental migrant – The species migrates and the range only covers the continental land masses.

Continental non-migrant – The species does not migrate, and the range only covers the continental land masses.

Mixed migrant – The species migrates, and part of its range covers a large region of land, and the other part of its range covers the ocean, such that the range is not "mostly continental" or "mostly oceanic," closer to half and half.

Oceanic non-migrant – The species does not migrate, but the range is covers mostly ocean, likely having a small portion on the shoreline.

Oceanic migrant – The species migrates and the range is mostly over the ocean.

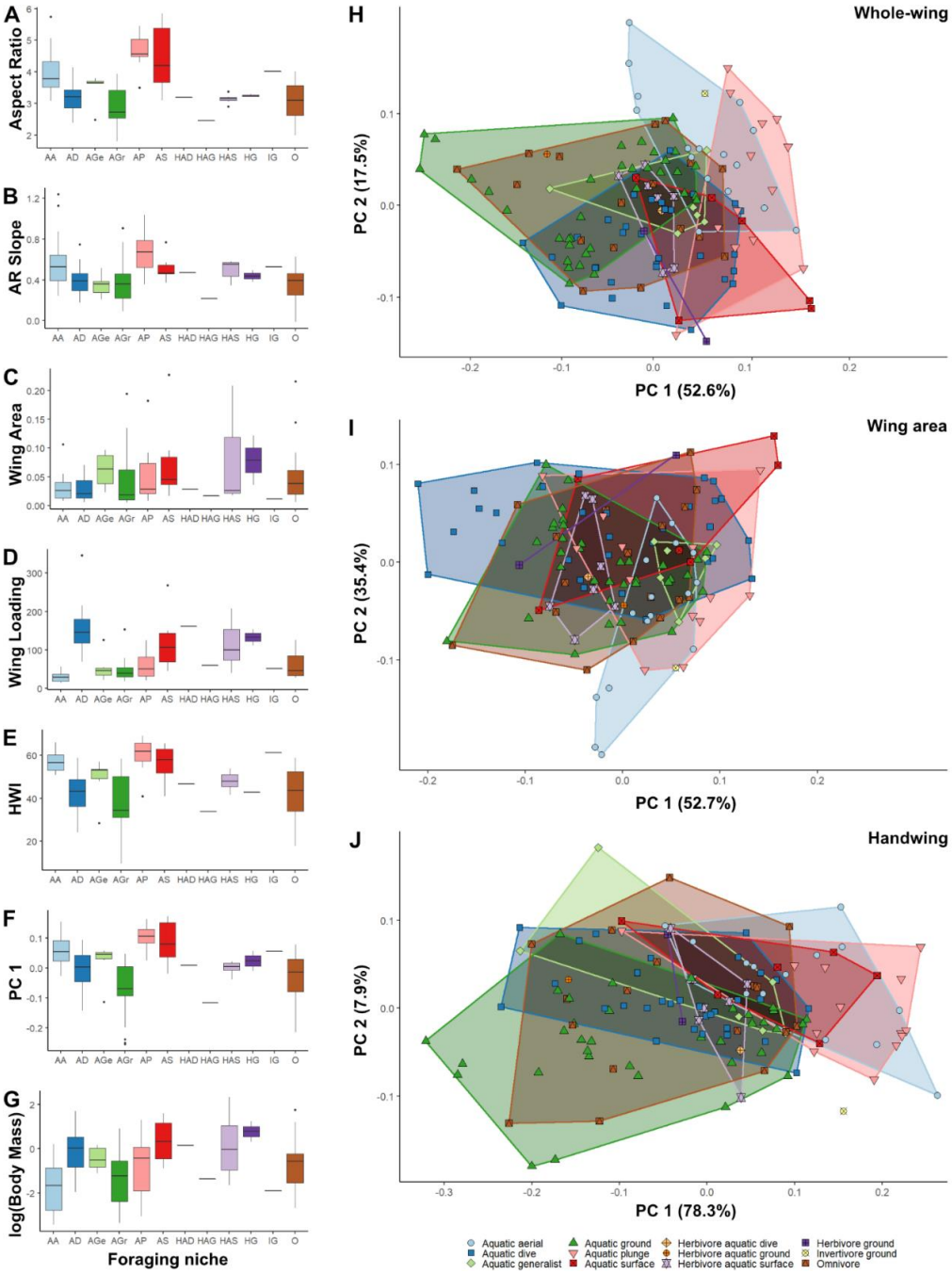

Suppl. Figure 2.2 Wing shape analysis with Pigot et al. (2020) foraging niche variables. (**A-G**) Boxplots depicting data on variables discussed in Suppl. Figure 3.; (**H-J**): morphospaces for whole-wing, wing area, and handwing shape data corresponding to Figures 7-9 respectively. Phylo-(M)ANOVAs tested in Suppl. Tables 4, 6, and 9 respectively. Abbreviations: AA, aquatic aerial; AD, Aquatic dive; AGe, Aquatic generalist; AGr, Aquatic ground; AP, Aquatic plunge;

(Suppl. Figure 2.2 continued) AS, Aquatic surface; HAD, Herbivore aquatic dive; HAG, Herbivore aquatic ground; HAS, Herbivore aquatic surface; HG, Herbivore ground; IG, Invertivore ground; O, omnivore.

Aspect ratio

The wing lengths of waterbirds in this study range from 12 cm in *Rallus longirostris* (Clapper rail) to 90 cm in *Pelecanus erythrorhynchos* (American white pelican). Large soaring birds like the albatross and frigate bird have high aspect ratio wings (AR = 5.1), whereas jacanas and rails have low aspect ratio wings (AR = 1.8-2.1).

Gruiforms have the lowest aspect ratio wings (1.8), procellariiforms have the highest aspect ratio wings (5.9). Procellariiforms and suliforms have the largest interquartile ranges in aspect ratio (3.2-5.0 and 2.7-4.6 respectively), though charadriiforms have the largest total range including outliers (2.0-5.3) (**Suppl. Figure 2.3**A). Gliding/soaring birds tend to have significantly higher aspect ratio wings (**Suppl. Figure 2.3**B, Suppl. Data 2), while other groups have medium to low aspect ratio wings. The aerial hunters and plunge divers tend to have the highest aspect ratio wings, although aerial hunters also have a large range in aspect ratio (**Suppl. Figure 2.3**C). Probers have low-medium aspect ratio wings, and dabblers, ground foragers, and surface divers have medium aspect ratio wings (**Suppl. Figure 2.3**C). Marsh birds have lower aspect ratio wings, whereas ocean and shoreline birds have medium to high aspect ratio wings (**Suppl. Figure 2.3**D). The aspect ratio of all migrating and all non-migrating birds does not differ significantly (Suppl. Data 2), although oceanic birds tend to have a higher average aspect ratio than continental birds (**Suppl. Figure 2.3**E). There is no significant difference between the aspect ratio of oceanic migrants and oceanic non-migrants, but aspect ratio of continental

migrants is significantly different from that of continental non-migrants (**Suppl. Figure 2.3**E, Suppl. Data 2).

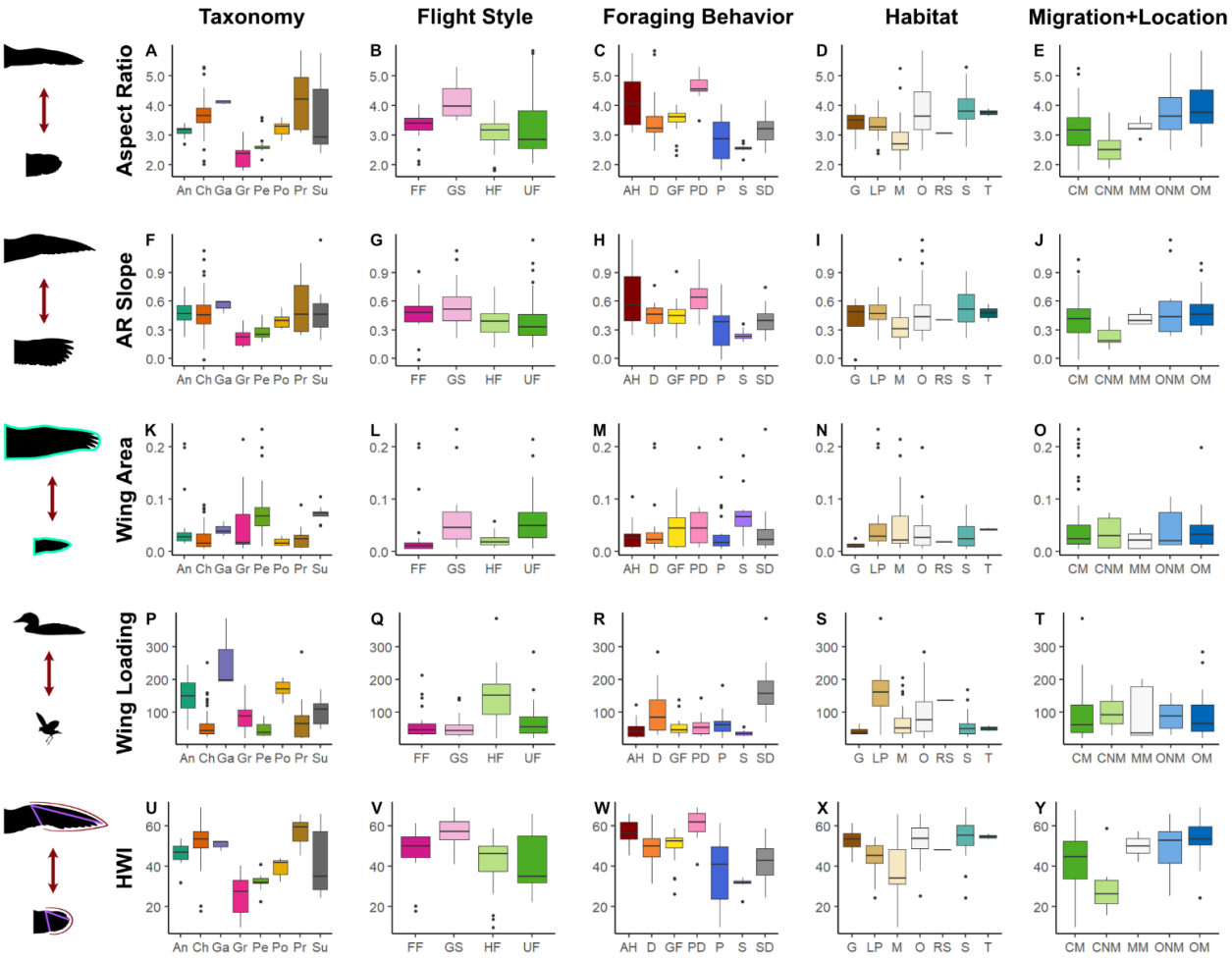

Suppl. Figure 2.3 Waterbird wing indices (y-axis) plotted against taxonomy, flight style, foraging behavior, habitat and migration patterns (x-axis). (A–E) Wing aspect ratio. (F–J) Slope of wing aspect ratio. (K–O) Single-wing area (m^2). (P–T) Wing loading ($N \cdot m^{-2}$). (U–Y) Handwing index. For boxplot statistics, see Suppl. Data 2. Abbreviations: *Taxonomy* An, Anseriformes, Ch, Charadriiformes, Ga, Gaviiformes, Gr, Gruiformes, Pe, Pelecaniformes, Po, Podicipediformes, Pr, Procellariiformes, Su, Suliformes; *Flight style* FF, forward/bounding flight, GS, gliding/soaring flight, HF, high-frequency flapping flight, UF, undulating flapping flight. *Foraging behavior* AH, aerial hunting, GF, ground foraging, P, probing, SD, surface diving, D, dabbling, PD, plunge diving, S, stalking. *Habitat* G, grasslands, M, marshes, RS, rivers/streams, T, tundra, LP, lakes/ponds, O, oceans, S, shorelines. *Migration + Location* CM, continental migrant, CNM, continental non-migrant, MM, mixed migrant, OM, oceanic migrant, ONM, oceanic non-migrant.

AR slope

Gruiforms and pelecaniforms have the lowest AR slope means (0.23, 0.28, respectively) across the wing (**Suppl. Figure 2.3**F). Procellariforms have the largest interquartile range in AR slope (0.28–0.77). An average AR slope of approximately 0.5 characterizes many waterbirds including anseriforms, charadriiforms, podicipediforms, procellariforms, and suliforms. There is no significant difference between birds that use forward versus gliding/soaring flight, as is the case comparing high-frequency flapping and undulating flight (**Suppl. Figure 2.3**G). Aerial hunters and plungers (**Suppl. Figure 2.3**H) tend to have higher AR slope means (0.62 and 0.65 respectively) compared to shorebirds that probe and stalk (0.34 and 0.25 respectively). Plunge diver AR slopes are significantly different from each group except aerial hunters (**Suppl. Figure 2.3**H). Prober AR slopes contain the lower end of the range. Dabblers, ground foragers, and surface divers have AR slope ranges that are not significantly different from each other (**Suppl. Figure 2.3**H). Marsh birds have a lower AR slope range (mean = 0.34) than birds inhabiting lake/ponds, oceans or shorelines (0.47, 0.49, 0.53 respectively; **Suppl. Figure 2.3**I). There is no significant difference between AR slope range of ocean birds and shoreline birds ($p = 0.202$; **Suppl. Figure 2.3**I). Distinctive migratory patterns do not generate differences between groups (Suppl. Data 2), although migration + location shows a significant difference between continental non-migrants (lowest AR slope range of 0.09-0.44) and each of the other categories (**Suppl. Figure 2.3**J).

Total wing area

Pelecaniforms and suliforms have the highest average wing areas (0.09 m^2, 0.07 m^2, respectively), and charadriiforms, podicipediforms, and procellariiforms have the lowest average wing areas (0.03 m^2, 0.02 m^2, 0.03 m^2, respectively; **Suppl. Figure 2.3**K). Pelecaniforms have

the largest total range (0.01-0.2 m^2), and gruiforms have the largest interquartile range (0.018--0.08 m^2), although neither are significantly different from other groups (**Suppl. Figure 2.3**K). Gaviiforms, podicipediforms, and suliforms have the smallest ranges in wing area (0.04-0.05 m^2, 0.01-0.03 m^2, 0.05-0.08 m^2, respectively). Birds which glide/soar and use undulating flight are not significantly different from each other ($p = 0.780$), and have wide interquartile ranges covering most of the total range of wing area (0.01-0.23 m^2, 0.01-0.22 m^2, respectively; **Suppl. Figure 2.3**L). Birds which use forward flight and high-frequency flapping flight have a very narrow range in the low end of wing area except for a few outliers (interquartile range 0.01-0.02 m^2, 0.02-0.03 m^2, respectively; **Suppl. Figure 2.3**L, Suppl. Data 2). Stalking birds have a significantly higher mean in wing area (0.08 m^2) compared to aerial hunters, dabblers, probers, and surface divers (**Suppl. Figure 2.3**M). No other foraging behavior pairings have been found to have significantly different wing area means. Ground foragers and plunge divers have the widest interquartile ranges in wing area (0.01-0.08 m^2, 0.02-0.08 m^2, respectively), and dabblers and probers have the narrowest interquartile ranges (0.02-0.04 m^2, 0.01-0.04 m^2, respectively; **Suppl. Figure 2.3**M). Grassland birds have the narrowest range of wing area (0.01-0.03 m^2), which differs significantly from lake/pond dwellers ($p = 0.042$; **Suppl. Figure 2.3**N). No other habitat pairings show significant differences between group means. Marsh birds have the widest range in wing area (0.01-0.2 m^2). Wing area is not found to be a significant factor in separating migratory status categories (Suppl. Data 2), nor migration + location categories (**Suppl. Figure 2.3**O).

Wing loading

Wing loading in this dataset ranges from 14 $N \cdot m^{-2}$ in *Oceanites oceanicus* (Wilson's storm petrel) to 346 $N \cdot m^{-2}$ in *Gavia immer* (Common loon) with a mean of 81 $N \cdot m^{-2}$. Gaviiforms have

the highest wing loading (232 $N \cdot m^{-2}$) followed by podicipediforms (171 $N \cdot m^{-2}$; **Suppl. Figure 2.3**P). High-frequency flapping birds have a significantly higher wing loading distribution (133 $N \cdot m^{-2}$) than birds with other flight styles, which are not significantly different from each other (**Suppl. Figure 2.3**Q). Wing loading was found to have a significant predictive value with regards to foraging behavior. Dabblers and surface divers higher wing loading (91 $N \cdot m^{-2}$, 152 $N \cdot m^{-2}$, respectively; **Suppl. Figure 2.3**R). Wing loading also was significantly related to habitat. Birds that live in lake/pond habitats have the highest wing loadings (148 $N \cdot m^{-2}$). Ocean-dwelling birds tend to have a large range in wing loading (14-268 $N \cdot m^{-2}$), the higher end of the range overlapping with the middle of the lake/pond boxplot (**Suppl. Figure 2.3**S). Neither migratory status nor migration + location have significant relationships with wing loading (Suppl. Data 2, **Suppl. Figure 2.3**T).

Handwing index

Handwing index (HWI) tracks trends in whole-wing aspect ratio. Gruiforms have low HWI (25.7), and anseriforms, charadriiforms, gaviiforms, and procellariiforms have high HWI (46.4, 52.3, 50.6, 57.2, respectively; **Suppl. Figure 2.3**U). Suliforms have the largest interquartile range (28.5-57.2) and the mean (42.5) is only significantly different from that of Gruiformes and Procellariiformes (25.7, 57.2, respectively; **Suppl. Figure 2.3**U). Gliding/soaring birds have a significantly higher mean (56.5) compared to other flight styles, and forward/bounding birds have a significantly different mean from high-frequency flappers ($p = 0.00963$; **Suppl. Figure 2.3**V). Undulating flappers have the largest range in HWI (22.0-66.0; **Suppl. Figure 2.3**V). Foraging behavior shows a significant relationship with HWI (phylo-ANOVA: F-statistic = 16.550, corrected p-value = 0.006, Suppl. Table 6). Aerial hunters and plunge divers have the highest HWI (57.0, 60.3, respectively), while probers have the lowest (9.5) and the largest range

(9.5-61.2; **Suppl. Figure 2.3**W). Habitat was found to have a significant relationship with HWI (phylo-ANOVA: F-statistic = 10.412, corrected p-value = 0.004, Suppl. Table 6). Marsh-dwelling birds have the largest range in HWI (9.5-65.7), including the low end of the total range (**Suppl. Figure 2.3**X), and ocean and shoreline birds have the highest HWI (52.4, 54.2, respectively; **Suppl. Figure 2.3**X). Full migrants and non-migrants overlap, the former with a smaller interquartile range (39.6-54.7, 27.5-55.3, respectively; Suppl. Data 2). Migration + Location shows a weakly significant relationship with HWI (phylo-ANOVA: F-statistic = 7.278, corrected p-value = 0.044, Suppl. Table 6). Continental non-migrants have significantly lower HWIs than any other group (**Suppl. Figure 2.3**Y). The HWI of continental migrants (43.7), however, differs significantly from oceanic migrants (53.5; **Suppl. Figure 2.3**Y), although there is no significant difference in HWI among oceanic birds or between mixed migrants and other birds (**Suppl. Figure 2.3**Y).

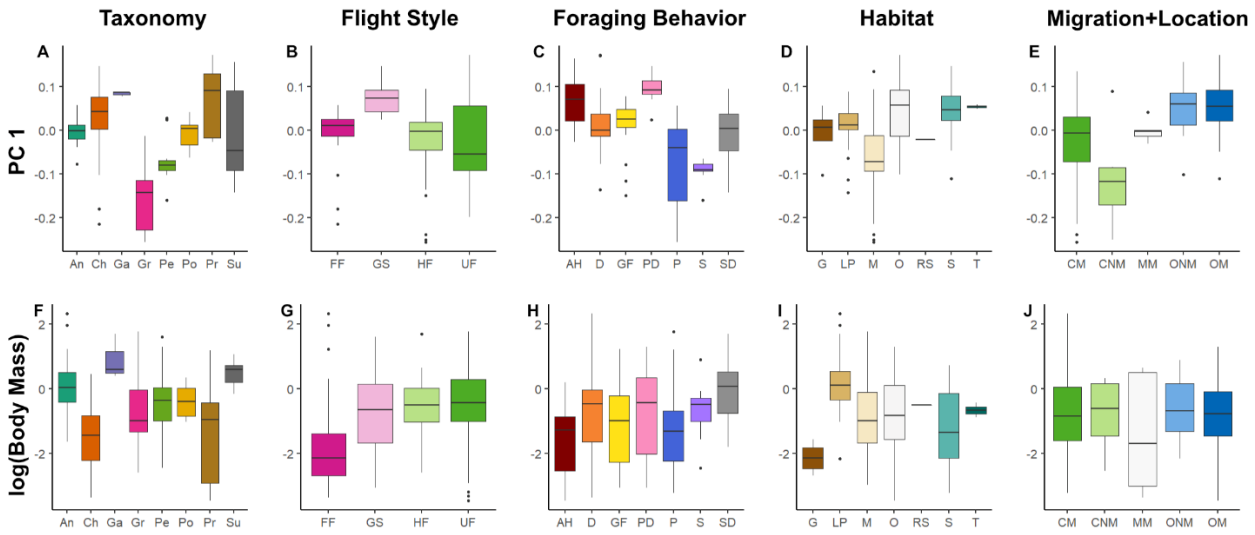

Suppl. Figure 2.4 Waterbird wing indices (y-axis) plotted against taxonomy, flight style, foraging behavior, habitat and migration patterns (x-axis). (A–E) PC 1. (F–J) log-transformed body mass. Abbreviations: *Taxonomy* An, Anseriformes, Ch, Charadriiformes, Ga, Gaviiformes, Gr, Gruiformes, Pe, Pelecaniformes, Po, Podicipediformes, Pr, Procellariiformes, Su, Suliformes; *Flight style* FF, forward/bounding flight, GS, gliding/soaring flight, HF, high-frequency flapping flight, UF, undulating flapping flight. *Foraging behavior* AH, aerial hunting, GF, ground foraging, P, probing, SD, surface diving, D, dabbling, PD, plunge diving, S, stalking. *Habitat* G,

(Suppl. Figure 2.4 continued) grasslands, M, marshes, RS, rivers/streams, T, tundra, LP, lakes/ponds, O, oceans, S, shorelines. *Migration + Location* CM, continental migrant, CNM, continental non-migrant, MM, mixed migrant, OM, oceanic migrant, ONM, oceanic non-migrant.

Suppl. Figure 2.5 Interactive plot of the functional metric morphospace colored by taxonomy, including species information, raw functional metric data, and log-transformed mass. (In a standalone .html file in Baumgart et al. 2021 supplementary.)

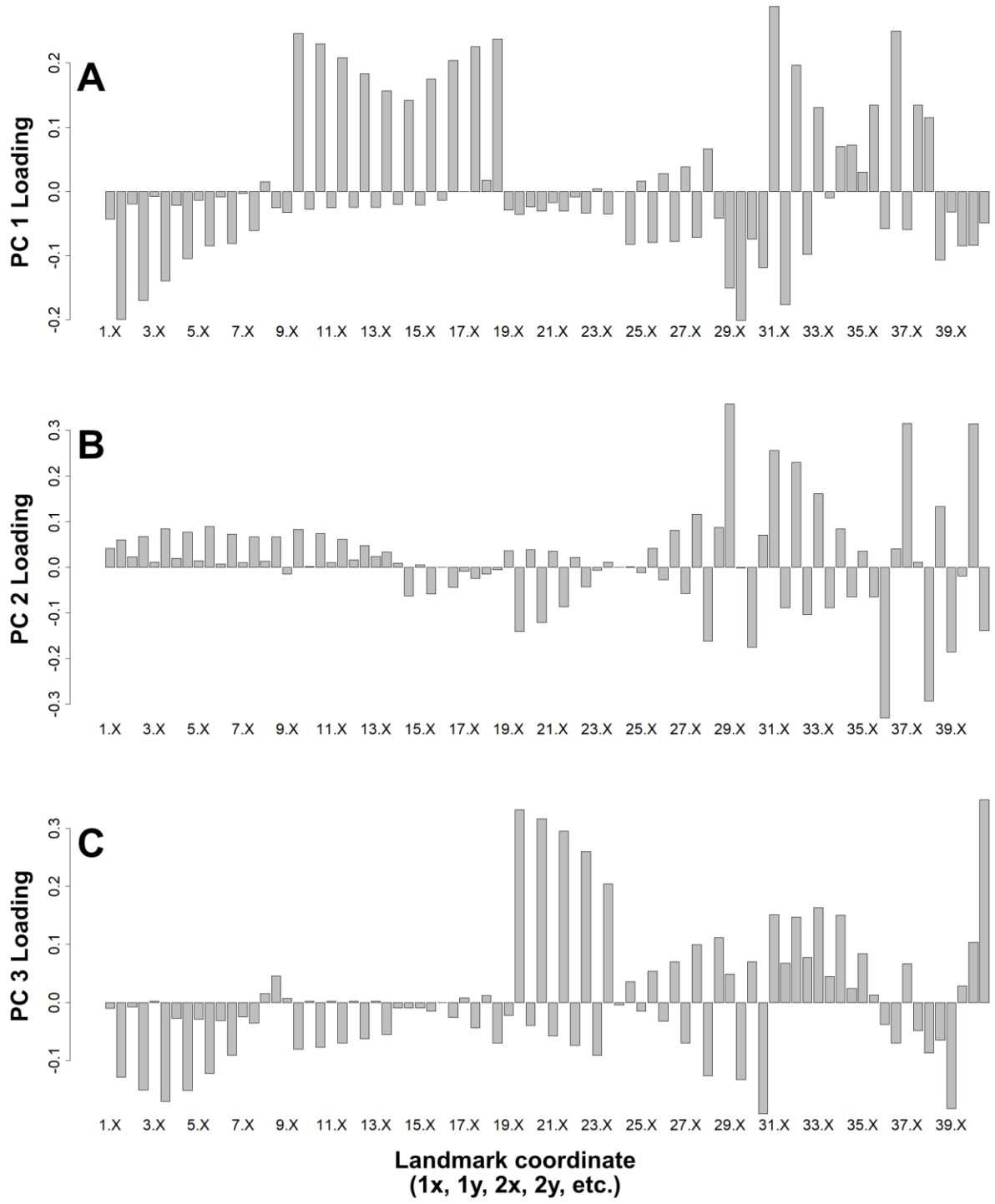

Suppl. Figure 2.6 Whole-wing morphospace loadings for each coordinate. **A**: PC 1 loadings. **B**: PC 2 loadings. **C**: PC 3 loadings. There is a separate loading for the x- and for the y-component.

Suppl. Figure 2.7 Interactive plot of the whole-wing morphospace colored by taxonomy, contains species information and ecological variables. (In standalone .html file in Baumgart et al. 2021 supplementary.)

Suppl. Figure 2.8 Interactive plot of the wing area morphospace colored by taxonomy, including species information and ecological variables. (In a separate .html file in Baumgart et al. 2021 supplementary.)

Suppl. Figure 2.9 Interactive plot of the handwing morphospace colored by taxonomy, including species information and ecological variables. (In a separate .html file in Baumgart et al 2021 supplementary.)

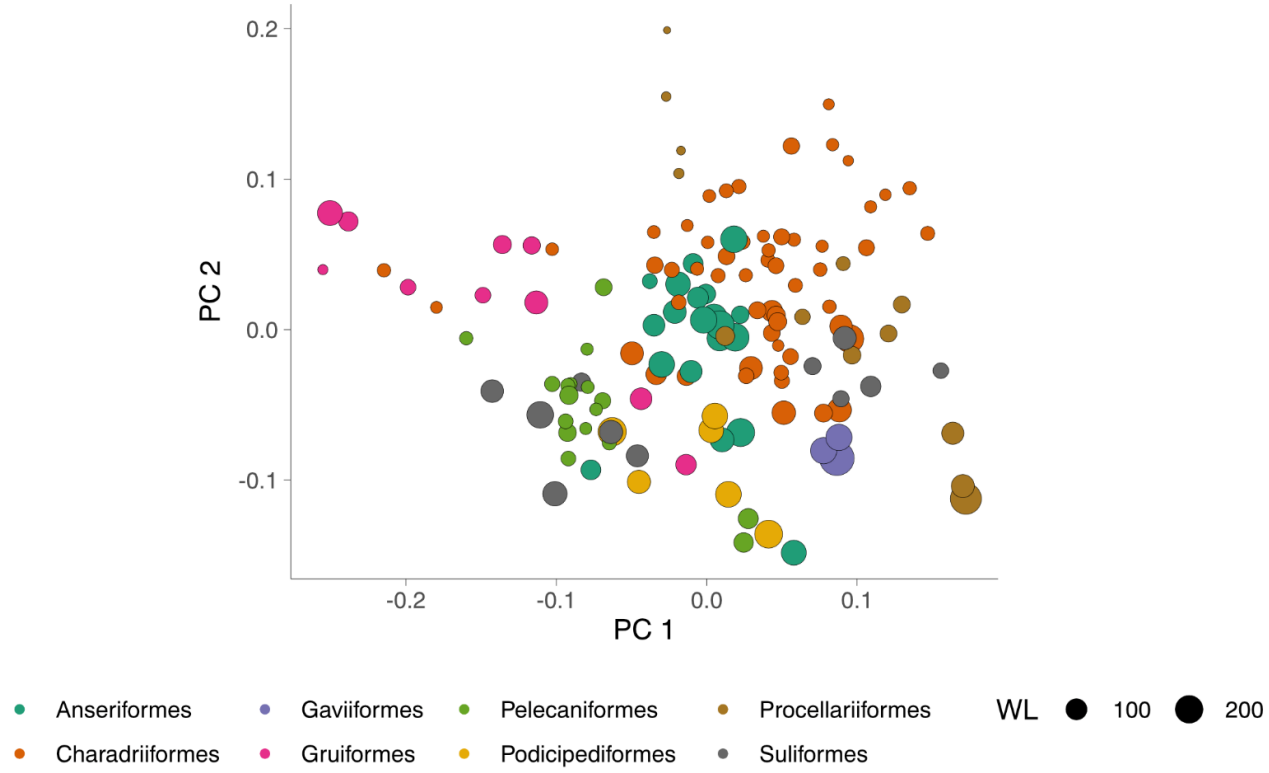

Suppl. Figure 2.10 Wing loading (WL, N/m^2) mapped onto whole-wing morphospace, colored by taxonomy.

SUPPL. DATA 1-2

Found in supplemental material for Baumgart et al. (2021):

https://academic.oup.com/iob/advance-article/doi/10.1093/iob/obab011/6276991#supplementary-data

Suppl. Data 1 Phylogenetic tree used in this dataset, pruned from Jetz. et al (2012). (In standalone .phy file.)

Suppl. Data 2 Boxplot significance tests and summary statistics. Each sheet within the Excel workbook shows the data for one of the boxplots, labeled in the name tabs at the bottom. Includes data on analyses for migratory status (full migrant, partial migrant, non-migrant); not plotted in Figure 5. (In standalone Excel workbook.)

SUPPL. TABLES 1-11

Suppl. Table 2.1 Species used in this dataset and corresponding variables.

In Excel spreadsheet in suppl. for Baumgart et al, 2021:

https://academic.oup.com/iob/advance-article/doi/10.1093/iob/obab011/6276991#supplementary-data

Suppl. Table 2.2 WingMorph metrics used in this study.

In Excel spreadsheet in suppl. for Baumgart et al, 2021:

https://academic.oup.com/iob/advance-

article/doi/10.1093/iob/obab011/6276991#supplementary-data

Suppl. Table 2.3 Pagel's lambda tests for phylogenetic signal for functional metrics used in this study. Null hypothesis = 0, no phylogenetic signal. (1 = high phylogenetic signal)

Variable	Lambda	P-value
Wing loading	0.827	5.185E-19
Body mass	0.950	7.100E-17
Aspect ratio	0.978	9.103E-33
Wing area	0.957	1.496E-22

Suppl. Table 2.4 Spearman's test for correlation between functional metrics. Top value = test statistic, Spearman's rho; bottom value = p-value. Colored boxes indicate statistically significant correlation between two variables. Abbreviations: AR, aspect ratio; WA, wing area; WL, wing loading; HWI, handwing index.

	AR slope	WA	WL	HWI
AR	98954 <1E-16	404502 0.68455	439566 0.574292	30332 <1E-16
AR slope		410782 0.815865	395210 0.507315	120778 <1E-16
WA			335936 0.020558	469680 0.162584
WL				507042 0.014512

Aspect ratio is significantly correlated with AR slope and handwing index. AR slope is also correlated with handwing index. Wing loading is correlated with wing area and handwing index. The remaining metrics are not correlated with each other. Loadings provided below, in Suppl. Table 5.

Suppl. Table 2.5 Loadings (eigenvectors) for the functional metrics for each PC.

	PC1	PC2	PC3	PC4	PC5
AR	0.555	-0.210	0.227	-0.772	0.000
AR slope	0.492	-0.259	-0.810	0.185	4.22E-16
WA	0.304	0.637	-0.010	0.042	-0.707
WL	0.304	0.637	-0.010	0.042	0.707
HWI	0.516	-0.278	0.540	0.605	-4.23E-16

Suppl. Table 2.6 Phylogenetically corrected ANOVAs for handwing index data.

Response variable	F statistic	df	P-value	Corrected P-value
Flight style	11.577	3	8.72E-07	0.418
Foraging Behavior	16.55	6	4.37E-14	0.006
Foraging Niche	7.311	11	1.57E-09	0.042
Habitat	10.412	6	2.13E-09	0.004
Migratory Status	1.271	2	0.284	0.46
Migration+Location	7.278	4	2.52E-05	0.044

Suppl. Table 2.7 PC scores for the whole-wing morphospace.

In Excel spreadsheet in suppl. for Baumgart et al, 2021:

https://academic.oup.com/iob/advance-article/doi/10.1093/iob/obab011/6276991#supplementary-data

Suppl. Table 2.8 Phylogenetically corrected MANOVAs for whole-wing morphospace data using the first six PCs, accounting for ~90.9% of the variance.

Response variable	Wilks statistic	df	P-value	Corrected P-value
Flight style	0.372	18	1.01E-18	0.668
Foraging Behavior	0.178	36	1.47E-28	0.017
Foraging Niche	0.11	66	8.46E-28	0.004
Habitat	0.414	36	6.21E-10	0.114
Migratory Status	0.942	12	0.802	0.965
Migration+Location	0.655	24	3.33E-04	0.481

Suppl. Table 2.9 PC scores for the wing area morphospace.

In Excel spreadsheet in suppl. for Baumgart et al, 2021: https://academic.oup.com/iob/advance-article/doi/10.1093/iob/obab011/6276991#supplementary-data

Suppl. Table 2.10 PC scores for the handwing morphospace.

In Excel spreadsheet in suppl. for Baumgart et al, 2021: https://academic.oup.com/iob/advance-article/doi/10.1093/iob/obab011/6276991#supplementary-data

Suppl. Table 2.11 Phylogenetically corrected MANOVAs for handwing morphospace data using the first three PCs, accounting for ~91.3% of the variance.

Response variable	Wilks statistic	Df	p-value	Corrected p-value
Flight style	0.487	15	1.89E-13	0.696
Foraging Behavior	0.369	18	7.07E-19	0.032
Foraging Niche	0.348	33	3.85E-14	0.042
Habitat	0.571	18	1.48E-05	0.061
Migratory Status	0.98	6	0.841	0.944
Migration+Location	0.707	12	8.93E-06	0.106

CHAPTER 3 APPENDIX

SUPPL. TABLE 3.1 SPECIMENS USED IN STERNUM ANALYSIS.

Including order, flight style and waterbird/landbird categorization.

	Spec. No.	Name	Order	Flight style	Waterbird/Landbird
1	MCZ 342282	*Aceros subruficollis*	Bucerotiformes	Forward flight	Landbird
2	FMNH 368823	*Actophilornis africanus*	Charadriiformes	Forward flight	Waterbird
3	YPM 104291	*Aechmophorus occidentalis*	Podicipediformes	High freq. flapping	Waterbird
4	MCZ 346514	*Ailuroedus buccoides*	Passeriformes	Forward flight	Landbird
5	MCZ 343828	*Alle alle*	Charadriiformes	High freq. flapping	Waterbird
6	MCZ 340260	*Alopochen aegyptiaca*	Anseriformes	Forward flight	Waterbird
7	YPM 109923	*Anhima cornuta*	Anseriformes	Undulating flight	Waterbird
8	MCZ 343615	*Anhinga anhinga*	Suliformes	Undulating flight	Waterbird
9	YPM 103994	*Anhinga rufa*	Suliformes	Undulating flight	Waterbird
10	MCZ 346739	*Anodorhynchus hyacinthinus*	Psittaciformes	Forward flight	Landbird
11	YPM 137647	*Anseranas semipalmata*	Anseriformes	Forward flight	Waterbird
12	MCZ 346994	*Anthracoceros coronatus*	Bucerotiformes	Forward flight	Landbird
13	MCZ 347208	*Aptenodytes patagonicus*	Sphenisciformes	Swimming	Waterbird
14	YPM 103006	*Apteryx australis*	Apterygiformes	Not flying	Landbird
15	MCZ 343763	*Aramides cajanea*	Gruiformes	High freq. flapping	Waterbird
16	MCZ 343706	*Ardea cocoi*	Pelecaniformes	Undulating flight	Waterbird
17	MCZ 347536	*Ardea herodias*	Pelecaniformes	Undulating flight	Waterbird
18	YPM 103855	*Athene cunicularia*	Strigiformes	Undulating flight	Landbird
19	MCZ 343601	*Balearica pavonina*	Gruiformes	Undulating flight	Waterbird
20	MCZ 340266	*Bombycilla garrulus*	Passeriformes	Forward flight	Landbird
21	MCZ 347936	*Bonasa umbellus*	Galliformes	Short flight	Landbird
22	MCZ 347953	*Branta canadensis*	Anseriformes	Forward flight	Waterbird
23	MCZ 346931	*Branta leucopsis*	Anseriformes	Forward flight	Waterbird
24	MCZ 347017	*Bubo virginianus*	Strigiformes	Undulating flight	Landbird
25	YPM 110394	*Bubulcus ibis*	Pelecaniformes	Undulating flight	Waterbird
26	MCZ 340459	*Buceros bicornis*	Bucerotiformes	Forward flight	Landbird
27	MCZ 337291	*Bucorvus abyssinicus*	Bucerotiformes	Forward flight	Landbird
28	MCZ 346978	*Burhinus capensis*	Charadriiformes	Forward flight	Waterbird
29	MCZ 335526	*Buteo jamaicensis*	Accipitriformes	Gliding/soaring	Landbird
30	MCZ 340358	*Catharacta antarctica*	Charadriiformes	Undulating flight	Waterbird
31	MCZ 347737	*Centropus sinensis*	Cuculiformes	Forward flight	Landbird
32	MCZ 342210	*Ceratogymna elata*	Bucerotiformes	Forward flight	Landbird
33	YPM 103840	*Chauna torquata*	Anseriformes	Undulating flight	Waterbird
34	MCZ 342155	*Chen caerulescens*	Anseriformes	High freq. flapping	Waterbird
35	MCZ 346997	*Ciconia nigra*	Ciconiiformes	Gliding/soaring	Waterbird
36	MCZ 342125	*Circus cyaneus*	Accipitriformes	Gliding/soaring	Landbird
37	MCZ 346497	*Clangula hyemalis*	Anseriformes	High freq. flapping	Waterbird

(Suppl. Table 3.1 continued)

	Spec. No.	Name	Order	Flight style	Waterbird/Landbird
38	MCZ 346435	*Colius striatus*	Colliformes	Forward flight	Landbird
39	MCZ 346026	*Corythaixoides leucogaster*	Musophagiformes	Forward flight	Landbird
40	MCZ 347531	*Crinifer zonurus*	Musophagiformes	Forward flight	Landbird
41	MCZ 340276	*Crypturellus noctivagus*	Tinamiformes	Short flight	Landbird
42	YPM 105038	*Cuculus canorus*	Cuculiformes	Forward flight	Landbird
43	MCZ 347051	*Cygnus olor*	Anseriformes	Forward flight	Waterbird
44	YPM 107504	*Dacelo novaeguineae*	Coraciiformes	Forward flight	Landbird
45	MCZ 1586	*Dromaius novaehollandiae*	Casuariiformes	Not flying	Landbird
46	MCZ 342991	*Dromas ardeola*	Charadriiformes	Gliding/soaring	Waterbird
47	MCZ 343061	*Dryocopus javensis*	Piciformes	Forward flight	Landbird
48	MCZ 343703	*Eudocimus ruber*	Pelecaniformes	Undulating flight	Waterbird
49	MCZ 346428	*Eudyptes chrysocome*	Sphenisciformes	Swimming	Waterbird
50	YPM 102975	*Eudyptes chrysolophus*	Sphenisciformes	Swimming	Waterbird
51	MCZ 346025	*Eudyptula minor*	Sphenisciformes	Swimming	Waterbird
52	YPM 4830	*Euryapteryx gravis*	Dinornithiformes	Not flying	Landbird
53	MCZ 347072	*Eurypyga helias*	Eurypygiformes	Forward flight	Waterbird
54	MCZ 343335	*Falco rusticolus*	Falconiformes	Undulating flight	Landbird
55	MCZ 337043	*Falco sparverius*	Falconiformes	Undulating flight	Landbird
56	MCZ 355463	*Florisuga mellivora*	Apodiformes	Hovering flight	Landbird
57	YPM 105483	*Fregata magnificens*	Suliformes	Gliding/soaring	Waterbird
58	MCZ 347016	*Gallus gallus*	Galliformes	Short flight	Landbird
59	MCZ 347919	*Gavia immer*	Gaviiformes	High freq. flapping	Waterbird
60	MCZ 346913	*Gavia stellata*	Gaviiformes	High freq. flapping	Waterbird
61	MCZ 343239	*Geococcyx californianus*	Cuculiformes	Forward flight	Landbird
62	MCZ 343032	*Geranospiza caerulescens*	Accipitriformes	Gliding/soaring	Landbird
63	YPM 102319	*Goura cristata*	Columbiformes	Forward flight	Landbird
64	MCZ 346875	*Gracula religiosa*	Passeriformes	Forward flight	Landbird
65	MCZ 246600	*Grus antigone*	Gruiformes	Undulating flight	Waterbird
66	MCZ 347823	*Haliaeetus leucocephalus*	Accipitriformes	Gliding/soaring	Landbird
67	YPM 104788	*Hemiprocne mystacea*	Apodiformes	Forward flight	Landbird
68	MCZ 337109	*Herpetotheres cachinnans*	Falconiformes	Undulating flight	Landbird
69	MCZ 347332	*Icterus galbula*	Passeriformes	Forward flight	Landbird
70	MCZ 341469	*Lagopus muta*	Galliformes	Short flight	Landbird
71	MCZ 342479	*Larus argentatus*	Charadriiformes	Gliding/soaring	Waterbird
72	YPM 109939	*Megaceryle torquata*	Coraciiformes	Forward flight	Landbird
73	MCZ 347151	*Melanitta perspicillata*	Anseriformes	High freq. flapping	Waterbird
74	MCZ 343049	*Meleagris ocellata*	Galliformes	Short flight	Landbird
75	MCZ 341900	*Mergus merganser*	Anseriformes	High freq. flapping	Waterbird
76	MCZ 347043	*Morus bassanus*	Suliformes	Undulating flight	Waterbird
77	MCZ 342988	*Netta peposaca*	Anseriformes	High freq. flapping	Waterbird
78	MCZ 341632	*Nothura maculosa*	Tinamiformes	Short flight	Landbird

(Suppl. Table 3.1 continued)

	Spec. No.	Name	Order	Flight style	Waterbird/Landbird
79	YPM 111466	*Numenius arquata*	Charadriiformes	Forward flight	Waterbird
80	MCZ 343442	*Nyctidromus albicollis*	Caprimulgiformes	Forward flight	Landbird
81	YPM 109620	*Nymphicus hollandicus*	Psittaciformes	Forward flight	Landbird
82	MCZ 346723	*Oceanites oceanicus*	Procellariformes	Undulating flight	Waterbird
83	MCZ 343617	*Opisthocomus hoazin*	Opisthocomiformes	Forward flight	Landbird
84	MCZ 347607	*Pandion haliaetus*	Accipitriformes	Gliding/soaring	Landbird
85	YPM 104940	*Paradisaea raggiana*	Passeriformes	Forward flight	Landbird
86	MCZ 343006	*Patagioenas fasciata*	Columbiformes	Forward flight	Landbird
87	MCZ 343648	*Patagioenas speciosa*	Columbiformes	Forward flight	Landbird
88	YPM 107559	*Pelecanus erythrorhynchos*	Pelecaniformes	Undulating flight	Waterbird
89	MCZ 347970	*Pelecanus occidentalis*	Pelecaniformes	Undulating flight	Waterbird
90	YPM 110024	*Phaethon rubricauda*	Phaethoniformes	Gliding/soaring	Waterbird
91	YPM 105267	*Phalacrocorax africanus*	Suliformes	Undulating flight	Waterbird
92	MCZ 346990	*Phalacrocorax gaimardi*	Suliformes	Undulating flight	Waterbird
93	MCZ 346743	*Phalacrocorax pelagicus*	Suliformes	Undulating flight	Waterbird
94	MCZ 343050	*Phoebastria immutabilis*	Procellariformes	Undulating flight	Waterbird
95	MCZ 342999	*Phoebastria nigripes*	Procellariformes	Undulating flight	Waterbird
96	MCZ 347572	*Phoenicopterus ruber*	Phoenicopteriformes	Forward flight	Waterbird
97	YPM 102558	*Platalea ajaja*	Pelecaniformes	Undulating flight	Waterbird
98	YPM 110028	*Priotelus temnurus*	Trogoniformes	Forward flight	Landbird
99	MCZ 346982	*Psarocolius angustifrons*	Passeriformes	Forward flight	Landbird
100	MCZ 346922	*Pterodroma externa*	Procellariformes	Undulating flight	Waterbird
101	MCZ 347048	*Puffinus griseus*	Procellariformes	Undulating flight	Waterbird
102	MCZ 343002	*Pulsatrix perspicillata*	Strigiformes	Undulating flight	Landbird
103	MCZ 346121	*Quiscalus quiscula*	Passeriformes	Forward flight	Landbird
104	MCZ 343316	*Rallus elegans*	Gruiformes	High freq. flapping	Waterbird
105	MCZ 347338	*Ramphastos sulfuratus*	Piciformes	Forward flight	Landbird
106	YPM 111118	*Raphus cucullatus*	Columbiformes	Not flying	Landbird
107	MCZ 337080	*Rissa tridactyla*	Charadriiformes	Gliding/soaring	Waterbird
108	MCZ 342764	*Rollulus rouloul*	Galliformes	Short flight	Landbird
109	MCZ 343699	*Rupicola rupicola*	Passeriformes	Forward flight	Landbird
110	MCZ 346960	*Sarcoramphus papa*	Accipitriformes	Gliding/soaring	Landbird
111	MCZ 347040	*Spheniscus humboldti*	Sphenisciformes	Swimming	Waterbird
112	MCZ 347813	*Sphyrapicus varius*	Piciformes	Forward flight	Landbird
113	MCZ 345022	*Sterna bergii*	Charadriiformes	Gliding/soaring	Waterbird
114	MCZ 343375	*Sterna fuscata*	Charadriiformes	Gliding/soaring	Waterbird
115	MCZ 347614	*Sterna hirundo*	Charadriiformes	Gliding/soaring	Waterbird
116	MCZ 343437	*Sterna maxima*	Charadriiformes	Gliding/soaring	Waterbird
117	MCZ 343323	*Streptoprocne zonaris*	Apodiformes	Forward flight	Landbird
118	YPM 102332	*Strigops habroptila*	Psittaciformes	Not flying	Landbird
119	YPM 110957	*Strix nebulosa*	Strigiformes	Undulating flight	Landbird

(Suppl. Table 3.1 continued)

	Spec. No.	Name	Order	Flight style	Waterbird/Landbird
120	MCZ 343007	*Strix virgata*	Strigiformes	Undulating flight	Landbird
121	MCZ 341626	*Struthio camelus*	Struthioniformes	Not flying	Landbird
122	MCZ 343831	*Tigrisoma lineatum*	Pelecaniformes	Undulating flight	Waterbird
123	MCZ 342774	*Tinamus major*	Tinamiformes	Short flight	Landbird
124	MCZ 346018	*Tockus erythrorhynchus*	Bucerotiformes	Forward flight	Landbird
125	MCZ 343173	*Treron pompadora*	Columbiformes	Forward flight	Landbird
126	MCZ 347505	*Tyto alba*	Strigiformes	Undulating flight	Landbird
127	YPM 107209	*Upupa epops*	Coraciiformes	Forward flight	Landbird
128	MCZ 337082	*Uria aalge*	Charadriiformes	High freq. flapping	Waterbird

CHAPTER 4 APPENDIX

SUPPL. TABLE 4.1 SPECIMEN SCANS USED.

Most are skeletonized; *, whole pickle scan. Abbreviations: BM, body mass; scan res, scan resolution; FS, flight style. All scans available on Morphosource.org, identified below using ARK IDs which can be copied into the browser as a URL.

Species	Specimen No. & ARK	BM, g	Scan res, mm	Order	Family	Family common name	FS
Boissonneaua flavescens*	CM B A1715 ark:/87602/m4 /M86702	8.2	0.026	Apodiformes	Trochilidae	Hummingbirds	HoF
Oceanodroma leucorhoa	NHMUK Zoo: S/1953.3.10 ark:/87602/m4 /M92379	41.4	0.038	Procellariiformes	Hydrobatidae	Northern Storm Petrels	UF
Melanerpes carolinus	UF O 42125 ark:/87602/m4 /M80832	73.2	0.043	Piciformes	Picidae	Woodpeckers	FF
Crypturellus tataupa	UMMZ B 201948 ark:/87602/m4 /M109590	219.5	0.049	Tinamiformes	Tinamidae	Tinamous	SF
Asio flammeus	UF O 41995 ark:/87602/m4 /M80816	315.0	0.071	Strigiformes	Strigidae	Owls	UF
Aix sponsa	UF O 47798 ark:/87602/m4 /M80944	681.0	0.071	Anseriformes	Anatidae	Ducks, Geese, Swans	HF
Fulica americana	UF O 46733 ark:/87602/m4 /M80912	724.0	0.062	Gruiformes	Rallidae	Rails, Crakes & Coots	HF
Spheniscus mendiculus*	FMNH B 106005 ark:/87602/m4 /M97861	2135.0	0.115	Sphenisciformes	Spheniscidae	Penguins	SW
Haliaeetus leucocephalus	UF O 46979 ark:/87602/m4 /M80928	4130.0	0.147	Accipitriformes	Accipitridae	Kites, Hawks, Eagles	GS
Chauna torquata	FMNH B 106314 ark:/87602/m4 /372259	4400.0	0.122	Anseriformes	Anhimidae	Screamers	UF
Gavia immer	UF O 39806 ark:/87602/m4 /M77157	5460.0	0.098	Gaviformes	Gaviidae	Loons	HF
Cygnus cygnus	FMNH B 104474 ark:/87602/m4 /372271	9350.0	0.096	Anseriformes	Anatidae	Ducks, Geese, Swans	HF
Vultur gryphus	NHMUK Zoo: S/1955.511 ark:/87602/m4 /M110010	11300.0	X,Y: 0.126; Z: 0.379	Cathartiformes	Cathartidae	New World Vultures	GS

(Suppl. Table 4.1 continued)

Species	Specimen No. & ARK	BM, g	Scan res, mm	Order	Family	Family common name	FS
Balaeniceps rex	NHMUK Zoo: S/1952.1.100 ark:/87602/m4 /M108630	5984.0	0.126	Pelecaniformes	Balaenicipitidae	Shoebills	UF
Pelecanus occidentalis	NHMUK Zoo: S/1973.66.16 ark:/87602/m4 /M92472	3438.0	X,Y: 0.126; Z: 0.252	Pelecaniformes	Pelecanidae	Pelicans	UF
Phoebastria irrorata	NHMUK Zoo: S/1963.28.4 ark:/87602/m4 /M92014	3395.0	X,Y: 0.125; Z: 0.375	Procellariiformes	Diomedeidae	Albatrosses	UF
Branta hutchinsii	UF O 45601 ark:/87602/m4 /M80880	2050.0	0.0915	Anseriformes	Anatidae	Ducks, Geese, Swans	FF
Alca torda	UF O 49661 ark:/87602/m4 /M81024	726.0	0.616	Charadriiformes	Alcidae	Auks	HF

SUPPL. TABLE 4.2 AIR SPACE PROPORTIONS (ASP) OF THE WHOLE HUMERUS.

Species	Air volume, mm^3	Bone volume, mm^3	Total volume, mm^3	ASP
Gavia immer	2776.9	1820.1	4597.0	60.4
Cygnus cygnus	50245.1	25606.1	75851.2	66.2
Boissonneaua flavescens	6.0	5.8	11.8	50.8
Chauna torquata	26261.0	12139.1	38400.1	68.4
Spheniscus mendiculus	518.6	1880.2	2398.8	21.6
Asio flammeus	2146.6	939.2	3085.8	69.6
Melanerpes carolinus	180.2	105.3	285.5	63.1
Branta hutchinsii	6145.3	4135.9	10281.2	59.8
Fulica americana	238.2	232.1	470.3	50.6
Haliaeetus leucocephalus	27446.4	16483.4	43929.8	62.5
Vultur gryphus	66542.3	40247.6	106789.9	62.3
Oceanodroma leucorhoa	62.3	104.6	166.9	37.3
Aix sponsa	1453.6	968.5	2422.1	60.0
Crypturellus tataupa	370.3	231.7	602.0	61.5
Balaeniceps rex	56812.6	22908. 8	79721.4	71.3
Pelecanus occidentalis	35455.0	18852.1	54307.1	65.3
Phoebastria irrorata	25455.2	20600.0	46055.2	55.3
Alca torda	565.4	1066.0	1631.4	34.7

SUPPL. TABLE 4.3 AIR SPACE PROPORTIONS (ASPS) IN EIGHT CROSS-SECTIONS ACROSS HUMERI.

A = air area, B = bone area, avg = average.

Species	Stats	CS 1	CS 2	CS 3	CS 4	CS 5	CS 6	CS 7	CS 8	Avg.
Gavia immer	A	83.1	33.1	23.8	20.8	18.6	16.6	18.6	52.8	
	B	32.5	18.6	15.1	13.6	13.0	12.6	12.9	32.6	
	ASP	71.9	64.0	61.2	60.5	58.9	56.8	59.0	61.8	61.8
Cygnus cygnus	A	564.7	188.9	145.8	133.1	110.8	113.8	118.6	385.5	
	B	170.0	103.6	101.8	77.5	76.5	68.3	74.4	150.7	
	ASP	76.9	64.6	58.9	63.2	59.2	62.5	61.5	71.9	64.8
Boissonneaua flavescens	A	1.65	2.14	1.03	0.73	0.69	0.67	0.95	0.91	
	B	1.03	1.49	1.08	0.76	0.78	0.71	0.89	1.29	
	ASP	61.6	59.0	48.8	49.0	46.9	48.6	51.6	41.4	50.9
Chauna torquata	A	296.3	190.8	120.8	83.2	97.6	92.7	98.7	265.2	
	B	126.1	77.9	57.5	53.2	49.6	47.3	46.5	106.4	
	ASP	70.1	71.0	67.8	61.0	66.3	66.2	68.0	71.4	67.7
Spheniscus mendiculus	A	39.5	40.9	3.2	2.6	1.9	2.0	6.0	20.1	
	B	48.5	48.0	38.7	31.2	33.6	32.4	34.8	29.3	
	ASP	44.9	46.0	7.6	7.7	5.4	5.8	14.7	40.7	21.6
Asio flammeus	A	64.8	34.0	23.9	17.7	14.1	15.5	17.9	53.0	
	B	15.6	12.8	8.9	8.4	8.5	8.6	9.0	23.6	
	ASP	80.6	72.6	72.9	67.8	62.4	64.3	66.5	69.2	69.5
Melanerpes carolinus	A	13.8	4.5	4.5	4.1	3.1	2.8	4.3	11.1	
	B	5.4	3.1	3.2	2.7	2.4	2.3	2.6	5.7	
	ASP	71.9	59.2	58.4	60.3	56.4	54.9	62.3	66.1	61.2
Branta hutchinsii	A	151.5	51.7	38.8	34.0	29.4	24.0	31.5	94.2	
	B	53.9	36.4	34.6	28.0	27.0	25.6	28.2	56.5	
	ASP	73.8	58.7	52.9	54.8	52.1	48.4	52.8	62.5	57.0
Fulica americana	A	20.5	6.4	3.6	2.7	2.3	2.4	4.1	10.0	
	B	10.8	5.8	4.4	3.9	3.9	3.9	4.0	8.2	
	ASP	65.5	52.5	45.0	40.1	37.1	38.1	50.6	54.9	48.0
Haliaeetus leucocephalus	A	296.2	203.2	129.1	83.5	77.8	96.7	117.0	223.4	
	B	149.9	91.0	69.1	57.4	60.0	61.4	70.6	196.8	
	ASP	66.4	69.1	65.1	59.3	56.5	61.2	62.4	53.2	61.7
Vultur gryphus	A	561.5	225.4	187.9	160.1	152.3	207.4	241.3	643.6	
	B	279.0	132.9	122.4	117.8	106.6	109.4	129.1	353.4	
	ASP	66.8	62.9	60.6	47.4	58.8	65.5	65.1	64.6	61.5
Oceanodroma leucorhoa	A	4.1	2.3	1.5	1.3	1.2	1.4	1.8	2.9	
	B	5.4	2.9	2.8	2.5	2.3	2.1	3.2	3.9	
	ASP	43.2	44.2	34.9	34.2	34.3	40.0	36.0	42.6	38.7

(Suppl. Table 4.3 continued)

Species	Stats	CS 1	CS 2	CS 3	CS 4	CS 5	CS 6	CS 7	CS 8	Avg.
Aix sponsa	A	41.0	30.8	17.4	14.2	14.8	14.0	15.7	28.8	
	B	33.3	31.0	19.3	11.5	11.2	10.9	12.1	29.8	
	ASP	55.2	49.8	47.4	55.3	56.9	56.2	56.5	49.1	53.5
Crypturellus tatuapa	A	21.4	16.5	12.3	5.6	4.5	4.4	8.5	15.1	
	B	10.4	9.3	5.9	4.4	4.2	4.4	5.1	9.8	
	ASP	67.3	64.0	67.6	56.0	51.7	50.0	62.5	60.6	60.0
Balaeniceps rex	A	511.3	452.3	256.9	173.1	155.7	117.1	174.9	349.2	
	B	177.3	105.0	79.2	67.2	60.6	64.3	71.8	225.4	
	ASP	74.3	81.2	76.4	72.0	72.0	64.6	70.9	60.8	71.5%
Pelecanus occidentalis	A	346.3	212.8	136.9	105.4	90.9	109.3	169.3	222.3	
	B	176.5	108.8	76.3	43.9	44.1	43.2	76.7	251.2	
	ASP	66.2	66.2	64.2	70.6	67.3	71.7	68.8	46.9	65.2%
Phoebastria irrorata	A	255.1	190.5	69.1	57.0	55.8	55.6	77.1	159.5	
	B	116.1	101.7	93.4	57.5	52.0	53.0	63.5	97.4	
	ASP	68.7	65.2	42.5	49.8	51.8	51.2	54.8	62.1	55.8%
Alca torda	A	26.6	12.1	7.4	4.4	4.0	4.4	6.4	18.5	
	B	26.5	26.4	14.6	12.4	12.4	11.6	13.0	23.6	
	ASP	50.1	31.4	33.6	26.2	24.4	27.5	33.0	43.9	33.8%